MOISTURE DYNAMICS IN OIL-FILLED POWER TRANSFORMERS

by

SRUTI CHAKRABORTY

Student ID:2012RCH9520

Under supervision of

Dr.MANISH VASHISHTHA

Department of Chemical Engineering

MALAVIYA NATIONAL INSTITUTE OF TECHNOLOGY,

JAIPUR-302017

December, 2017

In loving memory of

Dr. Asit Kumar Chakraborty

Without you I might never have dreamed of this day.

Thank you for being our light, Dadu.

Acknowledgments

I would like to take this opportunity to express my sincere gratitude towards each and every one who have helped me throughout the completion of this project and gain valuable experience.

First of all, I am very thankful to my supervisor, Dr. Manish Vashishtha. This project might not have happened without his excellent guidance and thorough support. His perpetual enthusiasm in research and scientific curiosity has highly motived me, and without his knowledgeable supervision and patient assistance it would not have been possible to prepare this thesis. I am equally grateful to my DREC experts who have contributed their valuable time and experience of various scientific and technological aspects that have finally helped in shaping up of this project. I am thankful to the Malaviya National Institute of Technology, Jaipur for providing the PhD scholarship and duly appreciate the help of all the faculty, staff and colleagues for their support and assistance throughout this project. I am utmost indebted to Dr. Sushil E.Chaudhari (Raj Petro Specialties Ltd., Mumbai) for being an exemplary mentor. It is entirely because of his encouragement, guidance and support that I have been able to pick up this topic despite being from the obvious end of the technical spectrum.

I am beyond any words to my wonderful family for their immense love, encouragement and patience during the completion of this project. I can't thank my parents enough who encouraged my desire for further education defying all social conventions while enduring my absence in all these years. I am beyond words for my little brother who's endless love and beautiful smile has made this thesis possible.

Last but certainly not the least, I am very grateful to the Almighty for his blessings...

Abstract

Power transformers are strategically placed components in a energy supply grid designed to transform the voltage and current levels as per the user requirement. In case of a premature failure, the total cost of repairing and re-installation exceeds the actual manufacturing cost. Hence, reliable transformer condition monitoring is of utmost importance.

Transformer deregulation due to moisture contamination is of particular interest among manufacturers due to its detrimental affect on the insulation components. Excess moisture can reduce the partial inception voltage level, compromise the dielectric strength of insulation, accelerate the rate of aging and increase the risk of bubble evolution in operational transformers. State-of-art techniques for moisture measurements are restricted by its non-accessibility to the most critical zones of the transformer thereby widening the scope of its application.

In the present work, an exhaustive twofold model is proposed to correlate the load-varied temperature profiles in transformer along with potential moisture movement schemes. The prime objective of this research is not only to improve the existing models for moisture measurement in oil and solid insulate respectively but also to suggest any potential contribution that can help in improving the accuracy of existing technologies. A CFD based thermal model with respect to transformer geometry and loading capacities have been proposed to monitor the time-dependent temperature profile within the utility. Such transient profiles have been applied directly to the an improved moisture-in-oil model that will provide a resultant distribution of moisture in oil and paper insulation of transformer without the need for intrusive measurements.

The observations in this study are found more reliable as compared to the available results due to its realistic approach. Other outcomes from this research include suitable recommendations in improving the winding design, reliable prediction of average moisture in various locations of transformer tank based on thermal behavior and suggestions to improve the sensor locations for on-line moisture sensing.

Contents

List of Figures

List of Tables

Nomenclature

A	Pre-exponential factor in Arrhenius equation
$\vec{A}$	Magnetic vector potential, V.s/m
a_w	Water activity in oil
α_c	Temperature coefficient of copper conductors, 1/K
B_m	Maximum magnetic flux density, Tesla
C_{avg}	Average moisture concentration in paper, %
C_d	Dissolved moisture in oil, ppm
C_i	Initial moisture concentration in paper, %
C_m	Equilibrium moisture concentration in paper, %
C_{oil}	Moisture concentration of oil, ppm
C_{paper}	Moisture concentration in paper, %
$C_{p,m}$	Measured moisture in paper, %
$C_{o,ss}$	Saturated moisture in oil, ppm
$C_{o,i}$	Instantaneous moisture in oil, ppm
C_s	Soluble moisture in oil, ppm
D_{eff}	Effective diffusion coefficient of moisture in paper, m^2/s
DP	Degree of polymerization
dV	Elemental volume, m^3
ε	Magnetic permeability, H/m
f	Operating frequency, Hz
Γ	Constant for determining thermal capacity of oil
j	Molar flux of moisture in cellulosic insulation, $mol/m^2.s$
J_s	Surface current density, A/m^2
K_h	Material coefficient of hysteresis losses, W
K_e	Material coefficient of Eddy losses, W
l	Insulation thickness, mm
L_{exp}	Expected life of transformer, years
M_a	Mass of untanked assembly, kg
M_t	Mass of tank, kg
M_w	Molecular weight of water
M_{paper}	Total mass of dry paper, kg
M_{water}	Total mass of moisture (water) in paper or oil, kg
M_{oil}	Total mass of oil, kg
P_c	Core losses, W
$P_{w,o}$	Winding losses due to Ohmic currents, W
$P_{w,e}$	Winding losses due to Eddy currents, W
Q_T	Total heat source due to transmission losses, W/m^3
$Q_{T,0}$	Heat source at reference temperature, W/m^3
RS_{oil}	Relative saturation of oil, %
RH_{air}	Relative humidity of air, %
σ	Electrical conductivity, S/m
ψ	Molecular potential per unit mass of oil
T	Absolute operating temperature, K
T_a	Ambient temperature, °C
T_c	Critical temperature of air, °C
T_{hst}	Hot-spot temperature, °C
T_{to}	Top-oil temperature, °C

T_h	Temperature rise of hot-spot over windings, °C
$T_{to,u}$	Ultimate top-oil temperature, °C
$T_{to,i}$	Initial top-oil temperature, °C
t_c	Thickness of laminate, m
τ_p	Time constant of moisture change in paper, hours
τ_o	Time constant of moisture change in oil, hours
τ_{corr}	Corrected time constant, hours
V_c	Critical vapor pressure of moisture in air, atm
V_p	Partial vapor pressure of moisture in air, atm
V_s	Saturated vapor pressure of moisture in air, atm
V_w	Volume of windings, m^3

Abbreviations

Sim	Simulated values
Fit	Fitted values
LVW	Low voltage windings
HVW	High voltage windings

Chapter 1

INTRODUCTION

With the recent socio-economic upsurge, the demand for uninterrupted power supply has grown exponentially among various sects of users. Installing high performance electrical transformer within the supply network not only improves the grid integrity but also caters to the exhaustive demand and supply of electricity over long distances with minimum transmission losses and maximum efficiency.

Over the years, transformation of power industry due to the techno-economic changes has led to an interesting opportunity for improving the performance of transformers (both existing and futuristic) by either design or operational modification. An electrical transformer is a static device that can convert a system of alternating current and voltage applied over an invariant frequency within two or more windings using electromagnetic induction as shown in Fig.1.1 [17–19].

These equipments can be broadly classified as "Power" and "Distribution" transformers on the basis of its feeder voltage rating. Typically, a power transformer is required to "step-up" or increase the feeder voltage that is obtained directly from the Generation Substation Unit (GSU) [20] across the transmission network. They operate at a higher voltage rating ($\gg$33 kV), heavy loading conditions, and are expected to
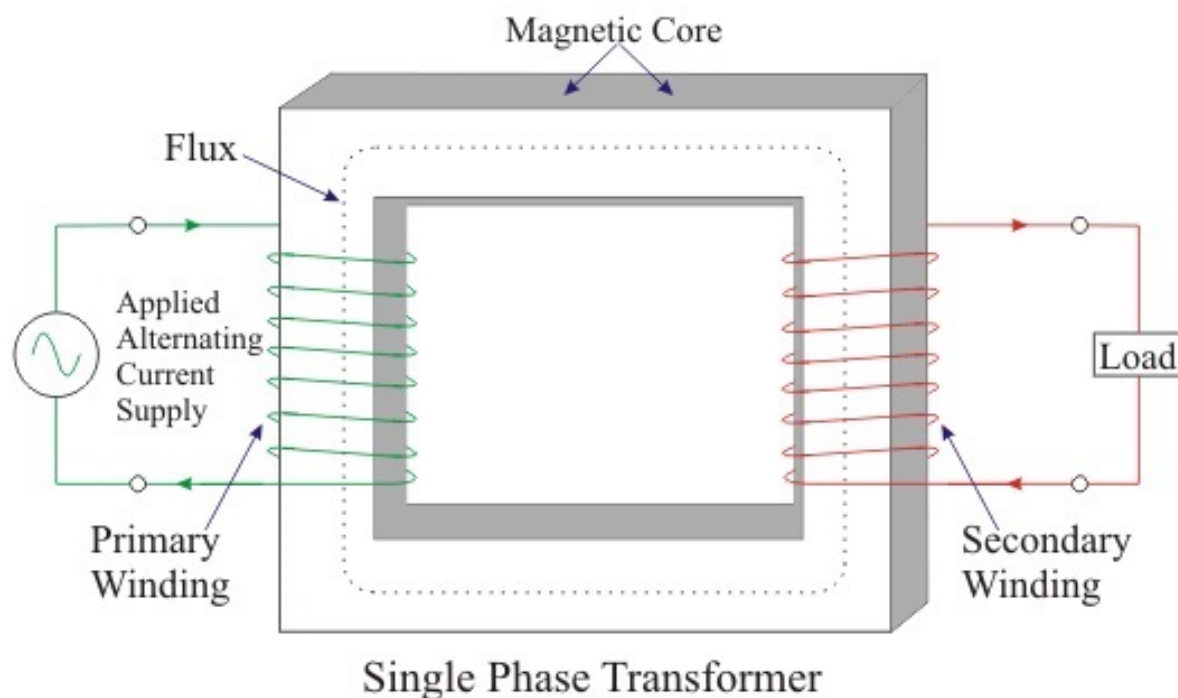
Figure 1.1: Schematic plan of a single phase transformer to show the electromagnetic induction and transformation of current and voltage levels, Source:https://www.electrical4u.com/single-phase-transformer

perform at 100% efficiency. On the other hand, distribution transformer operates at a relatively lower voltage rating (11 kV-230 V), and is required to "step-down" or decrease the incoming feeder voltage according as per user requirement.

Due to its high manufacturing and commissioning costs, the power transformers represent a substantial investment of the energy supply network. In order to maximize the economical revenue and restrict the operational cost below the capital investment, it is essential to continuously monitor the condition of a transformer. Typically, the periodic monitoring of transformer insulation can diagnose an operational efficiency and expected service life of the equipment based on various physico-chemical and dielectric parameters. Although these techniques are reliable enough to predict the risk of an unexpected fault generation, it may sometimes fails to correlate several electrical, thermal, physical and chemical phenomenon to foresee the remaining life of transformer

and its ultimate failure [21–26].

It is a well known fact that the resistive heating of the conducting coils (Cu or Al) due to an applied current and voltage will cause an internal heat generation within the transformer. This heat is capable of initiating an unwanted temperature rise within the active parts of the transformer that is otherwise required to be in thermal equilibrium with the surroundings of an encapsulated unit for safe operation. In case of improper heat dissipation, the hence increased temperature initiates a series of irreversible physico-chemical phenomenon that can eventually cause the equipment to fail.

Modern day transformers are generally filled with suitable dielectric fluids to maintain the thermal equilibrium between active and non-active parts of the equipment. Appropriate circulation of these fluids can restrict the overheating of transformer and increase the active in-service life. Since windings are the most perilous parts of an active transformer, a proper electrical and thermal insulation can delay, if not avoid, the inevitable transformer death due to internal heat generation.

Conventional insulation system containing cellulose based paper is immersed with mineral-based oil in order to provide thermal and electrical resistance to the active windings within a transformer. Although this combination has proven to be inexpensive yet effective, one can undoubtedly infer the effect of elevated thermal stresses on the rate of insulation deterioration and its consequence on the transformer performance [18, 19, 21, 24, 27, 28].

As the winding temperature rises, the cellulose chains of solid insulation undergoes an irreversible physico-chemical cleavage that results in generation of free water, oxygen and other potentially hazardous functional hydrocarbons. The surrounding oil, which not only absorbs the excess heat from the winding but also dissolves these degradation by-products, gradually begins to exhibit a retardation in its thermal-dielectric properties until its reaches a state of complete failure. The collective degradation of insulation resistance due to temperature rise, water formation and oxygen release is termed as

relative ageing [21].

Besides the internal heat, moisture presence within transformers is of utmost concern for both manufacturers and consumers. It is inevitable, unavoidable and very detrimental to the health of transformer insulation. Existing techniques for moisture determination within transformers rely heavily on the relative saturation limits of oil under isothermal conditions that restricted to smaller time periods.

Although partially reliable, these methods are not capable for direct estimation of moisture within the solid insulation due to its inaccessibility and limited understanding of moisture interaction behavior within and oil-cellulose-air complex under fluctuating operating conditions. In the present work, an attempt has been made to differentiate this interaction behavior and provide a holistic understanding of moisture dynamics within encapsulated power transformers based on insulate properties, temperature and moisture exposure conditions.

Unlike the previous studies [7, 19, 21, 22, 27–30], the migration behavior is associated directly with the dynamic thermal modeling of an oil-filled power transformer to pinpoint the locations of bulk moisture release, sorption/dissolution and accumulation within the encapsulated transformer.

Exhaustive studies on thermal modeling to identify the effect of operational parameters using computational fluid dynamics has provided a basis for moisture interaction mechanisms between oil and cellulose at various locations.

The ultimate objective of this research was not only to contribute towards the existing moisture dynamics studies in oil-filled transformers, but also to provide guidelines for a reliable health assessment scheme that can maintain the grid integrity by precise anticipation of fault causing factors without disrupting the energy transmission.

1.1   Transformer Insulation

Besides the design considerations for maximum performance, the choice of an efficient insulation has also become a crucial aspect of the transformer asset management. A conventional insulate must be an inert and non-interactive material with the capacity to isolate the active and non-active parts of transformer without interfering in energy transmission process.

1.1.1   Cellulose-based materials

Conventional wood pulp based cellulosic insulation has been a popular choice among the transformer manufacturers not just due to its excellent dielectric strength and thermal stability, but also because of its abundance and lower cost [4]. It is an inhomogeneous labyrinth of polysaccharide fibers containing anhydrous-1,4 β D-glycopyranose monomers as shown in Fig.1.2a [31].

Multiple glycopyranose monomers conjoin using glycosidic bonds to form a single parent cellulosic chain that will eventually determine the mechanical strength of insulate. The interconnected labyrinth of cellulosic microfibrils that leads to fibrous surfaces of the many layers of paper/pressboard material indirectly decides its mechanical, thermal and dielectric capacity as shown in Fig.1.2b. The remaining hemicellulose and lignin components are nothing but binding agents for conjoining these cellulosic monomers.

Cellulose based Kraft/Crépe paper and pre-compressed pressboard are the most widely used materials in transformer for insulation and isolation respectively as shown in Fig.1.3 [3]. The cellulosic chains can appear in both amorphous and crystalline form depending upon the processing technique. Paper and pressboard is naturally hydrophilic because of the strategic placing of hydroxyl bonds (O-H) within the polymeric chain that causes weaker molecule-dipole interactions because of the van der Waal forces thereby allowing a multilayer moisture seepage through the

material [1, 2, 8, 32].

On the other hand, strong hydrogen bonds on the surface of a cellulosic chain leads to single-layer moisture adsorption that is easy to remove by conventional drying techniques, yet ineffective while segregating the moisture entrapped within the multi-layers of the material thereby requiring modified drying operations [1, 4, 8, 28, 33].

A fresh paper contains higher number of glycopyranose units in a single chain and is referred to as the degree of polymerization (DP) of the insulate [32]. Upon thermal excitation, bond-cleavage and consequential chain scission decreases the DP value and ultimately causes the loss of insulate mechanical-life [23]. The increase in oil acidity due to decomposition of paper/pressboard material is a strong marker of relative ageing and is described by a dimensionless entity as shown in Eq.1.1.

$$\eta = \frac{DP_n}{DP_o} - 1 \tag{1.1}$$

where, DP_o and DP_n indicates the DP values for a fresh and aged sample. Normally, a fresh paper will have a DP value of about 1200-1500 depending upon its preconditioning. After initial moisture removal, it decreases to about 1000-1300 assuming that 0.5% water was retained within the paper sample.

Gradually under fluctuating thermal stresses, the glycosidic bonds break to form free water, oxygen radical, complex furans and other functional hydrocarbons due to the ageing discussed previously. This causes the inter-fiber forces to diminish and eventually the material losses its mechanical strength.

As a commonly acceptable standard, a paper sample is believed to be at the end of its service life, when the tensile strength has reduced to 20% of its original value [23, 34]. Such an initial assumption has also helped researchers in correlating the remaining life of transformer using moisture induced DP values and temperature as given in Eq.1.2.

$$L_{exp}(Yrs) = \Big(\frac{\frac{1}{DP_n} - \frac{1}{DP_o}}{A \times 24 \times 365}\Big) \exp\Big(\frac{13350}{T_{hst} + 273.15}\Big) \tag{1.2}$$

where, A is an experimentally determined pre-exponential factor

T_{hst} is the hottest-spot temperature on the winding obtained from thermal modeling of transformer, K.

Currently, some work is being done on thermal upgrading of paper to delay the inevitable ageing without compromising its dielectric strength. In order to understand more about the thermal upgrading of Kraft-paper, one can be redirected to [35] for further information.

1.1.2 Insulating oil

As discussed previously, insulating oils are the most vital components for ensuring proper thermal and electrical resistance within the transformer to ensure safer operations. The conventional hydrocarbon-based mineral insulating oils have enjoyed immense popularity as electrical insulates in the past six decades. Due to its petroleum-based origins, these are rich in alkanes, alkenes and aromatic components in both straight and branch configurations as shown in Fig.1.4 [5, 36, 37]. These oils are processed as per IEC 60296 to posses high breakdown voltage potential, lower dynamic viscosity, weaker thermal conductivity and slower deterioration rate. The oil quality in an operational transformer is then monitored as per IEC 60422.

Currently the two types of acceptable mineral insulating oils are namely, naphthenic and paraffinic that is distinguishable by the concentration of paraffin content within it. The omnipresent paraffinic content is mainly responsible for the flow retardation, especially below -25°C, thus necessitating careful mixing of naphthenic and paraffinic oils while proposing a suitable insulate for transformer application. Some of the manufacturers providing a competitive market for insulating oils are Shell, Naynas,
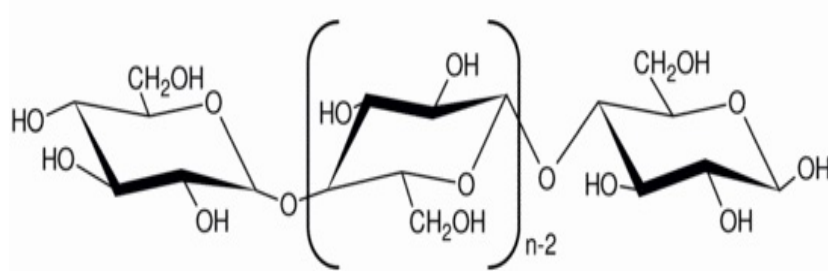
(a) Molecular configuration of a typical anhydrous-1,4 β D-glycopyranose chain as the backbone of cellulose-based insulating materials [1]
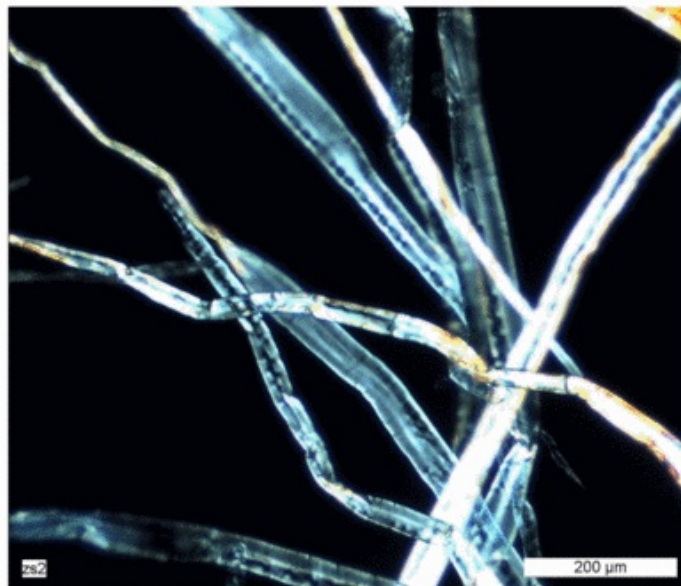
(b) SEM image of the labyrinth of microfibers within a single layer of a typical cellulose insulate [2,3]

Figure 1.2: Molecular and microscopic view of a typical cellulose insulate

Petro Canada, Labrolac etc.

As discussed previously, the by-products obtained from cellulosic decomposition is dissolved in the surrounding oil hence affecting the thermal and electrical resistance of oil. The end of oil's useful-life due to relative ageing is indicated by various parameters such as oil acidity, corrosive sulfur, dissolved gases, oxidation stability and moisture adherence. Despite so many advantages, the non-biodegradability, lower fire point and
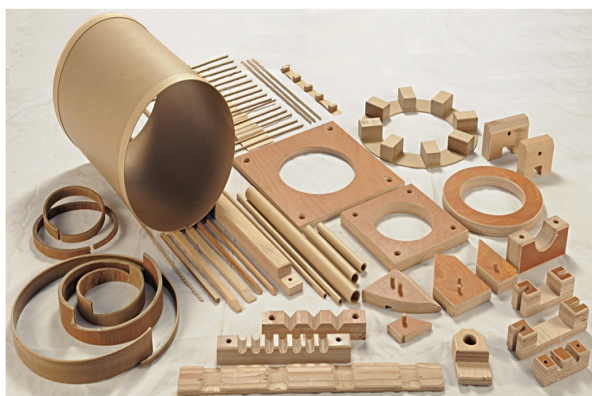
(a) Application of pressboard insulation
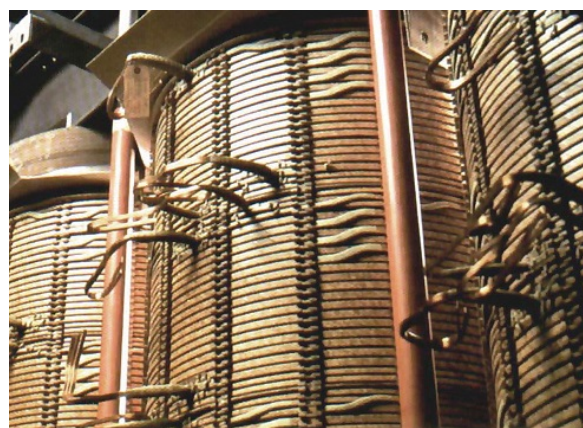
(b) Application of paper insulation

Figure 1.3: Various applications of cellulosic insulation in transformers [4]

low moisture adherence of mineral oil is particularly disadvantageous for the transformer operation and life-management [2, 3, 7, 11, 36, 38, 39].

At this point, it must be mentioned that the transformer oils are although naturally hydrophobic, yet very low quantities of water can be found associated (dissolved) within the oil. It is later discussed in this very chapter as how this moisture increases despite the initial reluctance and its role in transformer failure.
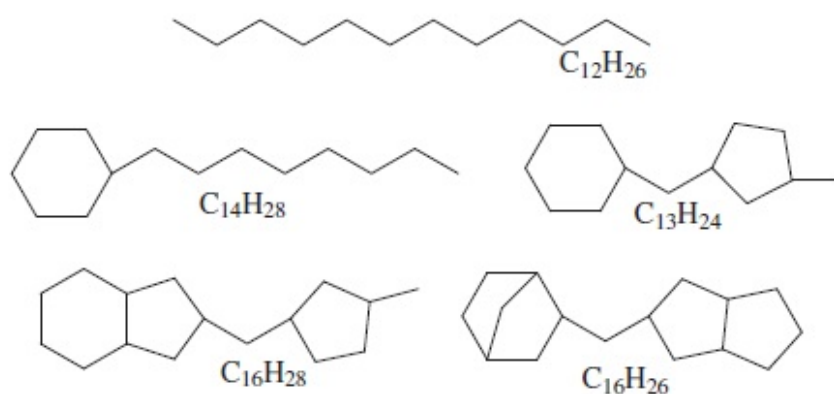
Figure 1.4: Various molecular arrangements of naphthenic oil based on permutations between chain configuration and functional groups obtained from sophisticated instrumental analysis [5]

1.2   Transformer Failure Analysis

A typical power transformer is always manufactured in accordance with the grid requirements.It is also expected that with cautious assessment, a transformer can operate successfully for about 40-45 years ideally [40]. On the contrary side, fluctuating electrical, thermal and mechanical stresses encountered during daily operations within the unit can lead to various internal and external causes that are responsible for the ultimate failure of a power transformer.

The chances of an external damage due to structural distortion of tank, gasket or sealing etc., is relatively lower due to the advanced manufacturing strategies [8, 19, 22, 27, 28]. On the other hand, moisture, oxygen and heat induced faults such as overheating, oil contamination, ageing, arcing etc., contribute more towards the loss of useful life in transformers and more cautiously diagnosed to improve the operational efficiency of the equipment [21, 23, 34, 41, 42].

Therefore, one can conclude that the strategic planning of transformer diagnostic research during manufacturing and commissioning can offer a reliable remaining life assessment scheme (RLA) of the equipment. Moreover, in order to obtain such schemes it is imperative to correlate the underlying factors and propose a cost-effective and energy efficient solution as given in Fig.1.5.
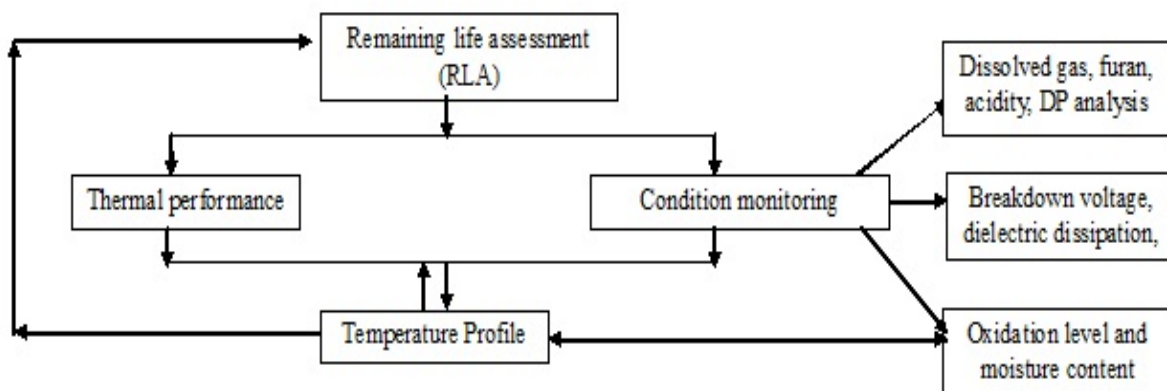
Figure 1.5: Transformer life assessment methods and significant parameters

While the internal heat can be regulated by monitoring the thermal performance of a transformer [24, 29, 40, 43–46], the moisture presence within transformers, partially regulated by drying, is still bound to increase gradually over the operational life-time of transformers [1, 2, 7, 8, 11, 47, 48].

Various sources suggest that an excess moisture within the transformers can decrease the inception voltage for partial discharge, exacerbate the dielectric strength, accelerate the insulation aging rate and aggravate the risk of premature transformer failure. Therefore, a reliable technique for moisture assessment within the utility can be the key to ensure longer in-service life, improved performance and maximum efficiency of the transformer [8, 11, 34, 38, 39, 47, 49, 50].

1.3   Moisture in Transformers

Previous investigations on prominent moisture sources within the encapsulated units suggests that there are three zones of moisture contamination within transformers as discussed below [2, 8, 11, 22, 25, 28, 41, 51]:

1.3.1   Residual water from insufficient drying

To isolate the most moisture-prone zone, solid insulation is distinguished into three parts viz. thick, thin "hot" and thin "cold" structures. The thick parts mainly comprise of wood-based supports at the bottom and top of the windings, lead supports, load tap changers, Bakelite cylinders etc. and contribute to almost 50% of the total insulation mass. Due to its high thickness, the entrapped moisture (2-4%) can take longer drying durations as compared to conventional paper or pressboard insulation.

Since this moisture is retained within the structural components as a result of insufficient drying, it is bound to come out gradually and contribute to the total water content within the utility.

Although the thick structure contribute towards half of the total weight of insulation, most of the *active* moisture resides within the thin "cold" structure containing pressboard-based spacers, barriers and end-caps. These materials are strategically placed within the windings to isolate two consecutive coils and are separated from the electromagnetic core through barriers. Moreover, since they operate at the bulk oil temperature, the moisture contributions from pressboard is generally low but not neglected.

On the other hand, the thin "hot" structure comprises of Kraft/Crèpe paper for insulating and isolating the conductor strands as shown in Fig.1.3(b). Since it operates at winding temperature, a mechanical deformation along with the physico-chemical changes in paper is also visible at the hot-spot temperature, where the localized heat raises the average winding temperature. With proper oil circulation, the thermal ageing can not only be delayed but also the moisture can be transported away from the bulk source in to less-active zones where it can be safely measured [24–26, 52, 53].

1.3.2   Atmospheric ingress through leaky seals/open breathers

Moisture contamination through atmospheric ingress is a three-step process, which includes sorption from atmosphere due to direct exposure of insulation driven by a thermal gradient, Knudsen diffusion of moisture within the micro-fibrils due to concentration gradient, and viscous air flow into the transformer during on-site repair/re-installation works due to difference in water vapor pressure on either sides [25, 28].

Moisture sorption in transformer insulation can be a twofold process i.e., absorption of water vapor within multiple layers of insulation, and adsorption of water vapor molecules to the free surface of cellulose and loose attachment to oil molecules. Unlike the cellulosic material, where the polar hydroxyl groups along the polysacchride chain causes hydrophilic nature, the aromatic content within oil controls its water affinity that in-turn is temperature dependent.

On the other hand, molecular or Knudsen diffusion has the least contribution in moisture ingress from atmosphere due to the low concentration gradients between surface moisture and capillary condensates. However, vast difference in water vapor pressure between transformer tank and external environment can create an inflow of moisture into the insulation thus leading to an ultimate transformer failure.

1.3.3 Accumulation from accelerated ageing

As discussed earlier, accelerated insulation ageing is the irreversible physico-chemical deterioration of dielectric materials due to the presence of moisture and oxygen under elevated thermal excitation [23, 41, 42, 54, 55]. Unfortunately, paper/pressboard ageing is concomitant to the internal water generation and subsequent loss of useful-life in electrical insulates. The cellulosic-bond cleavage leads to the generation of carbon oxides (CO, CO_2), free oxygen radical and complex furans thus resulting in free water formation [1, 23, 28, 56].

Ref. [57] reported an absolute 2% water generation within the transformer through DP correlations, whereas upon reaching 400 DP, as suggested by [32], shows a much lower increase of approximately 0.4% in the total water content. More interestingly, some practical experiences given in [58] reports an increment of 1.5-2.8% in water concentrations at some particular zones on the winding.

Overall it can be said that ageing will result in chain scission, hence reducing the DP values and furan formation that are directly related to localized and overall water contributions within the transformer. Proper quantification of these parameters is still a challenging task because ageing experiments are most performed within controlled conditions unlike the actual transformer that suffers from multiple stresses simultaneously at all the unknown locations. Moreover, it is neither possible nor advisable to propose a mathematical model for moisture generation through ageing based on constant conditions and must contain some experimental basis.

It was never the intention of this research to propose such models purely on the basis of theoretical calculations since performing such experiments was beyond the capacity of this thesis. Instead major contributions were made to trace the moisture migrations within the oil-filled power transformers in order to pin-point the location of potential hazard and hence save the transformer from an abrupt failure. For such an effective conditioning monitoring scheme, suitable life assessment models must be proposed in accordance with identification and measurement of winding hot-spots through proper multi-physics models.

1.4 Scope and Objective of Thesis

In order to propose models for understanding the mechanism of moisture drift within the transformer through on-line or off-line diagnostic methods, most of the prevailing literature addresses only one aspect at a time. These techniques either use relative humidity assessment, dielectric measurements to contemplate the remaining moisture within an insulate (either paper or oil) at any given time during the course of transformer operation. Moreover, except for the practical experiences using relative saturation vs load measurements in operational transformer, not much has been published about the moisture dynamic mechanisms in either oil or paper/pressboard. Also, material uniformity and strategically controlled conditions have always led to a series of assumptions that may or may not be completely accurate.

The relative humidity sensors assume that with load variations, top-oil temperature changes exponentially and it is sufficient to calculate the actual water concentration in oil. It also assumes that regardless of the load variations, the winding temperature is more or less constant and that all calculations for moisture in paper must also be done on top-oil temperature. After some suggestions were made by [24,59], some reports have surfaced where all calculations are done on bottom oil temperature [2,29].

At this conjuncture what should have been an interesting prospect about the effect

of mass-averaged (MA) oil temperature has been completely ignored.

Unfortunately, more sophisticated techniques using dielectric spectroscopy or voltage-current measurements have ignored the axial winding temperature completely and assume that they do not play any role in oil-temperature variation. This gives us a huge window of opportunity to explore, what if the winding temperature is as variable as the oil temperature? This would mean that rather than considering a constant heating source within windings, we are assuming that it changes as per the temperature and load variations.

Now, a transformer consists of several participating parts where some are heat generating while some are heat dissipating. Thus, in order to pinpoint the location of fault would mean that our desired area of investigation must be much closer to the actual winding and not at the far away tank walls. Therefore, in order to propose an elaborate mechanism of moisture dynamics within the oil-filled power transformers, some specific objectives were outlaid:

1. Understanding the mechanism of moisture migrations within oil-filled power transformer and analyzing the existing techniques for its measurement.

2. Understand the physics behind temperature rise under variable load conditions and analyze available techniques for temperature assessment.

3. Develop reliable thermal models to trace the effect of load variations and convection patterns on the solid insulate.

4. Locate the most failure-prone zone in transformer windings using thermal model so that appropriate hottest-spot temperature can be calculated.

5. Use predictive models to determine the effect of axial temperature rise in windings on the overall moisture change in transformer by either moisture-in-oil models or using non-isothermal diffusion equations.

6. Propose a quantitative model for moisture migrations in solid insulates with respect to the various influential parameters.

7. Propose a quantitative model for moisture in oil with respect to the axial thermal variations, loading patterns and ambient temperature.

1.5   Thesis Outline

To provide an enhanced understanding over the proposed topic of research and to enable and encourage the reader to understand and explore further on the many aspects of moisture dynamics within transformers, this thesis has been arranged as follows:

Chapter 2 is a survey on the existing moisture measurement techniques and their correlation with the thermal behavior of transformers. Such an analysis shall be very helpful in justifying the proposed objectives and observations obtained within the framework of this thesis.

Chapter 3 is a collection of the proposed models broken into two sub-modules where one can quantify the temperature rise in transformers and the other one is capable of assisting the moisture dynamics mechanism within individual insulates and consolidated transformer tank. Since extensive computational efforts have been taken to establish these models, in-depth analytical understanding of the associated software and computation technique is also presented for assisting the reader. In order to justify the accuracy of such models over restricted memory servers, some senstivity models are also discusses that shall enable the reader to extrapolate it over high-capacity computer and over highly-complex transformer geometries.

Chapter 4 is a collection of results obtained from the detailed thermal modeling of power transformers. A series of parametric investigations have been carried out in this section to quantify their influence on axial temperature variation. According to the objectives stated earlier, the expected conclusions from this study are two fold, where

the reader not only understand the effect of variable heat source on oil temperature behavior, but also becomes aware of the moisture-patterns to be expected while carrying out a diagnostic research.

Chapter 5 is the first-ever attempt of summarizing an entire moisture-dynamic mechanism based on its respective operation. This chapter not only provides the basis for understanding moisture migration through solid insulation by the virtue of diffusion, but also correlates variable temperature profiles obtained from the dynamic thermal models thus producing a more reliable and realistic understanding of transformer condition.

Chapter 6 summarizes the most important observations and explorations made from the present work in order to provide a holistic approach of the entire moisture dynamics model in oil-filled power transformers. It is but the intention of the author to contribute in a way such that future researchers can adopt the philosophy of moisture migrations discussed in this work to apply and enhance the existing knowledge on the subject matter.

Chapter 2

LITERATURE REVIEW

The present chapter details an in-depth analysis over the moisture and temperature measurements techniques within oil-filled transformers. Section 2.1 presents an overview of the available techniques for moisture measurement in transformers. Section 2.2 brings out the basics of internal heat generation within operational transformers and its association with the oil/winding temperature rise followed by the techniques to determine the thermal variation. Section 2.3 proposes the methodology to analyze the temperature rise patterns and further correlate them with moisture movement behavior in individual insulates. The chapter ends with an explanation on the influential parameters and its relevance through the proposed methodology over a partially-coupled model for moisture prediction within an oil-filled power transformer.

2.1 Moisture monitoring in transformers

As discussed earlier, continuous monitoring of moisture concentration within transformers is an imperative step towards improving the transformer integrity. Interestingly, transformer "wetness" is a relative component and varies with the physical rating of the equipment. According to some international standards [60],

allowable moisture within an oil-filled unit is distinguished below [41]:

1. Rated voltage <69 kV, maximum moisture allowed in oil is 55 ppm and paper is <3%.

2. Rated voltage between 69-230 kV, maximum moisture allowed in oil is 30 ppm and paper is within 2-3%.

3. Rated voltage >230 kV, maximum moisture allowed in oil is 15 ppm and paper is <1.25%.

Typically, there are two direct ways to determine the moisture content in oil directly, namely off-line (lab based) and on-line (sensor based). The traditional coulometric Karl Fischer Titration (KFT) is a lab-based technique that requires an oil sample withdrawal in order to determine the absolute water content in oil using chemical and electrochemical reactions. Typically, an ester is formed upon chemically reacting sulfur dioxide (SO_2) with methanol (CH_4) under an inert nitrogen (N_2) base. An intermediate stage allows the production of iodine (I_2) at the electrode end which is later consumed by the ester through oxidize thus producing an absolute concentration of inherent moisture (H_2O) [61].

Although this technique is widely acceptable, various studies have jointly agreed that besides sampling and instrumental error a considerable time lag between sample withdrawal and assessment can introduce unwanted contamination thereby restricting its application to lab-based investigations only [8, 11, 38, 41].

The commercially available humidity sensors can assist in predicting the moisture-in-oil concentrations continuously through on-line measurements. These modern day sensors are microprocessor-based transmitters containing a very thin polymeric film, which registers a change in its capacitance with moisture variation in oil. It measures the instantaneous water concentrations in terms of either water activity or relative saturation.

Water activity indicates the internal energy of dissolved moisture in oil and depends on the moisture potential and temperature of oil. Similarly, moisture potential is an indicator of thermodynamic condition of moisture in oil and can be expressed mathematically by Eq.2.1 [62].

$$\psi = \frac{RT}{M_w} \, ln(a_w) \tag{2.1}$$

where, a_w is the dimensionless water activity varying within a range of 0-1,

ψ is the moisture potential per unit mass of oil,

R is the universal gas constant, 8.314 J/(mol.K)

M_w is the molecular weight of water in oil, 18(g/mol)

and T is the absolute temperature in K.

On the other hand, relative saturation of oil is the measure of actual moisture dissolved in oil against its solubility limit over a wide temperature range. One can expect a correlation between water activity and relative saturation to obtain an absolute moisture concentration in oil (ppm) using a solubility coefficient. It was observed on several occasions that absolute moisture is rather prone to aging effects and may lead to measurement discrepancies. Therefore, one must work on the change in saturation level within the transformer to obtain an acceptable condition for moisture measurements in both paper and oil.

Moisture measurements in oil is easy since it is highly accessible from all the prime locations in a transformer. On the other hand, paper is strictly restricted to windings and therefore inaccessible throughout the operational duration of transformer. One can have access to paper or pressboard insulation directly only when the transformer is detached from the active network and allowed to cool down for a considerable period of time. Such intrusive measures for moisture-in-paper has insisted many researchers over the years to propose an indirect yet reliable method of estimation.

The traditional yet indirect methods for moisture in paper measurements uses either equilibrium charts or dielectric response measurement in time and frequency domains. Since moisture in paper is more significant than oil, a detailed discussion in the following subsections will allow the reader to understand the existing research gaps and relevance of the proposed solution. Alternatively one can suggest the use of dielectric response based measurements (return voltage, frequency domain, polarization current, dielectric dissipation) to correlate the dielectric properties of paper/pressboard with possible moisture contamination.

Again, all these techniques neglect the prime driving factor responsible for moisture migration i.e., axial winding temperature [8]. As a result, although oil moisture may reflect within permissible limits, there is a continuous risk of overestimating the paper insulation that is otherwise drier than expected. Since paper-water contamination is one of the catalysts for insulation degradation, it is imperative to discuss in-detail the available techniques in order to identify the possible research gaps.

2.1.1   Equilibrium Charts

The equilibrium charts are a set of partition curves that allows relative moisture measurement in an oil-paper-air complex under isothermal condition. These charts are based on thermodynamic equilibrium assumption within the insulation complex. It requires the insulation system to achieve maximum entropy in order to establish the desired equilibrium. At this stage, the moisture distribution within the insulate complex will depends upon the water solubility of an individual material.

As the name suggests, an equilibrium condition can only exist within the insulation complex when individual materials are at similar temperature and any chemical or thermodynamical change cease to exist. The determining time constant for such a system will exclusively depend on the material property and exposed temperature.

Creating thermodynamic equilibrium conditions in an operational transformer is

highly unlikely. Practically, it is only possible when the utility has been detached from the network and allowed to achieve an equilibrium with the ambient surrounding. A similar condition can also be reached if the transformer continues to operate at a constant load for a preferably long period of time.

Practically, such conditions rarely exist for an operational transformer. During its service time, even within a day, the load pattern varies thereby leading to disruption of the so-called thermal equilibrium state. These swift temperature movements allows the moisture to change its direction of migration.

Also since a moisture equilibrium is slower than a thermal equilibrium, it is imperative that a proper understanding of the transformer condition prevails prior to the use of equilibrium charts.

Over the years, various researchers have proposed several modifications for these equilibrium charts in order to relate moisture movements with the relevant operation. In order to obtain the dew point of an inert gas enveloping the core-coil assembly, [63] published the first-ever set of equilibrium curves using cotton fiber and extrapolated its values to suit Kraft paper insulation as shown by Fig.2.1.

In the same work, moisture migration within a temperature range of 10-110°C were studied using heat induced water vapor pressure changes for non-impregnated fibers. Apart from the conclusive design modifications, it also proposed that the same data can be extrapolated for Kraft paper if the moisture range is increase by 1.7 times irrespective of its impregnation condition.

Moreover, the data reported in the same work were indistinguishable for the sorption direction and hence highly debatable.

A summary of the same work performed years later by [33] disapproves of the moisture absorption factor proposed in [63] by experimental verification. The exhaustive investigations in this work reported that the factor cannot exceed a value of
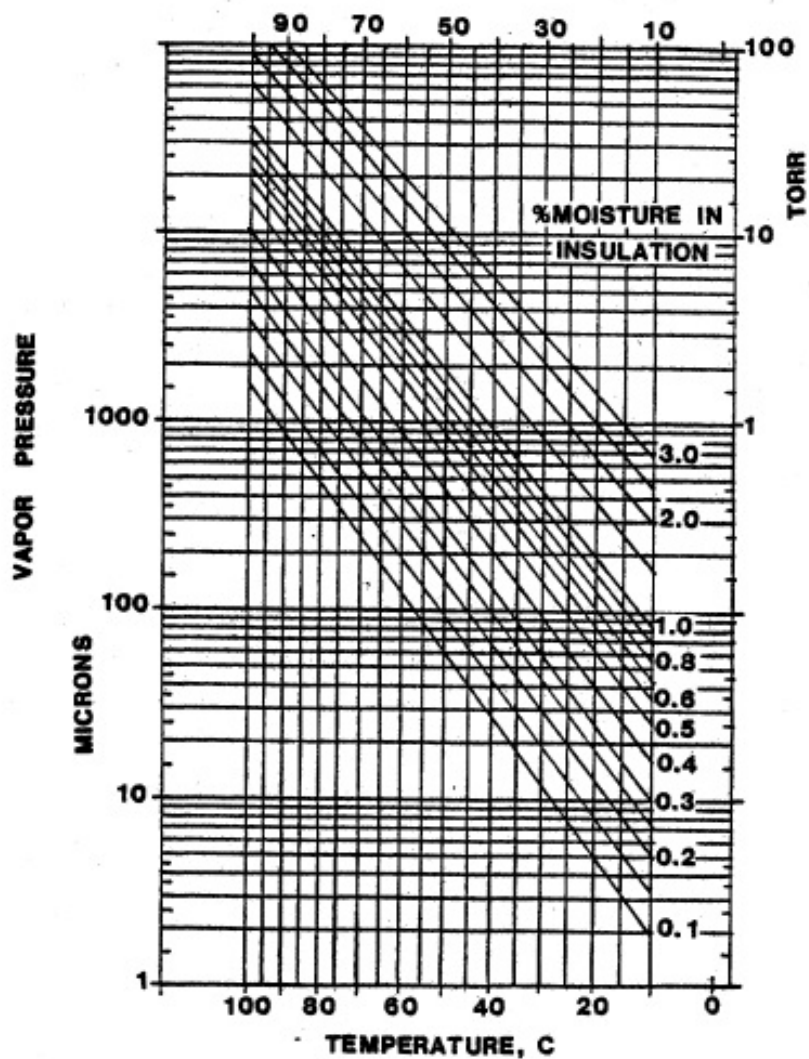
Figure 2.1: Piper charts for vapor pressure measurements. Taken from [6]

1.3 for textile polymers within a verified temperature range of 30-90°C.

In order to obtain moisture sorption behavior for a typical Kraft paper insulation, [64] carried out some exhaustive experimental investigations to reproduce transformer drying operations. In this paper, water absorption for Kraft paper insulation within a temperature range of 25-100°C were reported. The data was plotted in the form linear relationships between water concentration and equilibrium vapor pressure using Freundlich's isotherms.

Ref. [7, 11, 65] reported that the equilibrium charts proposed by [64] shows lower estimates for moisture-in-paper concentration because of the variation in absorption factor mentioned above. Experimental investigations by [16] suggests that practical establishment of an equilibrium between water vapor pressure in impregnated media with the ambient surrounding is relatively challenging and hence restricted.

Ref. [7] have proposed, what is currently known as the universal equilibrium chart for transformer insulation during drying operations. The primary assumption in this work suggests a thermal equilibrium between oil and paper due to non-fluctuating temperature of individual insulates. Fig.2.2 shows the typical drying curves for oil-paper system assuming equilibrium conditions.
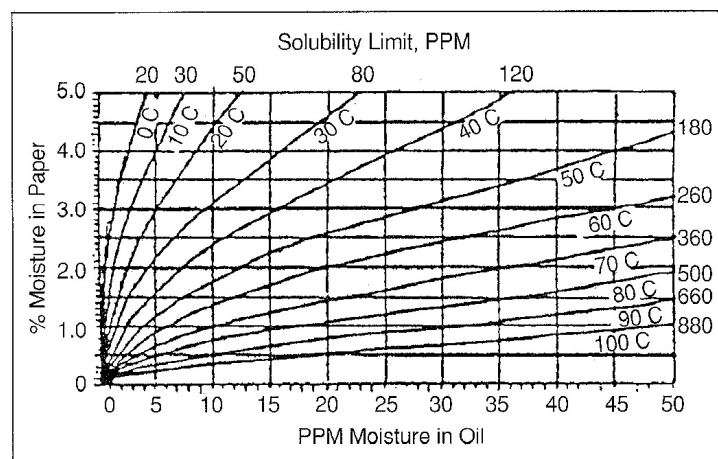
Figure 2.2: Oommen's curve for moisture equilibrium in oil-paper insulation complex [7]

In this case, partial water vapor pressure data can be obtained for paper using relative humidity measurements. Simultaneously, moisture concentration in oil is obtained using relative saturation data and converted as a function of relative humidity. Upon combining humidity and saturation data, one is expected to obtain absolute moisture in oil-paper systems under thermal equilibrium conditions similar to a typical drying operation.

In the above context, relative saturation is defined as the ratio of absolute moisture dissolved in oil to its solubility as shown by Eq.2.2.

$$RS_{oil}(\%) = \left(\frac{C_d}{C_s}\right) \times 100 \qquad (2.2)$$

where C_d and C_s represents dissolved and soluble moisture in oil (ppm) and RS_{oil} is the relative saturation of oil (%).

At this point, its must be noted that though hydrophobic initially, the moisture solubility in oil increases exponentially with temperature using an Arrhenius form according to Eq.2.3 [11, 26, 38].

$$\log C_s = \left(\frac{A}{T}\right) + B \qquad (2.3)$$

where constants A and B depends on the aromatic content of oil at an absolute temperature, T(K). Different coefficients have been proposed by various researchers as given in Table 2.1. The effect of these coefficients have been shown by Fig.2.3.

Table 2.1: Experimentally estimated constants for the water solubility in mineral oils as shown by Eq.2.3

Constants	Oommen [7]	Griffin [25]	Cigre [58]
A	7.42	7.09	7.3
B	1670	1567	1630

The relative humidity (RH) for oil is similar to its relative saturation (RS), and a strong indicator of the moisture mixing ability in oils. However, in case of air, it is defined as the ratio of partial water vapor pressure to saturated water vapor pressure under isothermal conditions as shown by Eq.2.4 respectively [7, 8].

$$RH_{air}(\%) = \left(\frac{V_p}{V_s}\right) \times 100 \qquad (2.4)$$

where V_p and V_s represents the partial and saturation water vapor pressure
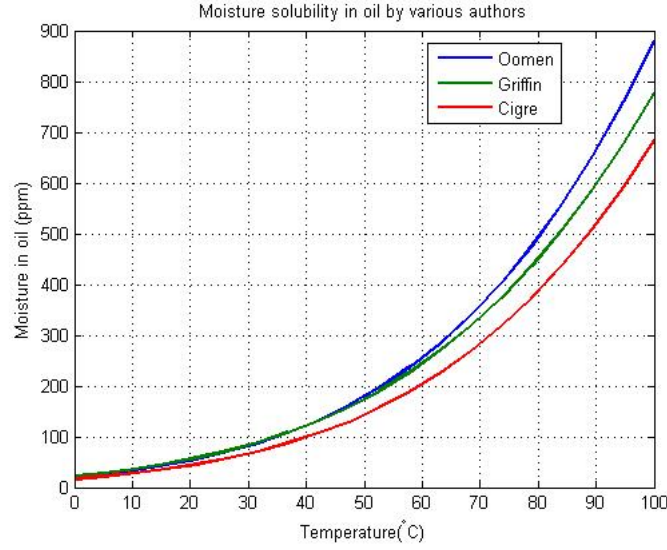
Figure 2.3: Estimation of water solubility in mineral oils using Eq.2.3 with coefficients proposed in Table 2.1

respectively, and RH_{air} is the relative humidity of air(%). It is a well known fact that the saturated vapor pressure of water in air is a strong function of temperature. There are various empirical correlations available to assist with the estimation of saturated vapor pressure values. Using a known RH_{air}, [8] suggested that the saturation vapor pressure of water in air is a strong function of temperature and can be determined using Magnus-Tete formula as shown by Eq.2.5.

$$V_s = 6.107 \times 10^{\frac{aT}{b+T}} \tag{2.5}$$

where, temperature (T) is in °C and the constants, a and b are reported as 1.5 and 235 at zero temperature. The saturated vapor pressure is calculated in hPa and requires to be converted into mmHg for further use. Moreover, the constants reported for this particular equation are highly debatable for a non-zero temperature using extrapolation. Ref. [12] suggested that the partial vapor pressure of water in air should be calculated using Keenan-Keyes correlation as shown by Eq.2.6. This formulation finds more application while modeling of vacuum drying of transformer insulation prior to oil impregnation.

$$log_{10} \frac{V_p}{V_c} = \frac{-T_c}{T + 273.16}\left[\frac{a + b \times T_c + c \times T_c^{3}}{1 + d \times T_c}\right] \quad (2.6)$$

where, T_c is the critical temperature of water vapor, 374°C, V_c is the critical pressure of water vapor, 1.65807×10^5 mmHg, a,b c and d are dimensionless constants with reported values of 3.2438, 5.868×10^{-3}, 1.1703×10^{-8} and 2.1878462×10^{-3} respectively.

For a typical drying operation, when the moisture in paper and surrounding air is in equilibrium with each other, the moisture content within paper can be calculated by the empirical correlation given in [66] as shown by Eq.2.7.

$$C_m = 2.173 \times 10^{-7} \times V_p^{0.6685} \times exp\left[\frac{4725.6}{T + 273.15}\right] \quad (2.7)$$

where,C_m is the local equilibrium moisture concentration in paper on percentage dry weight basis. If one can directly calculate the moisture concentration in paper using equilibrium charts assuming all conditions were satisfied, they can actually use Eq.2.7 to calculate the partial vapor pressure of water in paper using an algebraic inversion as given in Eq.2.8.

$$V_p = 9.2683 \times 10^9 \times C_m^{1.4959} \times exp\left[\frac{-7069}{T + 273.15}\right] \quad (2.8)$$

In the above set of equations, moisture in oil and paper can be defined as per Eq.2.9 and 2.10 respectively.

$$C_{oil} = \frac{M_{H_2O}}{M_{oil}} \quad (2.9)$$

$$C_{paper} = \frac{M_{H_2O}}{M_{paper}} \quad (2.10)$$

The moisture concentration in oil is given by μg/g through KFT and in PPM while using on-line sensors. Similarly, moisture in paper is reported mostly in % (gH$_2$O/g$_{paper}$)

and extensively converted into mol/m^3 for computational purposes.

During drying, when the temperature of external air (or oil) is higher than that of paper (or pressboard), the thermal gradient causes variable vapor pressure zones in paper and air. As soon as a temperature homogeneity is achieved, similar saturation conditions prevail within paper and air. On the other hand, when the transformer is operational, water solubility changes instantaneously because of the transient temperature series. In this case the moisture determination within transformers not only depends on the hotter material but also on the concentration gradients.

It is evident so far that although isothermal conditions are strictly required for some moisture concentration prediction, yet a realistic model will prevail only when instantaneous temperature can be monitored. One of the biggest drawbacks of moisture measurement using Eq.2.7 is its inefficiency to retain accuracy under extreme humidity levels. Although it can evaluate the equilibrium moisture in paper/pressboard, its precision is debatable due to different sorption behavior of Kraft paper and pressboard materials. Moreover, choice of surrounding media (i.e.,air or vacuum) plays a significant role in establishing sorption isotherms, thereby restricting the use of above equations only to oil-paper-air complex [28]. The proposed charts are also restricted by the desire to establish an ultimate thermal equilibrium condition prior to its use. It has already been proved that such conditions are rarely attainable in transformers, except during shutdowns.

In order to overcome this challenge, moisture sorption has been studied as a mass transfer problem rather than a thermodynamic condition by various researchers. The migration of moisture from paper to oil during drying operations is a classic example of Fick's laws assuming that the thermal transients significantly shift the so-called moisture equilibrium.

Early experiments by [67] shows that moisture content in paper can be modeled using Fick's first law in order to calculate the molar flux (j) across the insulation thickness

using a one-dimension form as per Eq.2.11.

$$-j = D\left(\frac{\partial C_m}{\partial x}\right) \tag{2.11}$$

where, x is the thickness of insulation, m

C_m is the local moisture distribution across the insulation, mol/m^3

D is the constant diffusion coefficient of moisture in paper, m^2/s

There are two major limitations of this theory. Firstly, the experiments were based on permeation of water within the multi-layers of Kraft paper. These experiments assume localized distribution of water across the insulate thickness instead of average distributions [68]. Secondly, it was performed under tightly controlled conditions, where the diffusion coefficient (D) was more or less a constant.

As soon as these limitations were realized, transient moisture diffusion was modeled according to Fick's second law as per Eq.2.12, where diffusion coefficient depends on both the concentration and temperature of the process.

$$\frac{\partial C_{(x,t)}}{\partial t} = \frac{\partial}{\partial x}\left[D(C,T)\frac{\partial C_{(x,t)}}{\partial x}\right] \tag{2.12}$$

where, $C_{(x,t)}$ is the spatial-temporal moisture discretization across normalized thickness (x) and a non-dimensional time (t).

If a constant diffusion coefficient is assumed, Eq.2.12 can be solved using Fourier series solution. Although the number of diffusing sides must be known in order to obtain an acceptable convergence. Eq.2.13 and 2.14 shows the two proposed schemes for moisture discretization assuming single and double sided exposure respectively [69].

Single-sided diffusion:

$$C_{(x,t)} = c_m - \frac{4(c_i - c_m)}{\pi}\sum_{n=0}^{\infty}\left[\frac{(-1)^n}{2n+1}e^{-t\times D\times B_n^2}cos(B_n x)\right] \tag{2.13}$$

Double-sided diffusion:

$$C_{(x,t)} = c_m - \frac{4(c_i - c_m)}{\pi} \sum_{n=0}^{\infty} \left[\frac{(-1)^n}{2n+1} e^{-t \times D \times B_n^2} cos\left(B_n \left(\frac{x-1}{2l} \right) \right) \right] \qquad (2.14)$$

where, c_i and c_m are the initial and equilibrium moisture in paper, mol/m³

n is the number of interactive layers (n=1 for single sided, n=2 for double sided)

x is the thickness of insulate, m

t is the discretization time, s

B_n is the reciprocal constant of thickness [13, 69, 70].

The constant B_n can be defined as by Eq.2.15 and 2.16 for single and double sided diffusion respectively as follows [69, 70]:

Single-sided diffusion:

$$B_n = \frac{n + 0.5}{l} \qquad (2.15)$$

Double-sided diffusion:

$$B_n = \frac{\pi(2n+1)}{l} \qquad (2.16)$$

The series solution along with its suitable coefficients given by Eq.2.13 and 2.14 with respect to the exposure sided will provide an inverse bath-tub type graph for local concentration over a localized thickness. It may be enough for single layer-homogeneous samples but certainly not sufficient to decide the intra-layer moisture within multilayerd components as Kraft paper and pressboard. Also, it is not possible to apply Fick's second law of diffusion in a continuous manner with continuously changing diffusion coefficients.

Most of the scientific literature available for moisture-in-paper models using Fick's second law proposes an experimentally derived diffusion coefficient [11,16,67]. Apart from the conventional techniques reported in [2,12,66], some authors have also used dielectric measurements to determine the diffusion coefficient of various impregnated and non-impregnated insulates [8,11]. An excellent review of various experimental and theoretical techniques to obtain diffusion coefficient for oil-impregnated and non-impregnated paper is available in [71,72].

There are two vital informations available by pursuing the existing scientific literature on determination of diffusion coefficients. Firstly, that the diffusion coefficients vary with the nature of material and most importantly its impregnated condition. And secondly, that there is absolutely no way to propose a theoretical diffusion coefficient for paper or pressboard material without experimental validations.

More explicitly, a lot of these available coefficients are for oil-impregnated paper and none have been proposed so far for an impregnated pressboard. Now interestingly, when the transformer insulation is immersed in oil after the initial drying, the paper does actually absorbs most of the oil which justifies the oil-impregnated diffusion coefficients. But so does the pressboard, which is still believed to be behaving like a non-impregnated insulate despite coming in contact with oil.

This leads one to wonder what could possibly be the effect of such assumption on the overall moisture performance within transformers and especially on drying operations? In order to find the solution to this problem, exhaustive studies were conducted using the available diffusion coefficients in complex drying conditions that shall be discussed later.

In conclusion, one can say that moisture equilibrium charts are strictly confined to drying operations only. Although much about its parametric influence is yet to be discovered. In case of operational transformers the fast moving transients of temperature and moisture makes it impossible to use the conventional Fick's second law continuously.

Most of the moisture distribution in an operational transformer must therefore be studied according to the conventional mass conservation equations where solubility becomes the dominant parameter. Unlike the existing dielectric response techniques that ignore the axial winding temperature, new methods must be developed to isolate the thermal gradients in paper, winding and oil. New mass conservation equations must be developed based on such improved models. Moreover, these models should be strictly in alignment with the fluctuating load patterns and transformer cooling conditions in order to realize the hot-spot temperature and average temperature rise for further application.

The axial temperature primarily changes with transformer loading and oil flow patterns. The choice of external(air or water) and internal coolant(oil, air or gas) depends on the physical size and rating of the transformer. Additional parameters such as loading pattern, winding configuration, internal heat generation etc., also affects the cooling scheme of transformers.

Nevertheless, a complete description is available in the upcoming section on the various aspects of heat generation and dissipation in transformers. Such an analysis can enable the reader to correlate winding and oil temperature rise with various thermal performance aspects and hence propose reliable models for moisture measurements in transformers at the crucial locations.

2.2 Transformer Thermal Performance

In order to evaluate the thermal performance of transformers, it is imperative to understand the source and magnitude of internal heat generation. It is a well known fact that the internal heat is a strong function of the total transmission losses. These losses can be originating from either the electromagnetic core or conductor windings. Traditionally, the factors such as hysteresis losses, joule heating and eddy current losses contribute significantly towards the internal heat generation [10, 17–19, 73, 74].

The core of a transformer is essentially a ferromagnetic material capable of generating an electromagnetic field. Present day transformer cores are made of soft iron to minimize the operational losses and restrict the magnetic flux leakage though strategic lamination. It is possible to correlate the total power losses with structural integrity of the core material using Eq.2.17 [75].

$$P_c = \kappa_h {B_m}^2 f + \kappa_e {K_h}^2 {B_m}^2 f^2 {t_c}^2 n \tag{2.17}$$

where, P_c is the total core loss, W

κ_h is the material coefficient of hysteresis losses

κ_e is the material coefficient of eddy losses

B_m is the maximum magnetic flux density, Tesla

f is operating frequency of transformer, Hz

t_c is the thickness of each laminate, m

and n is the number of laminates in a typical core.

The core losses contributes to less than 5% losses in new transformer thereby making them neglected during thermal assessments. This is because of its strong ability to restrict the magnetic flux leakage. On the other hand, winding or load-losses are the primary source of temperature rise due to resistive heating of winding and magnetic flux leakage due to Foucault (eddy) currents [10, 18, 19, 29, 40, 52, 73, 74, 76–78].

The Ohmic or Joule losses occurs due to the resistive heating of the winding and depends on the current density normal to the conductor surface as shown below:

$$P_{w,o} = \frac{1}{2\sigma} \int {J_s}^2 dV \tag{2.18}$$

where,σ_e is the electrical conductivity, S/m

J_s is the surface current density, A/m^2 dV is the elemental volume, m^3

In a quasi-static electromagnetic field, the Maxwell equations can estimate this current density within the functional domain as per Eq.2.19.

$$\nabla \times \frac{1}{\epsilon}(\nabla \times \vec{A}) = \vec{J_s} - \sigma_e \frac{\partial A}{\partial t} \tag{2.19}$$

where,ϵ is the magnetic permeability, H/m
A is the transient magnetic vector potential, V.s/m

Furthermore, Eq.2.20 can calculate the anisotropic eddy current losses in windings as follows [17, 18, 29, 74, 75]:

$$P_{w,e} = \frac{f^2 \pi^2 B_m{}^2 t_d{}^2}{3\omega} \tag{2.20}$$

where t_d is the thickness of conductor normal to the applied magnetic field,m
ω is the electrical resistivity, Ω.m
P_w, P_e are the winding losses due to Ohmic and eddy current respectively, W.

The total losses from the electromagnetic analysis can be converted into equivalent volumetric heat using a thermal-electrical analogy.

Eq.2.21 assumes that the total volumetric heat generated within a winding is a strong function of the transmission losses and structural integrity. It is the ultimate equation that will interpret the total internal heat generated within the solid windings due to various transmission conditions. This volumetric heat source estimation is a significant parameter in thermal modeling due to its linear temperature dependency is given in Eq.2.22 [18, 29, 44].

$$Q_T = \frac{P_T}{V_w} \tag{2.21}$$

$$Q_s(T) = Q_{T,0}[1 - \alpha_c(T - T_0)] \tag{2.22}$$

where, where, P_T is the summation of total winding losses,W

V_w is the winding volume, m^3

Q_T is the total heat source due to transmission losses, W/m^3

$Q_{T,0}$ is heat source at reference temperature, W/m^3

α is the temperature coefficient of copper conductors, 1/K

T_0 is the reference temperature obtained from heat-run tests, 348K

T is the operational temperature, K

In order to obtain the transmission losses from an operational transformer, electromagnetic analysis of the core-coil assembly can provide very satisfactory results. The only limitation in this approach is prior knowledge about the intricate structural details about the transformer to reciprocate the effect of selected geometrical configuration on heat distribution.

Since this data is also available with the manufacturer from their earlier experience, an exhaustive electromagnetic analysis of the transformer has been exempted from this research.

As mentioned earlier, the hot-spot temperature can determine both the remaining life of a transformer and its operational ability [10, 24, 43, 44, 52, 73, 79].

While electromagnetic analysis will ascertain the resultant heat generation within transformers, a coupled thermal-hydraulic model is sufficient to determine the axial oil-winding thermal behavior. The prime objective of such a model will be two-fold. Primarily, it should be capable of evaluating the oil and winding temperature rise during various conditions. Secondarily, it must also be capable of pin-pointing the exact location and magnitude of hot-spot temperature in order to estimate the remaining life of transformers.

Accuracy of hot-spot prediction is influenced by the axial temperature distribution in an oil-immersed winding. The flow determining parameters such as inlet flow rate, oil temperature, inlet channel width and contact area can cause a shift in the aforementioned thermal distribution. Therefore, prior to proposing an additional temperature rise of oil and windings, it is imperative to optimize the stationary model and isolate the effect of these parameters.

Conventionally there are several technique to determine the thermal performance of transformers using direct and indirect measurements. A summary of these techniques is available in Fig.2.4. The primary objective in the present work requires a CFD-based thermal model to predict the temperature behavior in accordance with the load pattern. In order to achieve the same, one must understand the direct measurements techniques so as to propose a future comparison to obtain the accuracy of the prposed CFD model.

2.2.1   Direct Measurements

Fiber-optic sensors provide a direct measurement of the temperature rise in the oil-immersed winding by inserting sensors probes at strategic locations while it is operational under variable loading conditions [54, 80–82].

It is also useful in monitoring various thermal, electrical and mechanical properties within the transformer by temperature-dependent loss estimation. The recent technological developments have made increased the applicability of theses sensors towards extra-high voltage exposure without getting damaged from internal stresses. Although it is the most accurate and easiest technique, yet the high embedding cost and risk of probe interference with the normal transformer cooling process can restrict its usage.

Alternative direct methods requires experimentally obtained temperature rise values at various locations by operating the transformer under variable load conditions. This is by far the most accurate method to determine the temperature rise and load bearing
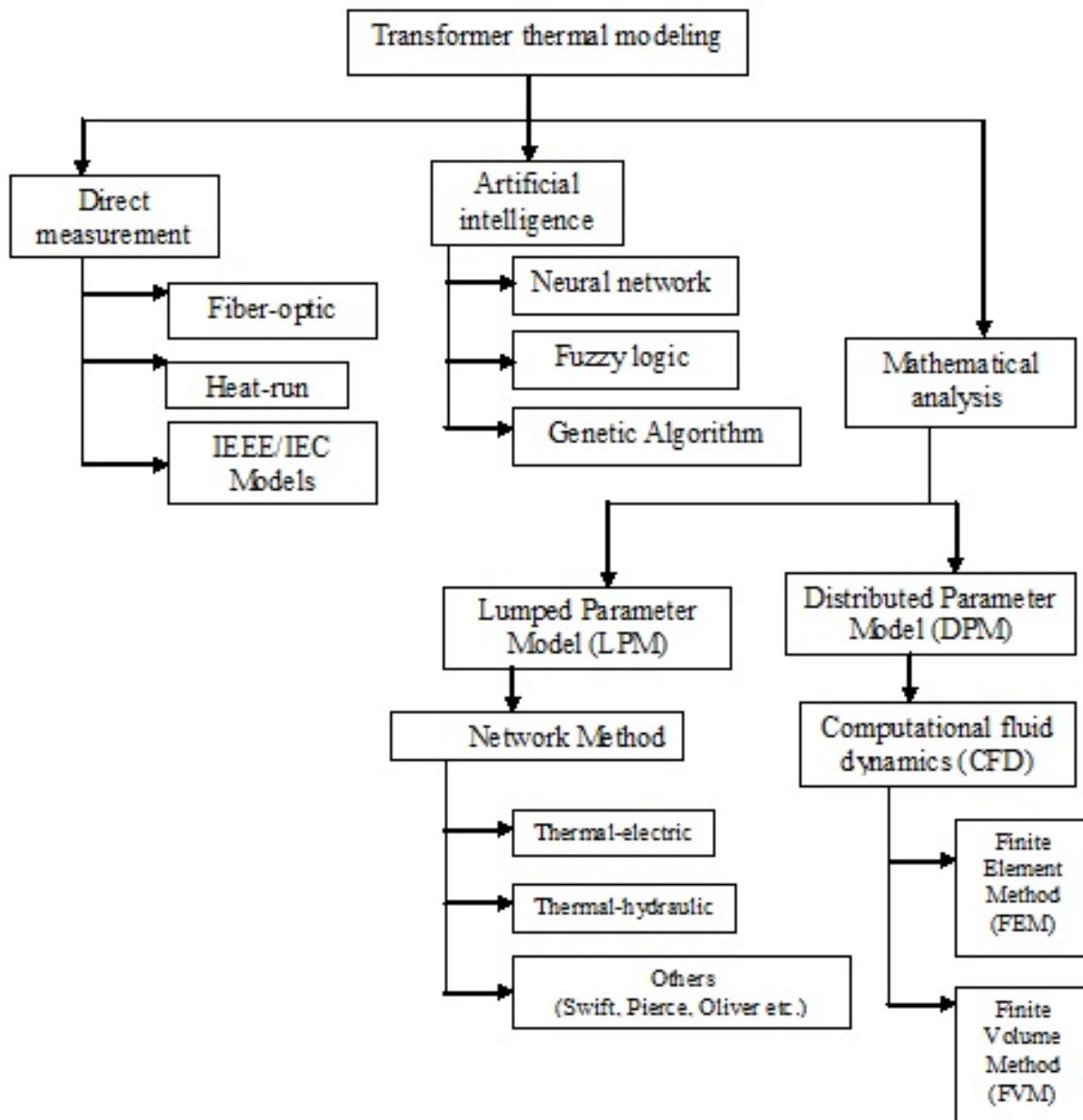
Figure 2.4: Summary of available methods for transformer thermal performance assessment

capacity of the transformer at any given instant within a load cycle.

Despite its appeal, heat-run tests are highly restricted to factory testing of transformer at the time of manufacture. This is because of the high cost of operation which makes the method unfit for use during on-site commissioning and continuous

temperature assessment.

Alternatively, some empirical equation based on ANSI/IEEE and IEC methods propose simple one-dimensional ordinary differential equations to estimate the temperature rise in oil. According to these methods, the hot-spot temperature is represented as the summation of oil and winding temperature rise above the ambient as given in Eq.??-2.28 [24, 43, 44].

$$T_{hst} = T_a + \Delta T_{to} + \Delta T_h \tag{2.23}$$

where, T_{hst} is the hot-spot temperature, °C

T_a is the ambient temperature, °C

T_{to} is the rise in top-oil temperature over ambient,°C

T_h is the rise in hot-spot temperature over winding, °C

The top-oil temperature rise in Eq.2.23 examines the total temperature change in transformer during loading by measuring the top-oil temperature at various stages. Such models to deliver the thermal performance of transformers are based on simple one-dimensional ordinary differential equations, where the transient response can be modeled using an exponential rise in the physical temperature values as depicted in Eq.?? [83].

$$\Delta T_{to}(t) = \left[\Delta T_{to,u} - \Delta T_{to,i}\right][1 - exp(-t/\tau_{to})] + \Delta T_{to,i} \tag{2.24}$$

where, $T_{to,u}$ is the ultimate rise in oil temperature, °C

$T_{to,i}$ is the initial rise in oil temperature, °C

τ_{to} is the thermal time constant of top-oil temperature, °C

Interestingly, Eq.2.24 also suggests that the top-oil temperature rise is also a function

of loading pattern such that the ultimate temperature rise can be obtained when the transformer is at full-load. Mathematically, it is expressed as below:

$$\Delta T_{to,u} = \Delta T_f \left[\frac{\mathbf{K}^2 R + 1}{R + 1} \right]^n \tag{2.25}$$

where, ΔT_f is the temperature rise in top-oil at full loading conditions,°C
$\mathbf{K}$ is the ratio of specified load to rated load and is better expressed as specified to rated current ratio.
R is the ratio of load loss at rated conditions to no-load losses.

This equation also suggests that the temperature rise in transformer changes exponentially with respect to time. The thermal time constant of oil is a relatively small value that explains the large temperature rise in oil and windings over the total loading time. It depends on the specific heat capacity of oil, physical mass ratio of tank components and rated power as given below.

$$\tau_{to} = \frac{\Gamma \times \Delta T_{to,av}}{P_T} \tag{2.26}$$

where, P_T is the total winding losses, W
$\text{T}_{to,av}$ is the average oil temperature rise above ambient, °C.

The constant Γ in Eq.2.26 is the cooling capacity of the transformer with respect to the mass ratio of participating media as shown below. The constants a, b and c defined in Eq.2.27 depends on the physical rating of the transformer.

$$\Gamma = a \times M_a + b \times M_t + c \times M_o \tag{2.27}$$

where, M_a is the mass of core-coil assembly, kg

M_t is the mass of transformer tank with fittings, kg

M_o is the equivalent mass of oil, kg.

Similarly, the resultant rise in hot-spot temperature during transient loading conditions can be evaluated using Eq.2.28 as shown below.

$$\Delta T_h(t) = \left(\Delta T_{h,u} - \Delta T_{h,i}\right)\left[\left(1 - exp(\frac{-t}{\tau_w})\right)\right] + \Delta T_{h,i} \qquad (2.28)$$

where, $\Delta T_{h,U}$ is the ultimate rise in hot-spot temperature at full loading, °C

$\Delta T_{h,I}$ is the initial hot-spot temperature rise,°C

τ_w is the winding time constant, hours.

The improved IEC techniques introduces a linear gradient in the form of hot-spot factor to evaluate winding and oil temperature rise as shown in Fig.2.5.

One of the biggest drawbacks in the aforementioned techniques is the determination of thermal times constants for oil. In a sensor-based method, these values are reported as at sensor response to the temperature rise of oil under variable loading conditions. In absence of any sensor or probe based measurement, some generic components are used to mimic the transformer thermal profile based on cooling and load pattern. However, such an assumption can certainly lead to erroneous temperature predictions without proper attention to the transformer age.

Unfortunately with such exhaustive advancements in the sensor-quality, its location in an operational transformer is still debatable. Therefore, alternative methods are being suggested using advanced computational techniques that are capable for determining the transformer thermal capacity with higher precision and reliability.

Such solutions are extensively based on mathematical modeling of coupled multi-physics governing the temperature rise phenomenon within transformers. These alternate solutions enhance the present understanding on transformer thermal performance for
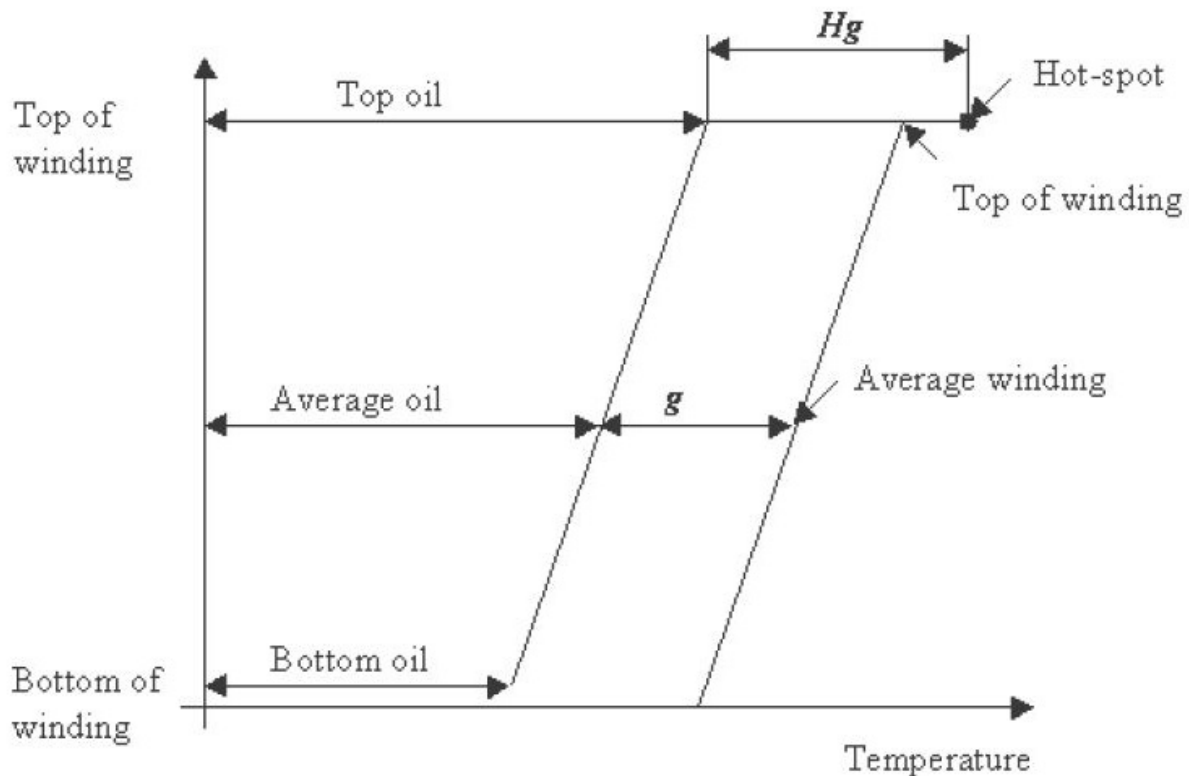
Figure 2.5: IEC model for transformer thermal analysis containing a winding to oil-temperature gradient ratio (g) and a hot-spot factor (H_g)

design optimization and improved operation efficiency without exceeding the capital cost of investment. A brief understanding of such methods is given in the subsequent section to assist the reader with modeling aspects and its relevance to the proposed work.

2.2.2 Modeling-Based Measurements

The main ideology to imply a model-based evaluation of temperature and flow fields depends on visualization of the specific sub-operations occurring at the same instant within transformers. Besides the non-uniform loss distribution as discussed in the previous section, oil circulation pattern also regulates the temperature rise limits within transformers.

The choice of an appropriate circulation technique depends on the physical size and

rating of a transformer. For example, forced cooling is better suited for larger power transformers with high heat dissipation requirements despite the additional noise (vibration) disrupting temperature rise measurements.

Similarly, natural cooling is the most efficient method for small and medium power transformers. It is capable of naturally removing the internal heat generated within the active windings of transformers. Although, it may not be always sufficient to use, one can suggest flow guiders to assist the velocity distribution and in return improve the thermal performance [40, 46, 52, 76, 77, 84–87].

Nevertheless, few combinations are discussed in Fig.2.6 that are common for small and medium power transformers [17–19, 74]
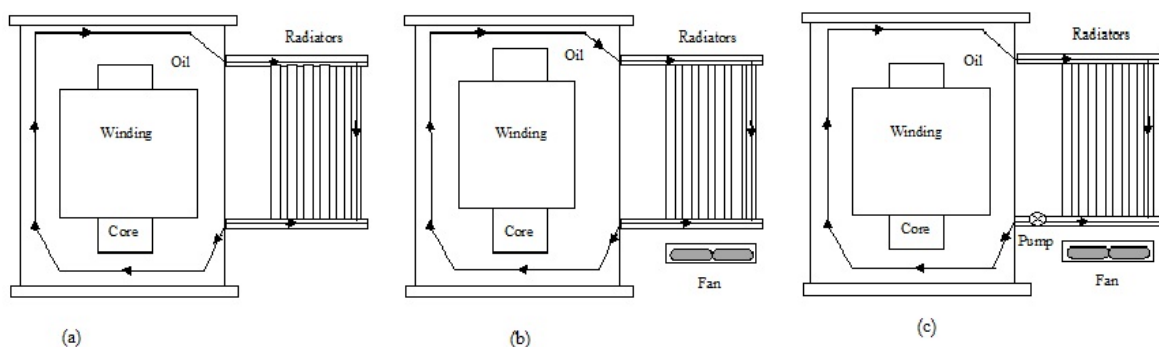
Figure 2.6: Various cooling methods in transformers (a) Oil natural air natural (b) Oil natural air forced (c) Oil forced air forced

One of the primary objectives of this research was to evaluate the winding and oil temperature rise during variable loading conditions. In order to achieve this, a medium voltage core-type power transformer with disc-type windings has been considered.

In the prescribed utility, the low-voltage winding (LVW) is placed near the core with extended conducting strands to accept the current and voltage input, whereas the high voltage winding (HVW) is placed away from it, thus justifying the mutual induction.

Naturally, the temperature in LVW of the transformer will be higher than the HVW. As a result, one can expect the formation of hot-spot temperature on the LVW itself

[10, 88]. Moreover, the oil far-away from the windings is expected to be relatively cold and hence irrelevant to the moisture dynamics prediction/participation.

It should also be noted that the moisture sensors mounted at various locations of the transformer are generally placed through a bypass line where the oil-field is ideally zero. It is obvious that all these factors will contribute to an approximate error in the moisture measurements, and therefore the prime objective should be on estimating the incipient error in moisture measurements of operational transformers due to these flow fields.

With the recent technological advancements, computational fluid dynamics (CFD) based thermal assessment of transformers can produce more reliable and relevant results without increasing the capital cost of the equipment. In this context, the thermal models are classified broadly into two categories namely, the lumped-parameter and distributed-parameter model.

The lumped parameter model (LPM) is based on a circuit method employing thermal-electric analogy to simulate the exponential temperature rise during transient analysis as given in [29, 74, 89–92]. Despite various advantages, it is evident from above that the LPM based solutions may not consider operational and geometrical complexities, thus failing to notice the thermal streaking and heat-pool formations within windings [29, 40, 46, 84, 87, 91, 93, 94].

Dynamic hot-spot modeling using bottom-oil temperature to avoid overshoots beyond the permissible limit is available in [90, 95]. Similarly, modeling of variable hot-spot temperature rise in power transformer (with external cooling) to accommodate the exponential changes in bottom-oil temperature is available in [96]. Ref. [74] mentions that despite the regular usage of top-oil temperature for hot-spot calculations, the modified expression using bottom-oil temperature [2] can be more reliable in transformer thermal evaluation. An excellent review and in-depth analysis of such models are given in [2, 29, 89, 91], but due to its non-relevance from the proposed method in this thesis, the same has been exempted from this study.

Previous works on the application of network methods to represent the temperature distribution in oil during stationary analysis is given in [46, 97, 98]. Ref. [45, 99–102] provides a more relevant transient model capable of accommodating the load variation-induced thermal changes around the conducting discs under variable cooling conditions and validated against the data available in [84, 101–103]. Another significant aspect of these methods is the heat source estimation by calculation of the total transmission losses [29, 40, 74]. Although, most of the authors accept that, the Ohmic losses are mainly responsible for winding temperature rise [10, 52, 77, 84, 95], few have actually simulated the combined effect of Ohmic and eddy current losses on internal heat generation in transformers [40, 73, 103].

A detailed critical review on LPM based techniques is available in [29], and therefore exempted from this work. Since the present work is largely influenced by the CFD-based methods, therefore, it is imperative to analyze the applicability of these techniques for satisfactory transformer thermal assessment. Conventionally, the CFD-based methods employ higher-order discretization techniques (i.e.,finite element,difference and volume methods) to evaluate the visually-aided coupled thermal-hydraulic behavior of oil in transformers.

Besides, variable winding geometry also plays a critical role in temperature distribution within transformers which are considered insignificant in LPM based measurements. In order to justify this, the apparent difference in temperature distribution of a naturally cooled power transformer with layer and disc windings is given in [79, 101] and [78, 104] using various CFD methods.

Similar studies shows the effect of buoyancy and thermal streaking has obtained a lot of interest due to its influence on the temperature distribution pattern in natural and forced cooled transformers [52, 77, 78, 94, 103, 104].

Similarly, other aspects *viz.*, the effect of winding configuration, variable flow rates, and internal temperature gradients have been addressed on several occasions throughout

the literature that has been largely neglected in thermal-electric or thermal-hydraulic methods [10, 52, 73, 78]. On the contrary, it is imperative to determine the temperature evolution in critical hot and cold zones of transformer insulation to predict the exact moisture content in these zones.

Hence it can be understood that in order to obtain a reliable moisture dynamic model for transformers, one has to look first into the precise thermal behavior of transformers. The temperature profiles thus obtained can be later fed to the moisture models to obtain a dynamic two-fold moisture distribution as discussed earlier. To allow the reader to navigate through such complex multi-physical modeling of the proposed problem, the next section proposes a simple flow chart to identify the mechanism and conjunction paths of prime importance.

2.3 Methodology

In order to proposed objectives, a detailed methodology is prepared and presented by Fig.2.7. Major aspects of this methodology including the mathematical modeling and simulation prospects shall be discussed in the upcoming chapters in this thesis.

The methodology primarily consists of four different physics combined together to obtain the dynamic moisture distribution in transformers. The electromagnetic analysis of core-coil assembly using the AC/DC module can provide insights to the winding and core losses encountered by the transformer during operation. These losses are converted into equivalent volumetric heat that is assumed constant and evenly distributed. Thus the winding losses act as the necessary heat source to identify the conjugate heat transfer and analyze the fluid flow patterns around complex winding geometries.

The evaluation of electromagnetic and thermal analysis along with associated flow field is carried out using fundamentals of computational fluid dynamics (CFD). A commercially available software COMSOL Multiphysics (v4.3b:2012) is used to evaluate

the thermal performance of transformers. Other mathematical operations and curve fittings to obtain several aspects during the transient measurements is carried out using MATLAB programming.

COMSOL Multiphysics is a commercially available CFD software based on the finite-element method for numerical approximation of higher-order and non-linear partial differential equations using various interactive tools to compute complex scientific and engineering problems [105, 106].

Unlike finite-volume or finite-difference techniques, the governing equations are approximated over a domain using Galerkin's residual-function technique. In this method, a shape (residual) function is automatically generated by simplifying the grid structure of the investigated surface or body. The residual thus generated is then multiplied with the dependent variable to achieve a converging solution of the proposed problem [107].

Although such an auxiliary approach may seem disadvantageous at first due to the excess mathematical computation, but while dealing with complex constraints finite element method does not require any back-of-envelope calculations for solving the PDE(s) thereby saving both computation time and effort.

On the other hand, MATLAB is a programming based language that finds immense physical importance during solution of ordinary differential equations and data interpretations using regression analysis.

The temperature profiles obtained during this analysis are incorporated into simple mass transfer equations to obtain the overall moisture distribution in transformers. These models primary consist of diffusion models operating on equilibrium temperature and overall mass balance equations to provide stationary and transient temperature-moisture patterns on the dominating oil-paper interface. Such results are extremely significant in determining the dominant aspects of inter-facial mass transfer and its role in overall temperature distribution in transformers.
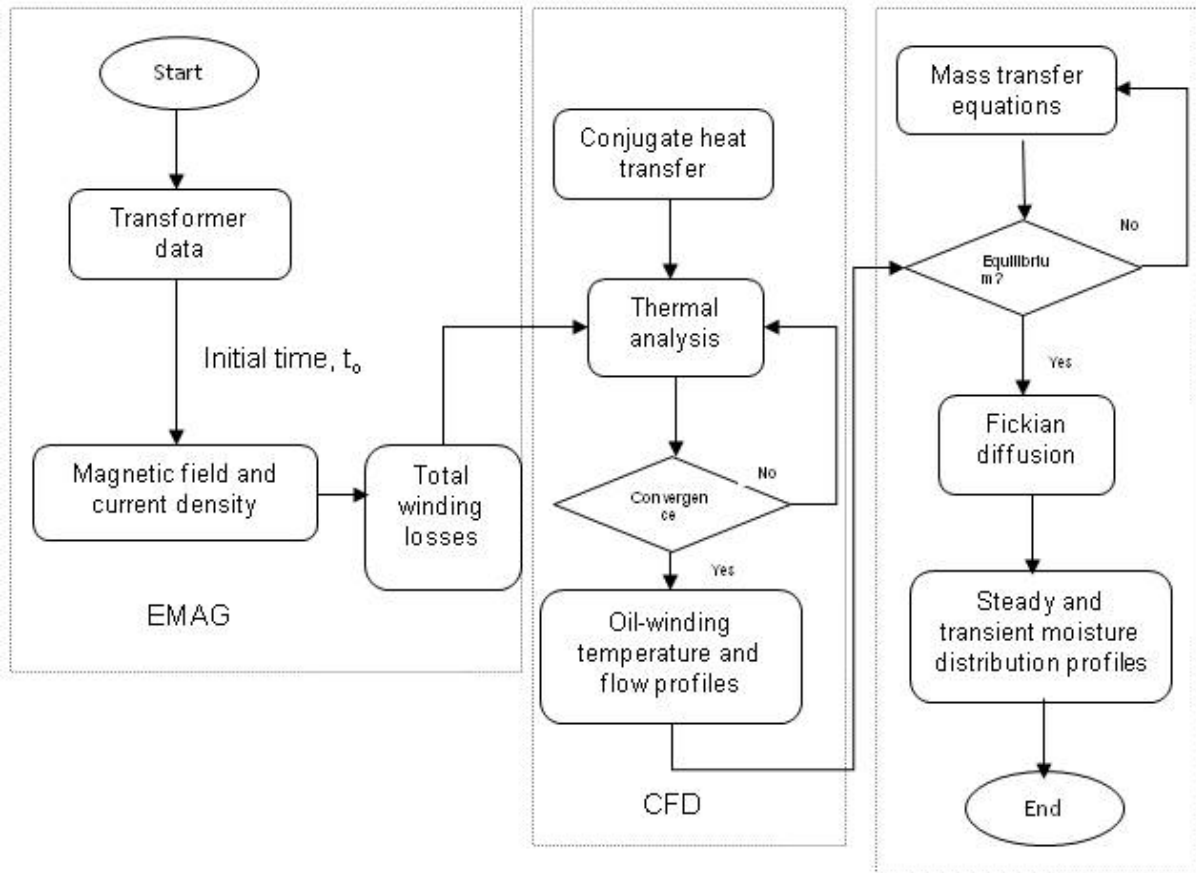
Figure 2.7: A typical methodology for multi-physics moisture dynamic studies in power transformers to correlate electrical-thermal-flow-moisture distribution using computational fluid dynamics approach

2.4 Summary

Moisture measurements and mitigation of moisture-related faults is an important aspect of transformer health management. In this regard, the temperature dependency of moisture increment, accumulation and subsequent dynamics is an inevitable aspect and can not be ignored. This chapter not only introduces the temperature dependency of moisture dynamics and significant aspects that predominates the overall moisture distribution in transformers. A simple methodology is introduced to estimate the multiphysics aspects of transformer health management and moisture analysis using

advanced computational tools and fundamentals of mathematical modeling. These results can significantly improve the present understanding of moisture dynamics in oil-filled power transformers.

Chapter 3

NUMERICAL MODELING AND ANALYSIS

The present chapter discusses multiple aspects of numerical modeling of moisture dynamics in oil-filled transformers using multiphysics approach. Section 3.1 discusses the basics of a moisture transport model for paper and oil separately thus allowing the reader to understand overall moisture distribution in the transformer. Section 3.2 provides the dynamic model for temperature variations in transformers in accordance with varying load profiles and ambient conditions. Section 3.3 discusses the various boundary conditions that will effect the thermal model of transformer windings. Section 3.4 proposes a set of boundary conditions as base settings for the desired model. Section 3.5 gives a brief description about the transformer geometry followed by its meshing scheme and grid analysis in Section 3.6. The chapter ends with an explanation for chosen boundary conditions for evaluating the moisture and temperature fields in transformer using the on-site information made available during the field survey in this project.

3.1 Dynamic Moisture Models

Dynamic moisture migration within an insulation complex is concomitant to the entailing dynamic temperature profile of oil and paper.

As the load increases, winding temperature becomes higher than the surrounding oil ($T_{paper} > T_{oil}$), hence resulting the moisture to migrate from paper to oil [7, 26, 41]. During this condition, the two mechanisms affecting the time taken to reach equilibrium are namely, diffusion and desorption. During diffusion, the moisture travels through the multi-layers of paper to reach the insulation surface, where a constant source of moisture-in-oil concentration can be located. Upon reaching the surface, desorption of moisture begins, which in turn depends on solubility of water in oil [108]. Since the moisture solubility in oil increases exponentially with temperature [7, 26, 36, 108], it is essential to calculate the instantaneous moisture-in-oil concentration over a fluctuating range of temperature to mimic the actual water distribution in an operational transformer. This procedure will stop when either the load is being removed or the oil has reached a saturation level whereupon free water formation is apparent [109].

A conditional reverse occurs when the temperature of winding drops abruptly($T_{oil} > T_{paper}$). At this stage, oil is still hotter than paper and therefore, moisture is supposed to be absorbed back into the insulation to maintain the moisture conservation. Interestingly, the oil impregnation of otherwise dry insulation will retard the resorption phenomena thus delaying the moisture conservation. At this stage the moisture uptake by insulation is by sorption isotherm (for surface moisture) and diffusion (average distribution) [7, 11, 64]. This condition is largely regulated due to the steady temperature of oil. One can alternatively propose the use of equilibrium curves to determine the equivalent concentration of moisture-in-paper under these circumstance. However, in the present work, separate models were proposed to determine the behavior of moisture up-take under different condition and verified against the available equilibrium data.

Therefore to propose a dynamic model for moisture interactions in transformer, one must create sub-models to interpret the behavior of such interactions separately for individual media and consolidate insulation complex. In this context, two simultaneous models have been proposed for moisture predictions in paper and oil respectively.

3.1.1   Moisture-in-paper Model

A moisture-in-paper model is an extremely handy technique to ascertain the condition of a damp transformer insulation and improving the applied drying models. For an inhomogeneous substance, heat moves faster than the accompanying moisture and hence, Fick's second law can be considered to express the water movement depending on its physical state [2, 3, 110].

Ref. [111, 112] assumed that moisture transport must be more dominant radially than axially due to higher aspect ratio of transformer windings, and thus suggested the use of one-dimensional partial differential equations to obtain local moisture distribution while avoiding structural complexity and added computation cost. Ref. [113] suggested that moisture distribution through the micro-pores and micro-fibrils is a strong function of the physical state of the associated water, assuming an analogous heat-mass conservation as shown by Eq.3.1- 3.3 [2].

$$\frac{\partial C_v}{\partial t} = \frac{\partial}{\partial x}\left(D_v \frac{\partial C_v}{\partial x}\right) + I \tag{3.1}$$

$$\frac{\partial C_w}{\partial t} = \frac{\partial}{\partial x}\left(D_w \frac{\partial C_w}{\partial x}\right) - I \tag{3.2}$$

$$\rho C_p \frac{\partial T}{\partial t} = \frac{\partial}{\partial x}\left(k \frac{\partial T}{\partial x}\right) - \lambda I \tag{3.3}$$

where, C_v and C_w are the local moisture concentration in vapor and liquid state

respectively, mol/m^3

D$_v$ and D$_w$ are the vapor and capillary diffusivity within a cellulose matrix, m^2/s

ρ is the density of cellulosic material, W/(m.K)

C$_p$ is the specific heat capacity of insulate, J/(kg.K)

T is the operating temperature of the insulate, K

λ is the latent heat of vaporization, J/kg

I is the rate of evaporation within the solid insulate during phase change, kg/(m^3.s)

Although Eq.3.1 and 3.2 provides an accurate representation of phase-oriented transport mechanism, yet it is quite challenging to continuously monitor the respective diffusion coefficients and physical mass of water during phase change. Therefore, a total (local) moisture is assumed by combining Eq.3.1 and 3.2 thereby neglecting the rate of change due to vaporization as shown below.

$$\frac{\partial C_v}{\partial t} + \frac{\partial C_w}{\partial t} = \frac{\partial}{\partial x}\left(D_v \frac{\partial C_v}{\partial x}\right) + \frac{\partial}{\partial x}\left(D_w \frac{\partial C_w}{\partial x}\right) \tag{3.4}$$

In Eq.3.4, the local moisture concentration is defined as the total mass of water present within a known mass of dry cellulose as shown below.

$$C_{loc} = \frac{C_w + C_v}{\rho_d} \tag{3.5}$$

Upon substituting, Eq.3.5 in 3.4, we can obtain the modified Fick's second law of diffusion for local moisture discretization over spatial-temporal scale as shown by Eq.3.6

$$\frac{\partial C_{loc}}{\partial t} = \frac{\partial}{\partial x}\left(D_{eff} \frac{\partial C_{loc}}{\partial x}\right) \tag{3.6}$$

where, D$_{eff}$ is the effective diffusion coefficient of moisture within the insulate, m^2/s

C$_{loc}$ is the local moisture concentration, mol/m^3.

Logically, the effective diffusion coefficient mentioned in Eq.3.6 is the combination of water and vapor diffusivity with an assumption that the mass transfer resistance is independent of cellulose inhomogeneity and a strong function of the local moisture concentration and temperature. Eq.3.7 shows an Eulerian approximation of Fick's second law with constant diffusion coefficient.

$$C_{i,j+1} = C_{i,j} + D_{eff}\left(\frac{C_{i+1,j} - 2C_{i,j} + C_{i-1,j}}{\Delta x^2}\right) \tag{3.7}$$

In practice, the effective diffusion coefficient in Eq.3.7 is not a constant value and varies with concentration and temperature over a local thermal equilibrium condition. According to the Arrhenius form of diffusion coefficient suggested by [16], a simple forward discretization can be enabled as shown by Eq.3.8.

$$D_{eff} = D_0 \exp\left[k'\frac{C_{i+1,j} - C_{i,j}}{\Delta x} + E_a\left(\frac{1}{T_0} - \frac{1}{T}\right)\right] \tag{3.8}$$

Upon combining Eq.3.7 and 3.8 one can obtain a holistic solution to the proposed model as shown below:

$$
\begin{aligned}
C_{i,j+1} = C_{i,j} + D_0\ e^{E_a\left(\frac{1}{T_0} - \frac{1}{T}\right)} \times \Bigg[&e^{k'\frac{C_{i+1,j}-C_{i,j}}{\Delta x}}(C_{i+1,j} - c_{i,j}) + \\
&e^{k'C_{i,j}}\frac{C_{i+1,j} - 2C_{i,j} + C_{i-1,j}}{\Delta x^2} \Bigg] + \Delta E_{i,j}
\end{aligned} \tag{3.9}
$$

where, (i×j) represents the discretization grid of moisture over spatial and temporal scales respectively and $\Delta E_{i,j}$ is the truncation error of the discretization scheme.

In order to solve the above set of equations, one must be aware of the applied operation to ascertain the initial and final boundary condition. Moisture diffusion models are applicable for both uptake and removal of moisture from paper/pressboard during oil-paper interactions.

In a typical drying operation, the paper/pressboard is rich in inherent water and assumes a homogeneous distribution of the initial state across the insulate thickness. Eq.3.10 shows the mathematical representation of this phenomena using constant surface moisture across all layers of insulate.

$$C_x|_{t=0} = C_s \qquad (3.10)$$

As the moisture is desired to be drawn out of the insulate, a stream of dry oil or air is exposed to the winding surface consisting of the wet insulation. At this stage, a minimum moisture retention of 0.5% is advised within the insulation in order to retain its mechanical and dielectric properties. Therefore, at the interface boundary, one can expect that the dry oil or air contains this desired equilibrium condition as shown by Eq.3.11. In order to initiate a consistency and convergence of solution, zero concentration gradient condition is applied at the other end of the insulate as shown by Eq.3.12.

$$C_t|_{x=0} = C_0 \qquad (3.11)$$

$$\frac{\partial C_{x,t}}{\partial x}|_{x=l} = 0 \qquad (3.12)$$

In case of factory drying, the choice of such boundary condition exhibits that the other end of the insulation is in contact with copper conducting strands and hence non-participatory. A reversal of this boundary is evident in almost all of the literature available describing the moisture interaction at oil-paper boundary. In these studies it is assumed that the paper initially contains about 0.5% of moisture and starts to absorb water from oil as soon as the winding temperature drops.

To assist the reader in understanding the diffusion mechanism, Fig.3.1 presents the rudimentary model of paper/pressboard interaction with surrounding oil, both near and

away from the winding within an encapsulated unit. Interestingly, local moisture discretization changes with density and thickness of material and therefore is not practically homogeneous.
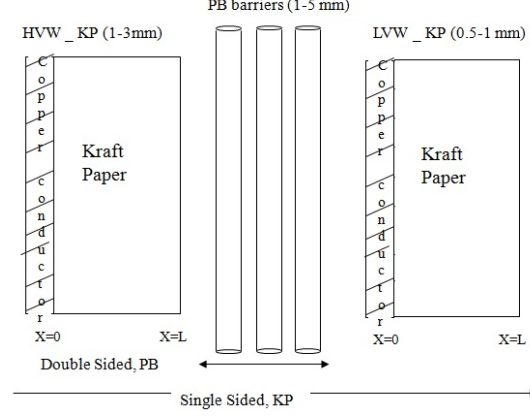
Figure 3.1: Moisture dynamic model of oil-paper-air insulation complex of transformers

In this case an average instantaneous moisture must be obtained using Eq.3.13 to isolate the nature of material type and more significantly its thickness of moisture-in-paper models.

$$C_{avg}(t) = \frac{1}{d} \int_{x=0}^{x=d} C_{loc}(x,t) \; dx \qquad (3.13)$$

During numerical approximations, minimization of the residual error between simulated data and analytical solution is imperative to reduce the redundancy error and increase accuracy of the fitted model. As per Eq.3.14 the root-mean-square-deviation (RMSD) is the difference between simulated and analytical (or in some cases experimental) data to calculate the probable error and convergence of the fitted model.

$$RMSD = \sqrt{\left[\frac{1}{n} \left(\sum_{i=1}^{k} C_{avg,sim}(t_i) - C_{avg,fit}(t_i) \right)^2 \right]} \qquad (3.14)$$

where, n is the number of simulation (or experimental) observations

$C_{avg,sim}$ is the simulated average concentration,(mol/m^3)

$C_{avg,fit}$ is the fitted average concentration,(mol/m^3)

Since fewer information is available for moisture dynamics in pressboard it is imperative to check the proposed model with analytical solutions in order to estimate the resolution error in the proposed model.

Fig.3.2 shows the error generated between simulated data and fitted curve for 1.5mm oil-impregnated pressboard with 2.2% surface moisture at 70°C. Similarly, Fig.3.3 shows the error generation between simulated and fitted data curve for 1.5mm non-impregnated pressboard with 2.2% surface moisture at 70°C.
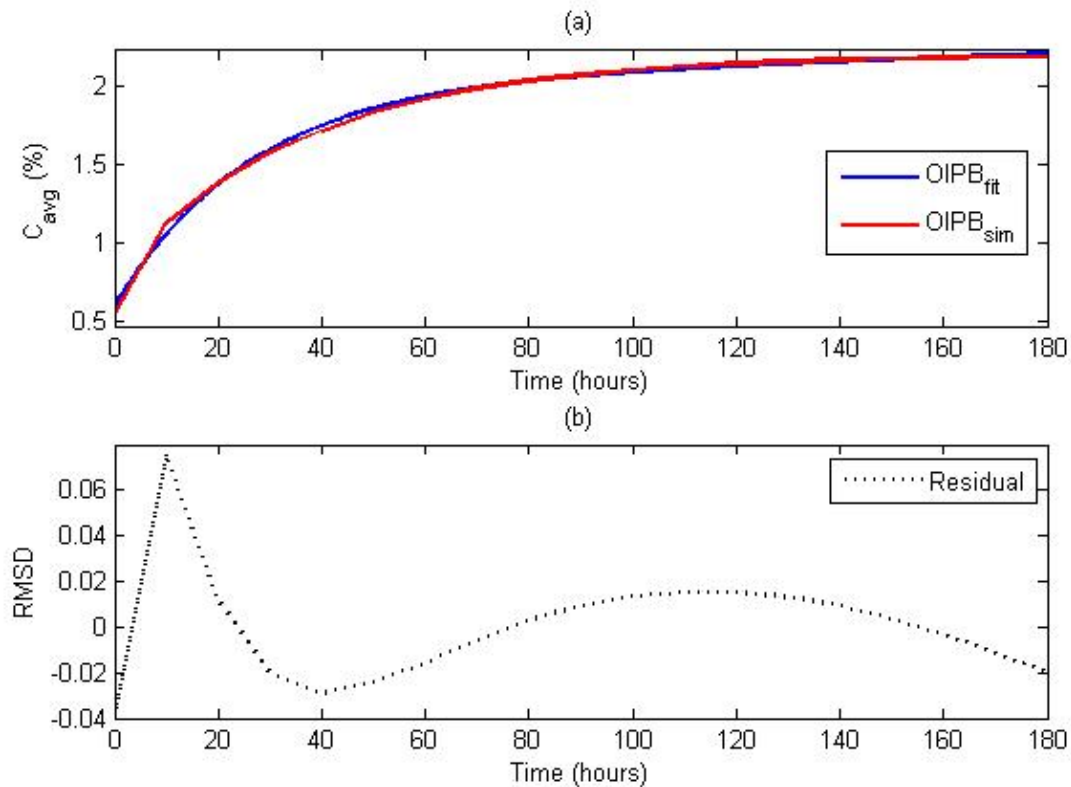
Figure 3.2: Error estimation in (a) average concentration distribution of 1.5mm oil impregnated pressboard in comparison with (b) the residual error

There are two most prominent observations made from these figures i.e., diffusion coefficients dominate the moisture interaction behavior for paper/pressboard; and that
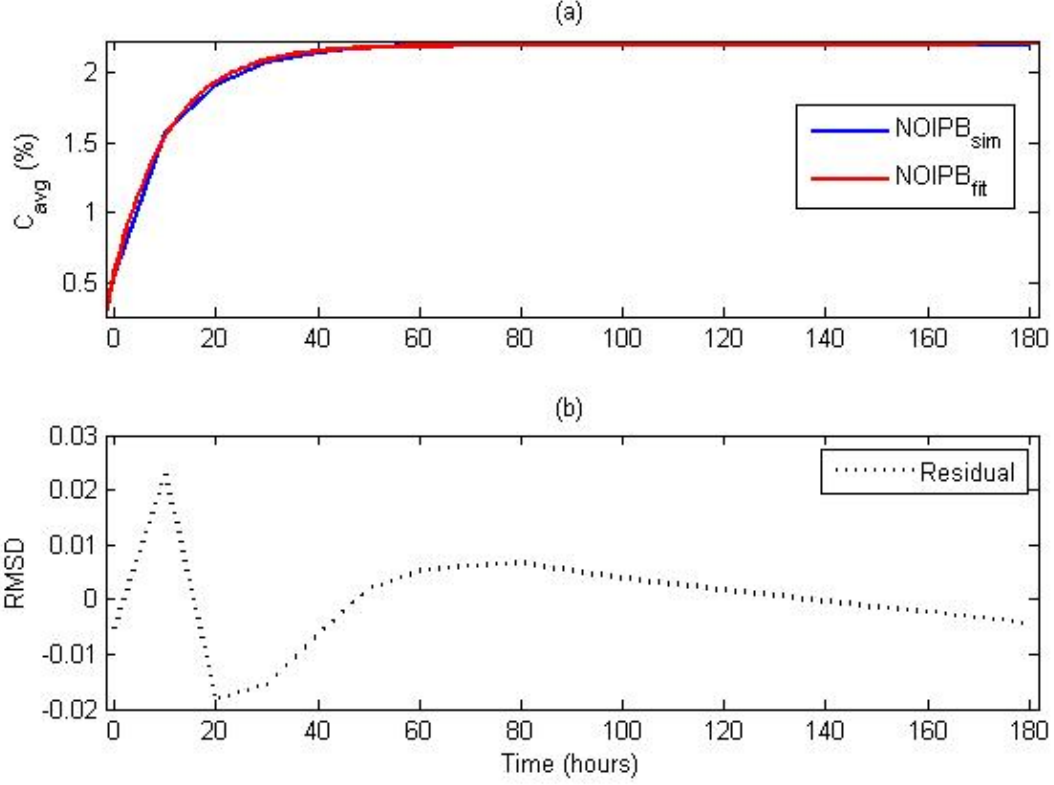
Figure 3.3: Error estimation in (a) average concentration distribution of 1.5mm non-impregnated pressboard in comparison with (b) the residual error

the sigmoidal shape of the residual suggests that the exponential curve is well-fitted to this data according to Eq.3.15, hence suggesting the accuracy of our proposed model.

$$C_{avg,e}(t) = a \ \exp(bt) + c \ \exp(dt) \tag{3.15}$$

where, constants a, b, c and d are obtained by fitting a curve of 95% confidence to achieve the most realistic expressions.

It is also evident that the average moisture concentration increases exponentially during temporal discretization of the insulation material. Therefore, it can be represented as a classical first-order system whose response time must be 63.2% of the change in physical values.

In conclusion, with reference to the dominance of diffusion coefficients reported by [11,12,16,16,68] one can safely distinguish the moisture transport across different insulates in transformers. Moreover, the following assumptions were made to accommodate Fick's second law of diffusion to evaluate the moisture-in-paper model:

1. Diffusion coefficient dominates the Fick's 2nd law, and is a strong function of local concentration, temperature and water vapor pressure.

2. Moisture transport is slower than conduction-convection thus neglecting the role of thermal time constants in diffusion studies.

3. A thermal equilibrium is partially attainable during an uninterrupted load cycle unlike moisture equilibrium, which shifts with small variables in temperature profile and hence unachievable especially in an operating transformer.

4. The aspect ratio (length to diameter) is greater than 1, thus suggesting a dominance of transversal diffusion over a longitudinal one.

While the afore mentioned assumptions help in simplifying the problem to a greater extent, following limitations restricts the use of such models to tightly controlled environments:

1. The model assumes an effective diffusion coefficient based on homogeneity of the material whereas in reality the insulate can contain variable fractions of cellulose, hemicellulose and lignin compounds.

2. Although Fick's law is incapable to modeling the physical deformation of insulate during drying, an added equation to model the decrease in tensile strength during drying might increase the complexity of the problem without a guaranteed solution.

3. Truthfully aging of solid insulation is not a parameter to be concerned about during factory drying due to higher physico-chemical strength of the material, whereas

it certainly is inevitable while field drying of relatively old transformers that are constantly facing elevated thermal and electrical stresses.

Another complex aspect of this model is that when the moisture is migrating from the paper to oil, a continuous sorption takes place which is concomitant with the shifting thermal transients. In this case, a suitable model is required to accommodate the transient moisture sorption in oil and paper with regard to the temperature, load and flow variations. The next section explores more about such a model that shall be helpful in understanding the moisture migrations within oil-filled transformers.

3.1.2   Moisture-in-oil Model

As mentioned earlier, the moisture changes exponentially with respect to temperature and the relative saturation shift. Fig.3.4 can be used as a based to estimate the dissolved (C_{diss}) and soluble moisture within a transformer with RS$\lesssim 20\%$ across a temperature range of 0-100°C. The choice of relative saturation limit is in order to avoid the detrimental effects of excess water on dielectric strength of oil [38].

Similarly, the moisture sorption in paper depends heavily on temperature and water vapor pressure as reported throughout the literature [2, 7, 12, 16, 39, 47, 66]. Therefore, using the discussion given in the previous chapter, one can plot a co-dependent relation between relative humidities and moisture content in paper as shown by Fig.3.5.

It is understood that despite the uneven distribution of moisture within transformers, the total weight of water is essentially conserved [2, 11]. In this case, a simple mass balance equation can predict the water partition in individual insulate as per Eq.3.16.

$$M_{t,w} = (M_p + M_b) \times \frac{C_{eq,ss}}{100} + M_o \times \frac{C_{o,ss}}{10^6} \qquad (3.16)$$

where

$M_{t,w}$ is the total conserved mass of water in transformers, kg

M_o is the mass of oil in tank, kg

M_p is the mass of paper in tank,kg

M_b is the mass of pressboard in tank,kg

$C_{o,ss}$ is the steady state moisture in oil, ppm

$C_{eq,ss}$ is the steady state equilibrium moisture in paper,%.
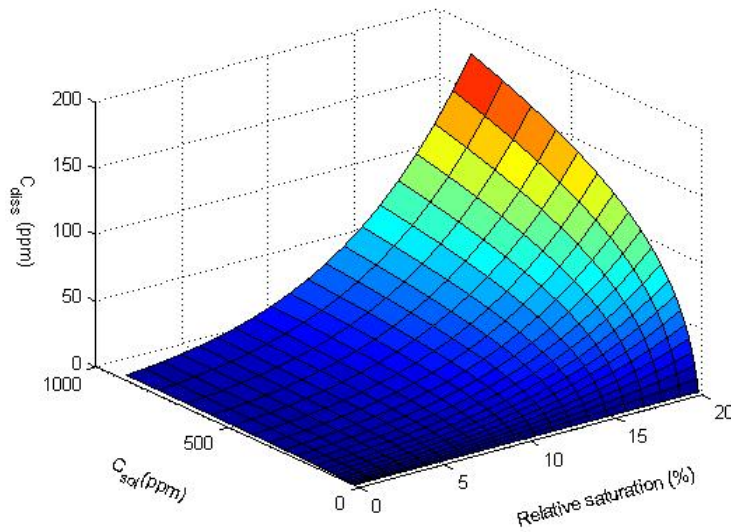
Figure 3.4: Typical water rise in naphthenic oil with variable temperature and RS<20%. The solubility coefficients are A=7.09, B=1570

It must be noted that to formulate an initial basis, Eq.3.16 may be adapted. However, in an operational transformer, the temperature transients will cause a shift in the relative saturation thereby affect the saturated concentration. Therefore, for a typical transient system it is more relevant to estimate the shift in equilibrium with respect to temperature variations as shown by Eq.3.17.

$$C_{eq}(t) = \frac{M_t}{M_p + M_b} - \frac{M_o}{M_p + M_b} \times \frac{C_{o,ss}(t)}{10^6} \qquad (3.17)$$

where, all concentration coefficients have been adjusted according to the transient
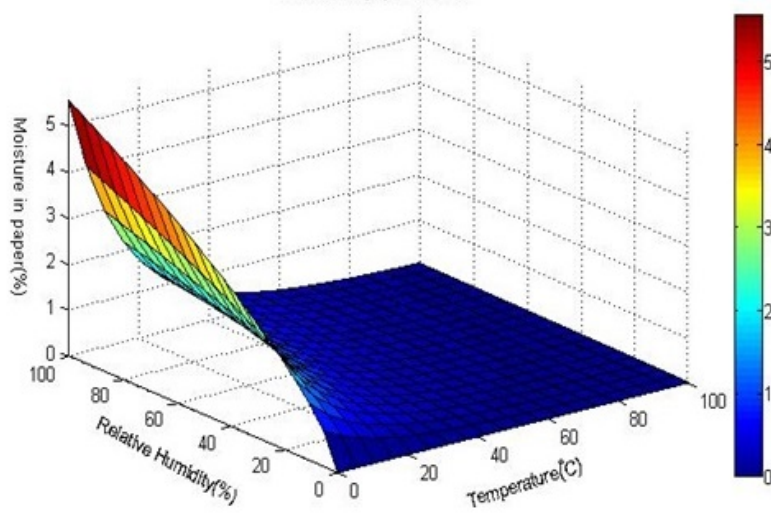
Figure 3.5: Typical water rise in cellulose based paper insulation with variable temperature and wide humidity range. The constants for pressure calculations are A=1.5, B=235 as per Magnus-Teten relation [8]

temperature variations. In order to formulate transient relationships, the moisture-in-oil model is again divided into two sub-sections as shown below:

Transient interactions at interface boundary

The interface boundary is where moisture from paper is interacting with the first layer of oil upon thermal excitation. In this case, the moisture transfer from paper to oil is similar to that reported in [13, 114].

$$\frac{dC_{p,m}}{dt} = \frac{C_{o,ss} - C_{p,m}}{\tau_p} \tag{3.18}$$

where, $C_{p,m}$ is the measured moisture in paper using equilibrium charts,%
$C_{o,ss}$ is the saturated moisture in oil measured using KFT, ppm
τ_p is the equilibrium time response of paper, hours.

Ref. [108] also proposed that this time response is constant through out the

operation for paper but may change for oil. This hypothesis was challenged by [13] who suggested that it will change with insulate thickness, moisture concentration and temperature. In their research, the effect of oil-impregnation and initial boundary condition was completely ignored.

Our investigations on the effect of various parameters on equilibrium time response of moisture in paper yields an empirical expression as shown below. The methodology and detailed discussions on the effect of these parameters on time response have been exhaustively shown in Chapter 5 later in this work.

$$ln\tau_{corr} = \gamma + a_0 \times T + a_1 \times C_p \tag{3.19}$$

where,

γ is a constant coefficient obtained a ratio of thickness and exposure sides

C_p is the constant moisture in paper at the interface boundary in percentage (%),

τ_{corr} is the corrected time constant, hours.

The values of coefficient a_0 and a_1 were obtained from curve fitting of simulated graphs. In this particular case, the constants a_0 and a_1 are -5.8×10^{-2} and 3.805 respectively. The correction coefficient γ is estimated to be -6.2 through curve fitting. As we will proceed towards the instantaneous moisture modeling in power transformers, Eq.3.19 can be used as a reference. These values have been exclusively used for moisture-in-oil modeling discussed later in the present thesis.

Transient interactions within oil

During transient migrations, the intensity of moisture solubility in oil not only depends on temperature but also on the response time required by the oil to adjust itself against shifting thermal transients. The time response of oil to self-adjust with respect to the shifting thermal transients can be experimentally determined. Since that was beyond

the scope of this thesis, an alternative method can be adopted as per the discussion of [108]. One may suggest that the increase in oil moisture will signify the decreasing concentration in paper and therefore, a removal model may as well be used to record the time constant. However, our investigations report that despite the universality imposed on moisture removal and uptake models, the time response will change with respect to various parameters. Although applicable, the use of such a technique will require utmost caution and shall be highly restricted.

Assuming that the oil-moisture rise is an ordinary first-order differential equation, the change in moisture-in-oil concentration at un-steady state shall is as shown by Eq.3.20. These equations assumed that the moisture was recorded near the winding, where some measurements were made using equilibrium charts. Since the time response of moisture dissolution in oil is also a function of temperature, a homogeneity in thermal distribution may predict this entity. It is mentioned in [108], that temperature is largely non-uniform for naturally cooled transformers especially at the location away from the winding.

$$\frac{dC_{o,i}}{dt} = \frac{C_{o,ss} - C_{o,i}}{\tau_p} \tag{3.20}$$

where $C_{o,ss}$ is the saturated moisture in oil at known temperature, ppm
$C_{o,i}$ is the instantaneous moisture in oil with variable temperature measurable by KFT, ppm
$C_{o,m}$ is the instantaneous moisture in oil measured by the sensor, ppm
τ_p is the equilibrium time response of paper, hours.

Traditionally saturated values are obtained at steady state i.e., when temperature variations cease to exist. In case of operational transformers, this condition is practically never achieved. Therefore, during moving transients, we assume a Dirac delta function that will be the representation of this time dependent temperature overshoot as given by Eq.3.21.

$$\frac{dC_{o,i}}{dt} = \frac{C_{o,ss} - C_{o,i}}{\tau_p} + \frac{\delta t}{\tau_p}\frac{dC_{o,ss}}{dt} \qquad (3.21)$$

where, δt is time instant of temperature overshoot, hours.

In order to obtain the mathematical value of this Dirac delta function one must be able to obtain the exact solution of Eq.3.21 using integration and re substitution. In case of operational transformers, moisture sensors are almost always mounted at the bottom of transformer tank. Specially in case of naturally cooled transformers, one can expect that the oil temperature shall be fairly low thus suggesting lower moisture levels near the sensor area. If it is to be assumed that the instantaneous moisture in oil is now what the sensor measures, one can assume the following.

$$C_{o,i}(t) = C_{o,m}(t) \qquad (3.22)$$

Ref. [115] suggests that in case of probe sensors, the location is usually inside a duct which is more of a bypass line, hence suggesting Eq.3.23 for instantaneous moisture measurement.

$$\frac{dC_{o,i}}{dt} = \frac{C_{o,a} - C_{o,i}}{\tau_o} \qquad (3.23)$$

Now, substituting Eq.3.22 in 3.23, one can obtain the exact equation for moisture read by sensor during daily transformer operation.

$$\frac{dC_{o,m}}{dt} = \frac{C_{o,a} - C_{o,m}}{\tau_o} \qquad (3.24)$$

where,

$C_{o,a}$ is the average moisture concentration near the probe location away from the winding,

ppm

τ_o is the time response of oil during shifting transients, hours.

To obtain the moisture dissolved within the remaining tank oil (all-locations) and especially near our sensor (not-bypass), one can obtain the following correlation.

$$C_{o,i} = \tau_m \frac{dC_{o,m}}{dt} + C_{o,ss} \tag{3.25}$$

where,

$C_{o,ss}$ is the average moisture in oil at steady state, ppm

$C_{o,i}$ is the instantaneous moisture measurable by a sensor, ppm

$\tau_{m,i}$ is the equilibrium time response of when the oil sensor was closer to the winding, hours.

In Eq.3.23, theoretical determination of τ_o is not possible, thus it has been assumed similar to the τ_m. Moreover, the saturated moisture in steady state is nothing but a hypothetical baseline. In order to model the transient moisture migration with reference to the effect of sensor measurement an by substituting Eq.3.21 into 3.20, one can obtain the following re-adjusted expression, with an assumption that the instantaneous moisture is same as measured moisture.

$$\tau_p \tau_m \frac{d^2 C_{o,m}}{dt^2} + (\tau_p + \tau_m) \frac{dC_{o,m}}{dt} + C_{o,m} = C_{o,ss} + \delta t \frac{dC_{o,ss}}{dt} \tag{3.26}$$

Eq.3.26 proposes that the instantaneous change in oil moisture ($C_{o,m}$)is affected by the sensor location and temperature indirectly. This second order formulation is very much similar to the one proposed in [108]. Except in the present work, time response for moisture migrating from paper to oil is not a constant value. Therefore, a revised equation can be obtained by substituting Eq.3.19 into 3.26 as shown below.

$$\tau_{corr}\tau_m\frac{d^2C_{o,m}}{dt^2} + (\tau_{corr} + \tau_m)\frac{dC_{o,m}}{dt} + C_{o,m} = C_{o,ss} + \delta t\frac{dC_{o,ss}}{dt} \qquad (3.27)$$

Again, re-substituting the expression of corrected time constant, one can modify the Eq.3.27 as follows:

$$\tau_m(\exp\left(\gamma + a_oT + a_1C\right))\frac{d^2C_{o,m}}{dt^2} + ((\exp\left(\gamma + a_oT + a_1C\right)) + \tau_m)\frac{dC_{o,m}}{dt} + C_{o,m} =$$
$$C_{o,ss} + \delta t\frac{dC_{o,ss}}{dt}$$
$$(3.28)$$

In the present work, an exhaustive CFD-based thermal model is employed over a control volume using finite-element scheme to understand the transient temperature behavior in oil and windings that shall be correlated to moisture migrations as proposed. Moreover, since the oil temperature immediately next to winding is a major influence on moisture-in-oil models, the obtained CFD results were more satisfactory as compared to the conventional IEEE/IEC methods.

3.2   Dynamic Thermal Models

In this section, a numerical model has been proposed to determine the temperature rise in oil and windings using computational fluid dynamics (CFD). The purpose of this model was twofold ie., obtaining an initial, steady state analysis of the temperature rise, and obtaining the load-varied rise to replicate the conditions of an actual transformer. All simulations were carried out on COMSOL Multiphysics with data extraction and curve fitting using the MATLAB.

In typical oil-filled transformers, oil enters near the bottom of winding with a known mass flow rate. As it comes in contact with the hot conductors, oil density changes thereby causing a viscous motion. This allows oil to circulate freely across the available

ducts/channels and hence absorb the excess heat from the windings through advection.

3.2.1 Governing Equations

A classical approach to transformer thermal modeling is by postulating the problem in terms of advection heat transfer through coupling of Navier-Stoke and general energy conservation equations [10, 15, 40, 52, 74, 77–79, 94].

Proposing a 3-d solution is no doubt the best approach, however such an effort will require excessive back-of-envelope calculations, intricate transformer construction data and of course higher computational effort. A smarter alternate is to propose the same problem using 2-d axisymmetric approach with an assumption that all the significant properties are showing an axial periodicity. This will not only save excess computational time and effort, but also produce reliable results without compromising the accuracy of model.

Navier-Stokes Equations

The Navier-Stokes equations governs the flow field of a weakly-compressible fluid by conservation of mass and momentum within the functional boundaries. In order to represent this, continuity equations within Eulerian frame of reference proposes that the rate of oil inflow is equal to outflow thus suggesting the conservation of total mass as shown in Eq.3.29.

$$\frac{\partial \rho}{\partial t} + \rho \left[\frac{\partial u}{\partial x} + \frac{\partial v}{\partial y} \right] = 0 \tag{3.29}$$

Similarly, Newton's second law of motion can be used to express the momentum conservation in oil field, where the total forces applicable on a body i.e.,hydrostatic pressure, viscous force, and buoyancy forces are equal to the total mass of fluid element. The oil viscosity appears to change exponentially with temperature rise and therefore, a

Lagrangian frame of reference is desired to solve the momentum conservation equations. Since the problem is postulated in two-dimensions, the respective equations for momentum conservation are:

x-direction:

$$\frac{\partial(\rho u)}{\partial t} + \rho\left[u\frac{\partial u}{\partial x} + u\frac{\partial v}{\partial y}\right] = -\frac{\partial P}{\partial x} + \frac{\partial}{\partial x}\left(\mu\frac{\partial u}{\partial x}\right) + \frac{\partial}{\partial y}\left(\mu\frac{\partial u}{\partial x}\right) \qquad (3.30)$$

y-direction:

$$\frac{\partial(\rho v)}{\partial t} + \rho\left[v\frac{\partial u}{\partial x} + v\frac{\partial v}{\partial y}\right] = -\frac{\partial P}{\partial y} + \frac{\partial}{\partial x}\left(\mu\frac{\partial v}{\partial x}\right) + \frac{\partial}{\partial y}\left(\mu\frac{\partial v}{\partial x}\right) + F_y \qquad (3.31)$$

where,

$\frac{\partial \rho}{\partial t}$ is the average mass change in oil, $kg/m^2.s$

u, v are radial and axial flow velocity, m/s

ρ is the density of oil, kg/m^3

In the Eq.3.30 and 3.31, the first term on the right hand side is the radial and axial gradient of hydrostatic pressure respectively. The last two terms on the right side of Eq.3.30 and 3.31 are nothing but the component of viscous force in radial and axial direction respectively. The last term, F_y, is the buoyancy forces due to density variation. As it changes with temperature, an additional effort is required to model the temperature-induced density change in oil using Boussinesq approximation.

Boussinesq approximation

Ref. [116] suggested that kinematic viscosity and volumetric expansion coefficient of oil dominates the winding-oil temperature rise phenomena. The effect of buoyancy on winding temperature model was then considered by [14, 94, 117], who strongly recommended the use of Boussinesq approximation to ascertain the temperature rise in critical and inaccessible zones.

In the present study, it is used within the functional domain as shown by Eq.3.32 and 3.33 to replicate temperature-dependent density variations.

$$F_y = (\rho - \rho_\infty)g \tag{3.32}$$

$$\rho_\infty = \frac{\rho}{\beta(T - T_\infty)} \tag{3.33}$$

Conventionally, such an assumption is applicable when despite infinitesimally small variations in fluid density, the buoyancy is strong enough to drive the flow. In this case, the density variation is not neglected while calculating buoyancy forces where the temperature moderation in density is very infinitesimal i.e., β(T-T$_\infty$)≪1.

where,

ρ_∞ is the density of oil at bottom fluid temperature, kg/m^3

μ is the dynamic viscosity of oil, Pa.s

F$_y$ is the buoyancy force in axial direction, N/m^3

β is the volumetric expansion coefficient of oil, g/g.K

g is the gravitational acceleration, 9.81 m/s^2

T$_\infty$ is the bottom fluid temperature, K

Energy Equation

Since winding losses are the main culprit for internal heat generation, the inherent temperature travels across the winding in axial and radial direction due to conduction. As transformer windings are made by wrapping of Cu-strands with insulation paper, the thermal conductivities are bound to change with insulation thickness in the resultant direction thus incorporating the need for spatial corrections [55, 118].

Practical experiences suggest that axial thermal conductivity of Cu was far higher than the radial one. Moreover, due to high aspect (height to diameter) ratio, the temperature

traveled faster in the axial direction as compared to radial one [118].

Within a bounded region, such that a≤x≤b, 0≤y≤H and t≥0, Eq.3.34 can be used to determine the heat conduction within windings in two dimensions as shown below, where (a,b) and (0,H) are the radial and axial limits.

$$\frac{\partial T}{\partial t} = k_x \frac{\partial^2 T}{\partial x^2} + k_y \frac{\partial^2 T}{\partial y^2} + Q_c \qquad (3.34)$$

In order to dissipate this heat accumulation and consequentially avoid the unwanted temperature rise, efficient oil cooling is required. The oil circulating within the windings removes this excess heat by advection and dissipates it to the non-active components of the transformer by either convection (natural/forced cooling) or radiation (natural cooling).

In this regard, the Newton's law of cooling is imposed to determine the convective heat transfer coefficients responsible for heat dissipation through participating surface during the thermal-fluid analysis of transformers as shown by Eq.3.35.

$$Q_a = h_\infty A(T - T_\infty) \qquad (3.35)$$

Similarly, the overall heat dissipation from radiation heat transfer can be given by Eq.3.36 based on Stefan-Boltzmann's law as shown below to replicate the dissipation of heat from non-participating tank walls towards the ambient surrounding:

$$Q_r = \kappa e(T^4 - T_{amb}^4) \qquad (3.36)$$

Therefore, while the total heat dissipation, (Q_t) from transformer is a combination of convection and radiation heat transfer, and a conservation equation must mean that this total heat dissipation is equal to the total heat generation, (Q_c) from windings as shown by Eq.3.37.

$$Q_t = Q_a + Q_r, \qquad Q_t = Q_c \qquad\qquad (3.37)$$

Upon extrapolating this fundamental idea over winding thermal performance, it can be assumed that the total energy consumed by oil during heat dissipation is equal to the amount of energy generated within the windings.

Based on the aforementioned assumption, Eq.3.38 gives the total energy conservation equation, where the summation of heat storage and temperature flow is equal to the diffusion and generation of heat within oil-immersed transformer windings.

$$\rho C_p \left(\frac{\partial T}{\partial t} \right) + \rho C_p \left[\frac{u \partial T}{\partial x} + \frac{v \partial T}{\partial y} \right] = \frac{\partial}{\partial x} \left[k_x \frac{\partial T}{\partial x} \right] + \frac{\partial}{\partial x} \left[k_y \frac{\partial T}{\partial y} \right] + Q_s \qquad (3.38)$$

where,

C_p is the specific heat capacity of oil, J/(kg-K)

k_x, k_y is the thermal conductivity of copper, W/(m-K)

Q_s is the internal heat generated from losses, W

$Q_{c,x}$, $Q_{c,y}$ is the conduction heat transfer in x- and y- directions respectively, W

Q_a is the advection heat transfer due to oil circulation, W

Q_r is the radiation heat transfer at the wall-ambient surface, W

κ is the Stefan-Boltzmann constant, 5.670367×10^{-8} W/(m^2-K^4)

e is the emissivity coefficient

A is the interactive surface area for heat conduction/convection, m^2

T is the operating temperature of oil/copper, K

T_{amb} is the ambient air temperature, K

At this point, it must be mentioned that since windings are the sole component of interest with proper relevancy to the proposed idea, an entire transformer tank modeling was found unnecessary. Moreover, since the low voltage windings were found closer to the

core, it was only logical that solely this part was modeled in order to find the temperature rise limits under extreme conditions.

3.3 Boundary Conditions

The coupled set of equations i.e., Eq.3.29-3.31 and 3.38 represents a well-poised conjugate heat transfer problem with four dominating equations and four unknowns. A combination of Dirichlet, Neumann and Robin boundary conditions are required to obtain the desired function or value that will be later imposed on functional boundaries.

Dirichlet boundary conditions are used when specified values or functions are available for both the inlet and outlet boundaries. In order to postulate an appropriate boundary formation, Eq.3.39-3.41 can be used for velocity-temperature conditions during a stationary analysis as shown below.

$$u_{in} = U|_{in}, \quad v_{in} = V|_{in} \tag{3.39}$$

$$u_{out} = U|_{out}, \quad v_{out} = V|_{out} \tag{3.40}$$

$$T_{in} = T|_{in}, \quad T_{out} = T|_{out} \tag{3.41}$$

Similarly, for a transient analysis, the oil/winding temperature rise can be simulated as per IEEE/IEC recommendation as shown in Eq.3.42 [24, 43, 44].

$$T_{in} = T|_{in}, \quad T_{out} = T_{in} + \Delta T \left[1 - exp\left(\frac{-t}{\tau_{oil}}\right)\right] \tag{3.42}$$

where, ΔT is the constant temperature difference between top and bottom oil, and τ_{oil} is the time constant required to achieve a thermal equilibrium, as given by Eq.3.43.

$$\tau_{oil} = \frac{(0.132m_A + 0.0882m_T + 0.400m_O) \times \Delta T_\infty \times 60}{P_T} \tag{3.43}$$

where,

T_{in}, T_{out} is the fluid temperature at inlet and outlet respectively, K

M_a is the mass of un-tanked assembly without oil, kg

M_t is the mass of tanked assembly without oil, kg

M_o is the mass of oil, kg

ΔT_∞ is the average temperature rise of oil above ambient at stationary state, K

P_T is the total load losses, W.

Similarly, Neumann conditions are used in absence of specific values or function over participating boundary, where a gradient or flux can be imposed on either sides of the functional domain instead of these constant values to solve the velocity-temperature formulations within the regime while identifying the symmetrical boundaries, if any. Eq.3.44 and 3.45 shows Neumann based inlet and outlet velocity-boundary formations for a fully-developed hydrodynamic profile within the circulation region.

$$u_{in} = \frac{du}{dt}|_{in}, \quad v_{in} = \frac{dv}{dt}|_{in} \tag{3.44}$$

$$u_{out} = \frac{du}{dt}|_{out}, \quad v_{out} = \frac{dv}{dt}|_{out} \tag{3.45}$$

Similarly, Eq.3.46 shows the heat flux condition at the solid boundaries in x- and y-direction respectively. This is highly desired when a non-conjugate heat transfer analysis is required to simply estimate the winding temperature rise in absence of insulating oil in transformers.

$$q_x = -k_x \frac{dT}{dx}|_x, \quad q_y = -k_y \frac{dT}{dy}|_y \tag{3.46}$$

A typical Robin boundary condition is a combination of Dirichlet and Neumann formulation thereby producing a correlation between constant value and gradient. In

other words, Robin boundary conditions are applicable on radiator banks and tank walls, such that the resultant convective heat transfer coefficients at the appropriate temperature gradients can be imposed, as shown in Eq.3.47.

$$q' = \frac{Q}{A} = k\frac{dT}{dx} = h_\infty(T - T_\infty) \tag{3.47}$$

where,

q' is the heat flux, W/m²

Q is the total heat generated within the conducting coils, W

A is the total surface area of conductors, m²

h_∞ is the convective heat transfer coefficient at reference temperature, W/m².K

T_∞ is the reference temperature, K

T is the operating fluid temperature, K

It is not easy to find an analytical solution to Navier-Stokes equation, given the obvious complexities, therefore, following dimensionless numbers have been promptly used.

- **Reynolds number (Re)**: It indicates the flow pattern of oil by asserting the dominance of either inertia over viscous force (i.e.,turbulent flow) or vice-versa (i.e.,laminar flow) within the flow regime. It is also used to approximate the bulk oil velocity (u_b) within transformers and windings as given by Eq.3.48

$$Re = \frac{\rho u_b L}{\mu} \tag{3.48}$$

  where, L is the characteristic length of flow regime. In case of disc-type windings, the hydraulic diameter (d_h) replaces L in order to suit the small channel/duct flow area. Whereas in case of transformer tanks, the total height of oil flow (H) replaces L to suit the large flow interaction are.

  For disc-type windings, usually, the characteristic length is replaced by hydraulic

diameter (d_h) of the flow duct under analysis, whereas for the transformer tank, it is equivalent to the circulation height of oil(including radiators).

- **Prandtl number (Pr)**: It is an indicator of the thermal diffusivity within the system due to fluid conductivity, and is given by the ratio of momentum to thermal diffusivity of oil and expressed as shown in Eq.3.49.

$$Pr = \frac{C_p \mu}{k_f} \tag{3.49}$$

Generally, for mineral insulating oils, where Pr $\gtrsim$ 70, a fully-developed hydrodynamic profile is more likely to build up along the flow channel/duct boundary, hence rejecting the affect of thermal boundary layer thickness on temperature-velocity formulations.

- **Nusselt number (Nu)**: It is a significant parameter in determining the extent of cooling and is defined by a ratio of convective to conductive heat transfer at the interaction boundary as per Eq.3.50.

$$Nu_{loc} = \frac{h_{loc} L}{k_f} \tag{3.50}$$

where, Nu_{loc} is the local Nusselt number due to the local heat transfer coefficient, h_{loc} in a flow regime. However, for large regime area, an average Nu is highly desired that can be obtained by surface integration of the localized as given below:

$$Nu_{loc} = \frac{1}{L} \int_0^L Nu_{loc} dS \tag{3.51}$$

Previous experience on modeling of disc windings using these parameters express a passive convection (i.e. $Nu_{loc} \lesssim 1$) suitable for simulating natural convection within thin winding ducts.

- **Grashof number (Gr)**: It is one of the most prominent parameter pertaining to the conduction-convection studies in oil cooled transformers. Mathematically, it is the ratio of buoyancy to viscous forces in a flow regime as shown in Eq.3.52, and has the ability to indicate the strength of applied convection mode.

$$Gr = \frac{g\beta\Delta T L^3 \rho^2}{\mu^2} \tag{3.52}$$

A relative ratio of Re and Gr (i.e.,Re/Gr$^{1/2}$), also known as Robinson number, is one of the most widely used parameters in determining type of convection (i.e.,natural or forced) within transformers.

- **Rayleigh number (Ra)**: It quantifies the fluid motion as a ratio of conduction to convection heat transfer encountered by the body within the flow regime. It is imperative to obtain a constant heat flux condition in order to impose Ra on wall boundaries.

$$Ra = Gr \times Pr \tag{3.53}$$

Since the initial mass flow rate of oil was unknown, an approximation was used on the basis of available winding geometry and the known cooling mode of transformer. As the investigations were solely based on naturally cooled oil-filled power transformer, laminar flow regime (Re<2000) was logically acceptable. Moreover, applying a flux boundary condition will require an additional mathematical effort, some of which are purely hypothetical. Therefore, the base settings were done in a logical manner to overcome this shortcoming as discussed in the forthcoming section.

3.4   Base settings

In order to obtain the flow-temperature visualization, a disc-type geometry was studied. The investigated transformer was attached to a 225/26.4 kV feeder line with natural cooling of windings with detailed geometrical description available in [9, 10, 15]. Table 3.1 summarizes the geometrical configuration a particular segment of low-voltage winding that is investigated in the present work.

In order to establish a base model for stationary analysis information about some specific parameters is required that can be later modified to suit a time-dependent

Table 3.1: Geometrical configurations of a slice of LV winding proposed over thermal modeling in oil-filled power transformers [9, 10, 14, 15]

Specification	value
Total discs	78
Turn per disc	232
Disc width (mm)	50.8
Disc height (mm)	15
Width of axial channel (mm)	8.9 (inner),6.4(outer)
Height of radial channel (mm)	4.1
Inner distance from core (mm)	316.2
Total washers	4
Total Cu-strands	18
Total stick	18

analysis. The following subsections estimates these parameters based on the available transformer data.

3.4.1 Area and Volume Calculations

As oil enters from the bottom of winding, the inlet location and channel width defines the initial oil flow velocity. The oil flow velocity or mass flaw rate is a strong function of the inlet channel area, which is otherwise known as the effective cross-sectional area. With reference to Fig.3.6, the effective area and volume can be calculated using Eq.3.54 and 3.55.

In the same figure, R_{inc} is the inner distance from core, $R_{1,2,3}$ are the distances from the core including inner channel, slice of winding and outer channel respectively. Moreover, to apply finite element methods, all interactive nodes in a channel are indicated by numbers. It must be noted at this stage that in order to avoid complexity a simpler model is represented, whereas in actual modeling, the channels and ducts have themselves been

divided in to finite number of nodes.

$$A_{lvw} = \pi \ (R_3{}^2 - R_2{}^2) = \pi \ (0.38233^2 - 0.3759^2) = 0.015316 m^2 \qquad (3.54)$$

$$V_{lvw} = n_{lvw} \ \pi \ (R_2{}^2 - R_1{}^2) \ h_d = 78 \times 0.007 \times \pi \ (0.3758^2 - 0.325^2) = 0.06107 m^3 \quad (3.55)$$
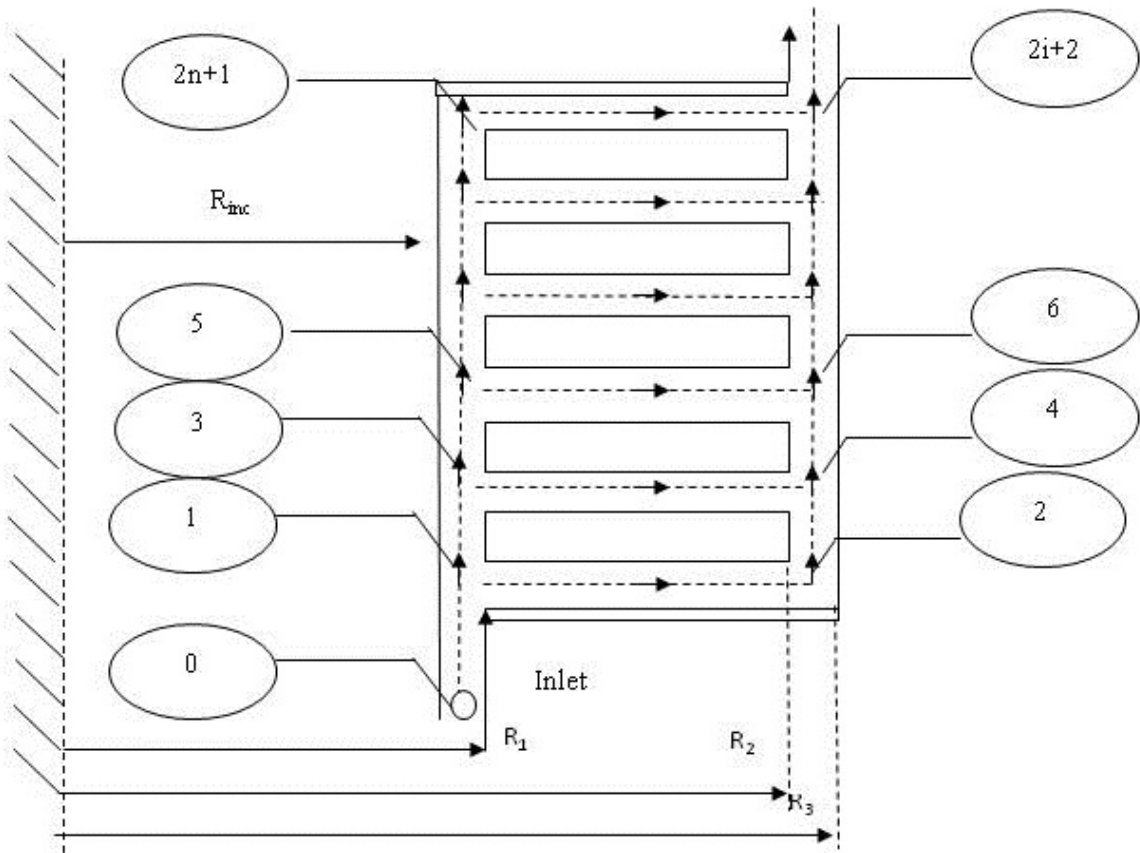
Figure 3.6: Interactive radii of the particular section of transformer geometry studied in the present work. Representation of 1°C in slice model [9]

3.4.2   Material Properties

One of the prime factors contributing towards the winding thermal performance are the thermodynamic properties of materials involved that are listed in Table 3.3 and 3.2.

Table 3.2: Thermodynamic properties of insulates and conductors [10,15]

Property	Copper	Kraft paper	pressboard
Density (kg/m^3)	8933	930	1200
Thermal conductivity(W/m.K)	383	0.04	0.19
Specific heat(J/kg.K)	385	1340	1340

Table 3.3: Various thermodynamic properties of naphthenic-base transformer oil [10]

Property	Function
Density(kg/m^3)	1098.72-0.712T
Dynamic viscosity (Pa.s)	0.08467-4$\times10^{-4}$T+5.0$\times10^{-4}$T^2
Thermal conductivity (W/m.K)	0.1509-7.101$\times10^{-5}$T
Specific heat(J/kg.K)	807.163+3.58T
Volumetric expansion (1/K)	7.5$\times10^4$

3.4.3   Oil-flow Rate

As per our previous assumption, Reynolds number (Re) can be used to calculate the inlet flow velocity of oil as shown below.

$$Re = \frac{\rho u d_h}{\mu} \qquad (3.56)$$

where d$_h$ is the hydraulic diameter and equivalent to the inlet diameter assumed 6.4 mm in this particular case. This would mean that the inlet of oil was located on opposite side from the exit hence allowing a zig-zag flow pattern. An acceptable Re of 42 was adopted after several hit and trail methods to obtain a resultant velocity of 0.00612 m/s.

Using the Prandtl number (Pr) correlation, one can evaluate that at oil inlet temperature with respect to the oil properties, it is higher than 70 and thus flow is fully developed hydro-dynamically.

Similarly, by using Grashof number (Gr) one can estimate that in case of a single pass with dimensions specified as above, the limit is well within 1.51×10^8 and hence natural convection prevails.

Rayleigh's number (Ra) will agree to this base settings in order to prove that convection dominates the proposed temperature rise mechanisms.

3.4.4   Volumetric heat density

Usually, for stationary state analysis, a constant heat source is mentioned as per the power losses and volume of winding. In this case, two separate heat source can be identified as follows:

$$Q_{lvw} = \frac{n \times P_w}{V_{lvw}} \qquad (3.57)$$

The aforementioned equation is valid in case of stationary analysis, however when a loading pattern is to be simulated, the winding losses becomes a time dependent function. In this case, since the power losses at variable loads were calculated using the following correlation:

$$P_w(t) = L^2(t) \times P_{w,hrt} \qquad (3.58)$$

where, L is the time dependent loading pattern and $P_{w,hrt}$ is the winding loss obtained from heat-run test at reference temperature of 75°C. The loading was varied in accordance with IEC 60354 and the initial winding losses was kept at 676.9 W/disc as reported in [9, 10].

3.5   Transformer description

The internal construction of this transformer is shown by Fig.3.7 and consists of disc-type winding representing the high and low-voltage windings respectively. The geometry of insulated windings is similar to that reported in [10]. The reader can refer to the published works by [10, 15, 29] to study more about the transformer specifications.
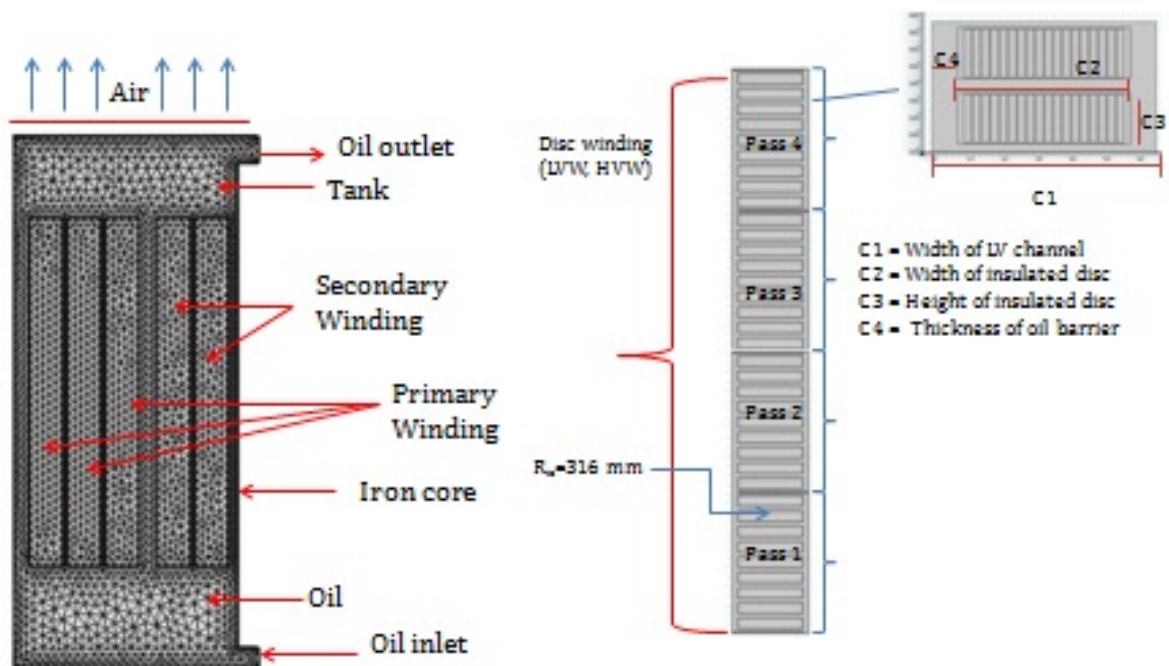
Figure 3.7: Schematic representation of the transformer tank, winding and disc geometry

3.6   Meshing and Grid Analysis

COMSOL Multiphysics has some in-built features that allows the user to adopt either automatic or manual meshing of the functional domain based on the governing physics or structural complexity. In case of any 2D-axisymmetric geometries, discretization of a functional domain can be achieved by applying either triangular or quadrilateral elements.

In the present work, first a comparison of the in-built triangular and quadrilateral meshes is done to achieve a benchmark for the future simulations. Later on, the observations from user-controlled meshes are compared with an automatic physics-controlled mesh to obtain a satisfactory discretization scheme. Fig.3.8 shows the proposed meshing schemes near the winding inlet with and without refinements respectively. To isolate the effect of residual function and unnecessarily dense meshing of the output variable, comparative observations have been also summarized in Table.3.4.
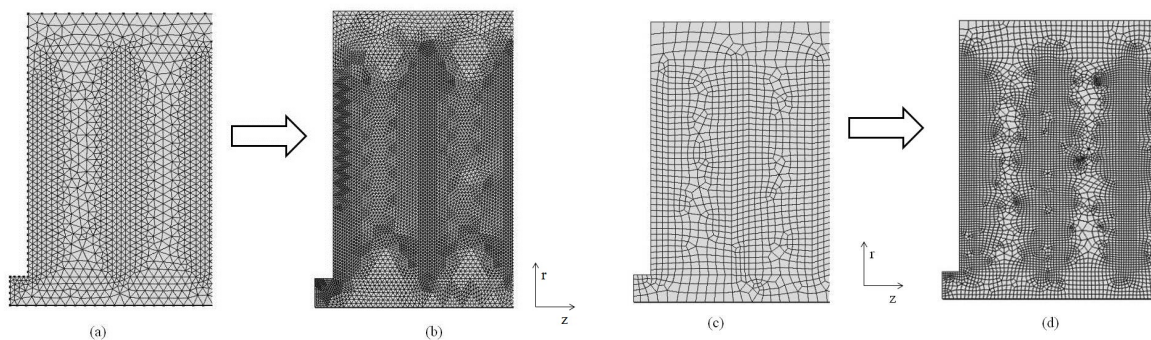
Figure 3.8: Proposed grids to study output variables on (a) non-refined triangular, (b) refined triangular, (c) non-refined quadrilateral, (d) refined quadrilateral mesh schemes

Grid analysis of any meshing scheme defines the independence of output variables on the nature of grid [107]. It also requires one to obtain an optimum number of elements to achieve the desired solution and relies on convergence ability of the applied solver. In order to analyze the grid acceptability , mesh resolution and element quality are the two most important parameters in COMSOL Multiphysics. The mesh resolution can directly influence the accuracy of a proposed solution by justifying the shape of nodal element.

Since nodal elements (triangle, quadrilateral, tetrahedral etc.) influences the solver technique, highly dense meshing with low resolution in areas of significance can predominantly reduce the accuracy of solution. Moreover, it is an indirect

Table 3.4: Mesh sensitivity analysis on input and out variables

	Free triangular			Free quadrilateral		
Parameter	Mesh1	Mesh2	Mesh3	Mesh1	Mesh2	Mesh3
N_{elem}	8284	27740	35708	8554	24310	34982
$T_{hst}(^\circ C)$	92.97	78.813	82.4	92.4	80.749	86.598
$U_{max}(m/s)$	0.0592	0.0726	0.0728	0.062	0.0731	0.0733

representation of element quality as a ratio of its volume to edge length that varies within [0,1], where 0 represents low resolution (lower accuracy) and 1 represent highest resolution.

On the other hand, the element quality of a mesh represents the extent of irregularities in the element shape and must be avoided at all costs to preclude solver convergence. Fig.3.9 shows the mesh quality plots obtained by automatic and manual meshing respectively of the disc winding in COMSOL(V4.3) [107].
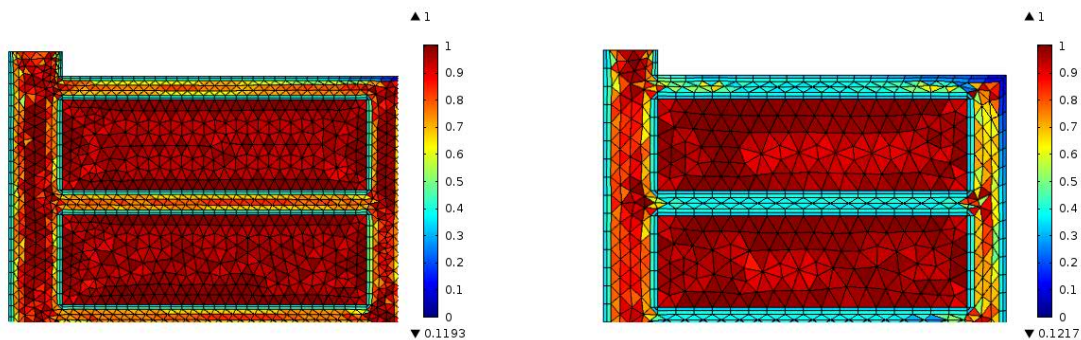
(a) Automatic meshing of disc windings with higher resolution around corners

(b) Manual meshing of disc windings with lower resolution around corners

Figure 3.9: Comparisons on mesh quality ans resolution using automatic and manual meshing

In the present work, the inlet temperature of oil was known previously, however that at the exit was unknown. Similarly, although it is assumed that the Cu-strands are operating at a higher temperature, the actual specific value is unknown, and is presumably

changing with oil flow behavior. It is also observed that with improvements in the mesh resolution, the accuracy of solution can be increased. This is more evident from Table.3.4, which suggests that besides the obvious bulk oil temperature, significant changes in hot-spot temperature has been recorded. Whereas, the velocity variations are however very minimal.

Thus in conclusion, it can be said that temperature variations are the driving aspects for dynamic moisture migrations. In order to estimate reliable temperature profiles one must look into the various sub-parameters that are affecting the accuracy of this model simultaneously. A reliable moisture dynamics model can therefore be proposed only when one has the understanding of the dynamic temperature variations in transformers.

Fig.3.10 shows the effect of structured refined and non-refined meshes on oil exit temperature that has been obtained by numerical approximation of the governing equations at the channel outlet.
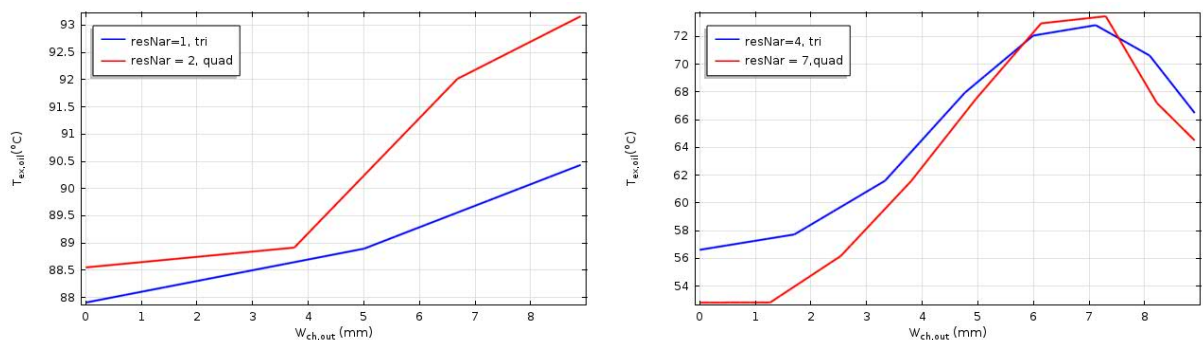
(a) Non-refined structured meshing with low resolution around corners

(b) Refined structured meshing with high resolution around corners

Figure 3.10: Comparisons on oil temperature at exit with various meshing schemes

3.7 Summary

This chapter discusses the numerical models fr moisture diffusion and desorption with respect to thermal performance assessment of oil-filled transformer windings. The

models also discusses the coupling of multiple physics and thereby assisting the reader to understand the multiphysics models for moisture measurement in oil-filled power transformers. In the upcoming chapters theses models are analyzed using on-site data available from operating transformers.

Chapter 4

RESULTS OF THERMAL MODELING

This chapter is a discussion on the CFD-based thermal modeling of transformers with respect to variable operating conditions. Section 4.1 discusses the preliminary model of an insulated disc subjected to resistive heating. Section 4.2 is the discussion on a winding model under stationary conditions to isolate the effect of geometry on oil temperature rise. Section 4.3 documents the time-dependent load contributions towards temperature rise models for oil and winding. The chapter ends with summarizing the major findings from thermal modeling of disc-type transformer under stationary and transient operating conditions.

4.1   Disc heating model

As discussed previously, resistive heating of Copper (Cu) conductors leads to an increase in winding temperature, which in turn increases insulation temperature. Ref. [10, 73] are the only sources where effect of insulating domain is identified as a potential contributor towards average disc temperature. Incidentally these models use

the presence of paper to pin-point the location of hot-spot but disregarded any possibility of a thermal gradient between insulating paper and Cu-strand.

A disc-conductor is generally a consolidated set of Cu-strands woven together in multiple turns and insulated by Kraft paper of known thickness. A 2-d heat conduction model can be proposed for a simple conductor geometry as shown in Fig.4.1.
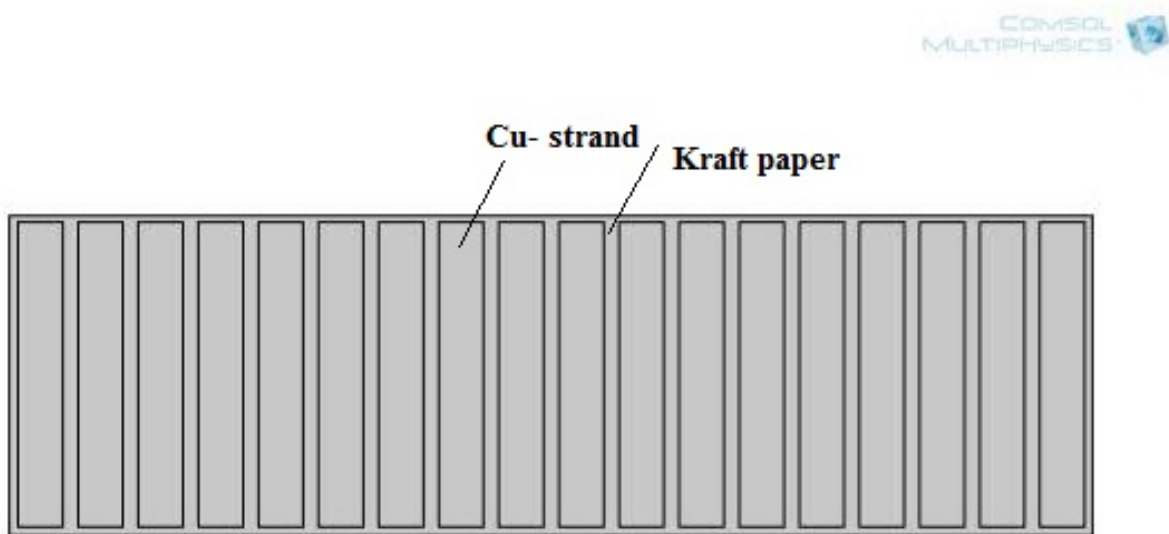
Figure 4.1: Simulated conductor geometry [10]

A simple heat transfer model for the aforementioned geometry can be proposed by applying a known velocity field across the heated component. In this case, a known velocity of oil flow was introduced from the bottom of disc to replicate the actual oil-disc interaction. A known disc-heat source was employed to calculate the temperature rise in insulator and conductor by interactions with external flow field.

Fig.4.2(a) and (b) shows the thermal gradient between paper and conductor on left and right side of the disc and proposes that this gradient is indeed very small thus rejecting the additional mathematical effort to represent paper as a participating media.

This observation is very significant for the future simulations because it clearly suggests that paper indeed works on bulk conductor surface temperature and therefore further simulations on moisture diffusion from cellulose and the distribution between oil

and paper near winding must be done on average winding temperature.

(a) Cu-Paper inner temperature gradient

(b) Cu-Paper outer temperature gradient
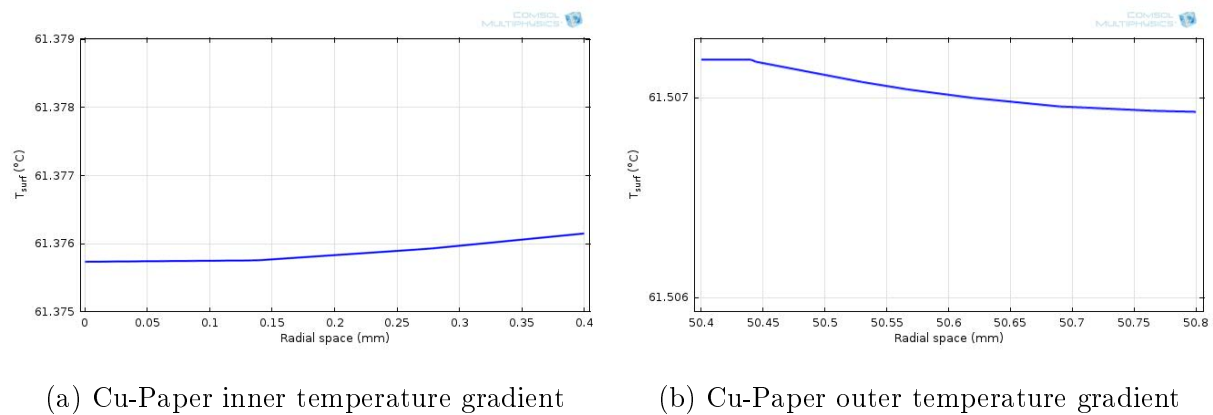
Figure 4.2: Temperature gradient between Kraft paper and Cu conducting strands

Although the insulation thickness is a deciding parameter in determining the thermal gradient between paper and Cu-strand, it is highly unlike to exceed more than 2°C. As seen from the aforementioned model, the temperature of paper is relatively closer to that of Cu-strands hence, the discs can be considered as a consolidated Cu block thus reducing an additional computational effort. Moreover, only the average temperatures obtained within the disc windings during stationary state is of prime significance due to its effect on moisture diffusion studies that will be discussed later in Chapter 5.

As the oil temperature is more active upon load variation, a thorough winding model can suggest the instantaneous moisture in oil obtained under aforesaid conditions. The oil temperature thus obtained can be used further to determine the instantaneous water solubility and equilibrium shifts respectively.

4.2   Winding Model: Stationary Mode

During transformer cooling, oil enters at the bottom and exits from the top of the windings. In case of natural cooling transformer, oil-guides are installed strategically to increase the rate of heat transfer by introducing a zig-zag flow pattern. Assuming the proposed windings behaves in a similar way, a stationary model is proposed to estimate

the effect of oil flow circulation on temperature distribution within a winding.

As a benchmark, Fig.4.3 exhibits the pattern of oil and temperature rise in disc-type windings at various locations. In order to obtain this, the base settings discussed in Chapter 3 have been applied to the in-built CFD module of COMSOL Multiphysics.

The heat transfers from one disc to another and eventually throughout the winding by conduction. As an oil circulation is introduced, the heat transfer from the winding to oil by convection. Therefore the overall temperature distribution in transformers is a strong function of the oil flow distribution. The aspect ratio of a conventional disc type winding is generally more than 1.

This would mean that the heat will transport rapidly in the axial direction as compared to the radial direction. If we consider a slice model, the heat transport in axial channels would be much faster than radial ducts.
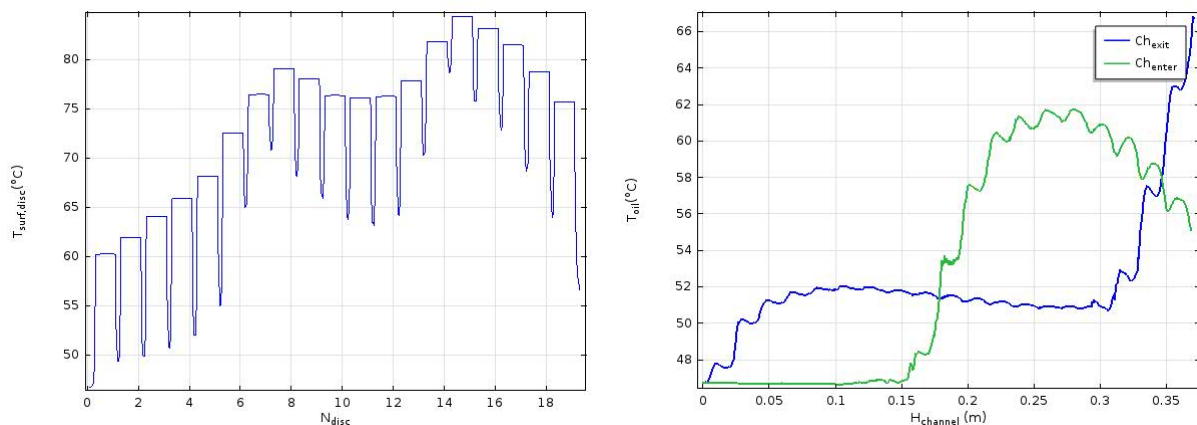
(a) Simulated surface disc temperature. The maximum surface temperature is obtained at the 15th disc (hot-spot location)

(b) Simulated centerline temperature within the entrance and exit axial channels of the second pass from the bottom of a winding

Figure 4.3: Simulated disc and oil temperature of the second pass of the low-voltage winding containing total 78 discs. The base velocity is 0.061 m/s and the base temperature is 46.7°C applied to the inlet located in the outer channel

The stationary state CFD analysis of single pass of this winding reveals a reference

maximum temperature of 84.39 °C at the 15th disc surface. A centerline tracing in the exit channel produces a maximum velocity of 0.0627 m/s. The step-type graph showing the surface temperature of discs in Fig.4.3(a) is essentially the surface temperature calculated across a centerline trace which intersects both oil and conductors. The depression in this graph is the indicator of oil field presence within two conductors. Similarly, a sigmoidal graphs showing the centerline oil temperature in entrance and exit field is the indicator of zig-zag flow due to opposite positioning of the inlet and outlet channels.

A single pass model may not be sufficient to obtain the top-oil temperature variation even during the stationary stage. However a consolidate winding temperature rise model suggested in [15] shows that the proposed section is where one can expect the transient time response rather than towards the top. Hence, this particular section has been subjected to obtain a benchmark of load-induced temperature variations that will be used for justifying moisture distribution in operational transformers.

Now that we have our desired benchmark, it is possible to apply load variations to the proposed thermal model in order to obtain the desired transient temperature rise profiles. A series of case studies have been performed in this regard that have been discussed below.

4.3   Effect of Daily Operations

The daily operating cycle of a transformer fluctuates heavily. This is primarily because of the load behavior and daily ambient variations. Although it is not easy to simulate the exact behavior of transformer windings during load variation, an attempt has been made. It is assumed that since loading directs affects the power losses in winding, the resultant heat source becomes a transient term. Based on this hypothesis, following case studies have been explored.

4.3.1 No-load variation

The no-load condition in transformer indicate the absence of a applied current and voltage to the primary winding. In this case, due to the absence of winding losses, core-losses leads to whatever minimum heat that is generated. Naturally, the temperature difference at the top and bottom of the winding will be negligible thus suggesting a total thermal equilibrium condition. Simulating a no-load condition does not provide an appreciable distinction between oil and winding temperature and hence, restricted for moisture dynamic predictions only.

4.3.2 Daily load variation

In this case, a typical load pattern was modeled, first assuming a step rise and them assuming a combination of load patterns on the transformer windings.Fig.4.4 is presents a perfect quantification of temperature rise assuming a the proposed steps.

It can be seen from the same figure that an initial step is introduced as soon as the transformer was charged. It was assumed that the transformer was rated at its full capacity. The change in winding losses was measured as per our discussion in Chapter 3. The temperature variations during step loading shows that the time taken by the oil-immersed winding to respond and achieve a thermal equilibrium is must faster (<1 hour). Thus it can be established that the temperature moves faster than moisture and hence, time response for thermal transients would be much smaller (within few minutes).

Further more, the effect of these loading on the maximum surface temperature per disc was also studied as shown in Fig.4.5.

Similarly, the oil temperature variation immediately near the winding due to a typical daily loading condition is given by Fig.4.6, where it is observed that despite the fast fluctuations, the exit temperature kept on increasing. It means that not only the flow guides are allowing a proper mixing of oil within axial and radial channels but also causing
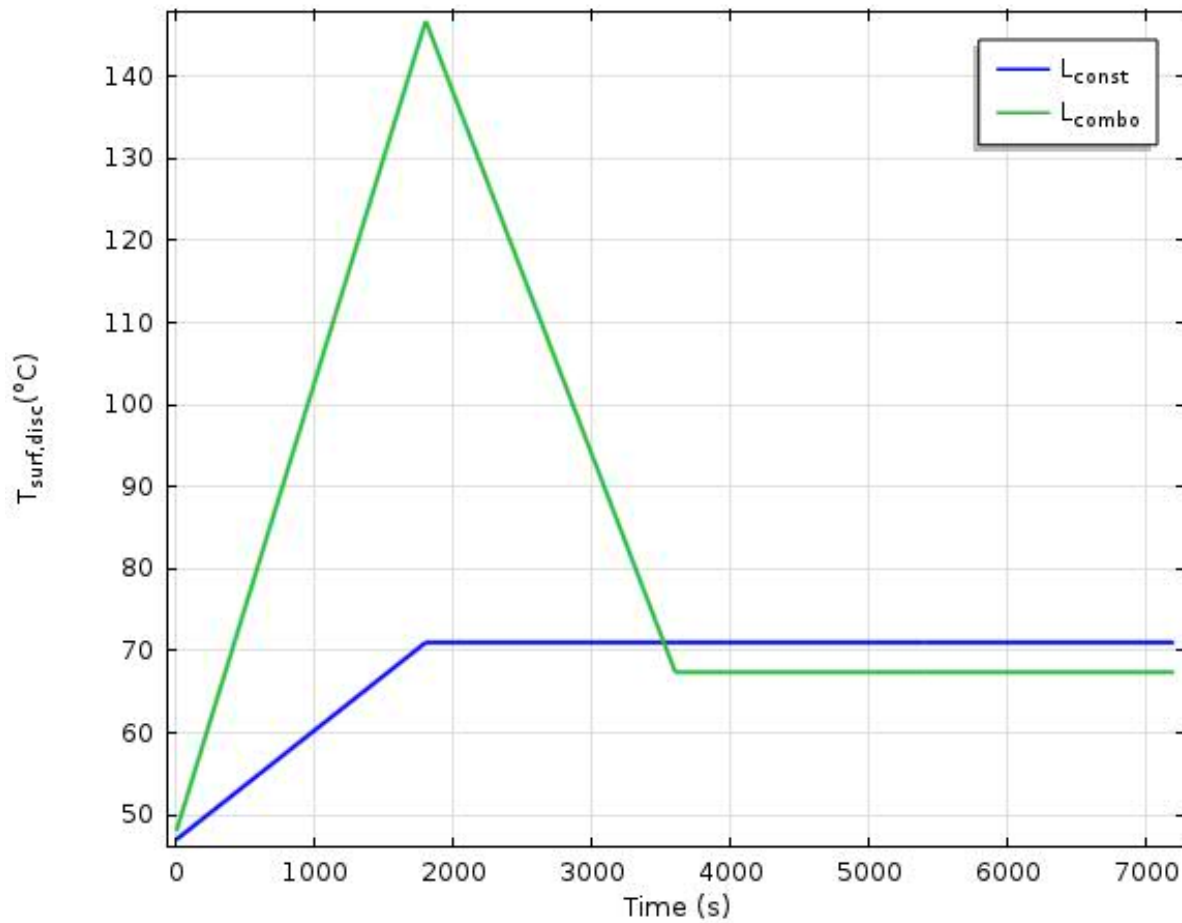
Figure 4.4: Comparisons on the loading behavior of windings using constant (step) and combination variation

.

a uniform mixing.

A comparison with Fig.4.7 can tell the reader a lot about the effect of a hydro-dynamically developed profile on oil temperature rise. The sigmoidal shape at the top suggests that due to the presence of another barricade near the exit, the oil direction was modified again hence leaving the top-most less hotter.

In order to create a sustainable model to co-simulate temperature and moisture distribution in transformers, a two step process needs to be implemented. The first step determines the temperature distribution in consolidated windings and at various
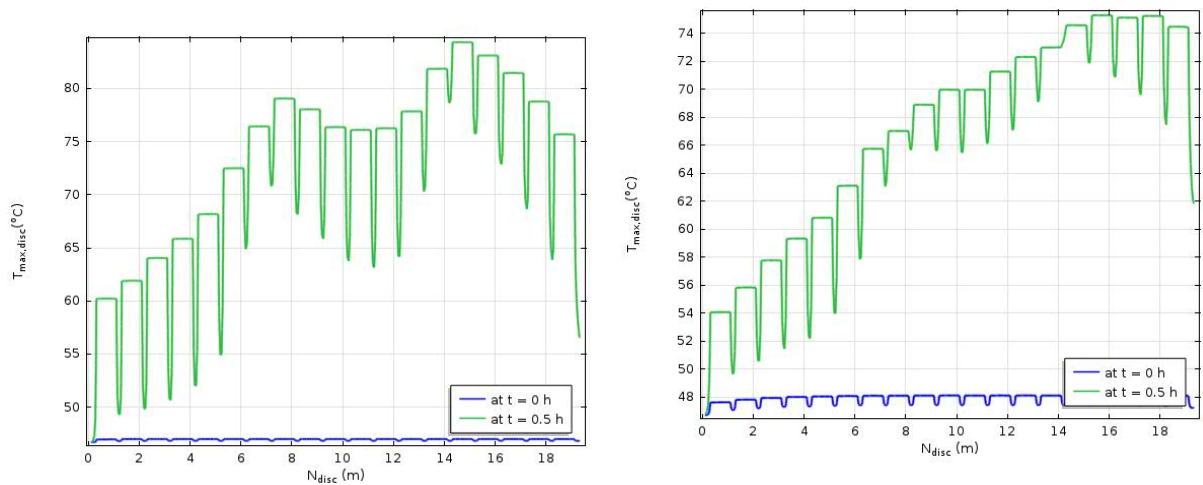
(a) Maximum surface temperature per disc recorded after the first step introduction

(b) Maximum surface temperature per disc recorded with a combination of loads to replicate the daily loading cycle

Figure 4.5: Comparative analysis of transformer winding temperature rise according to load pattern variation

locations of the transformer tank. The second step utilizes this temperature variation as a reference to calculate the moisture concentration in oil and paper thus considering the affect of load and ambient temperature.

Another significant contribution was to establish that the paper insulation not only insulates but also provides a reluctance to temperature rise in oil-immersed windings. In this case, although the hot-spot location may not vary so much, but the magnitude varies largely shown in Table 4.1. Moreover these results are obtained while applying a combination of loads that have been formulated according to the logic mentioned earlier.

In conclusion, one can say that the predicted temperature was in agreement with the prescribed value. A shift in hot-spot magnitude was very evident with inclusion of paper insulate in thermal model. Since these values are much below the IEEE prescription, it is safe to assume that aging is non-existent, at least at this stage. The oil and winding values have been utilized further to quantify moisture migrations under different conditions.
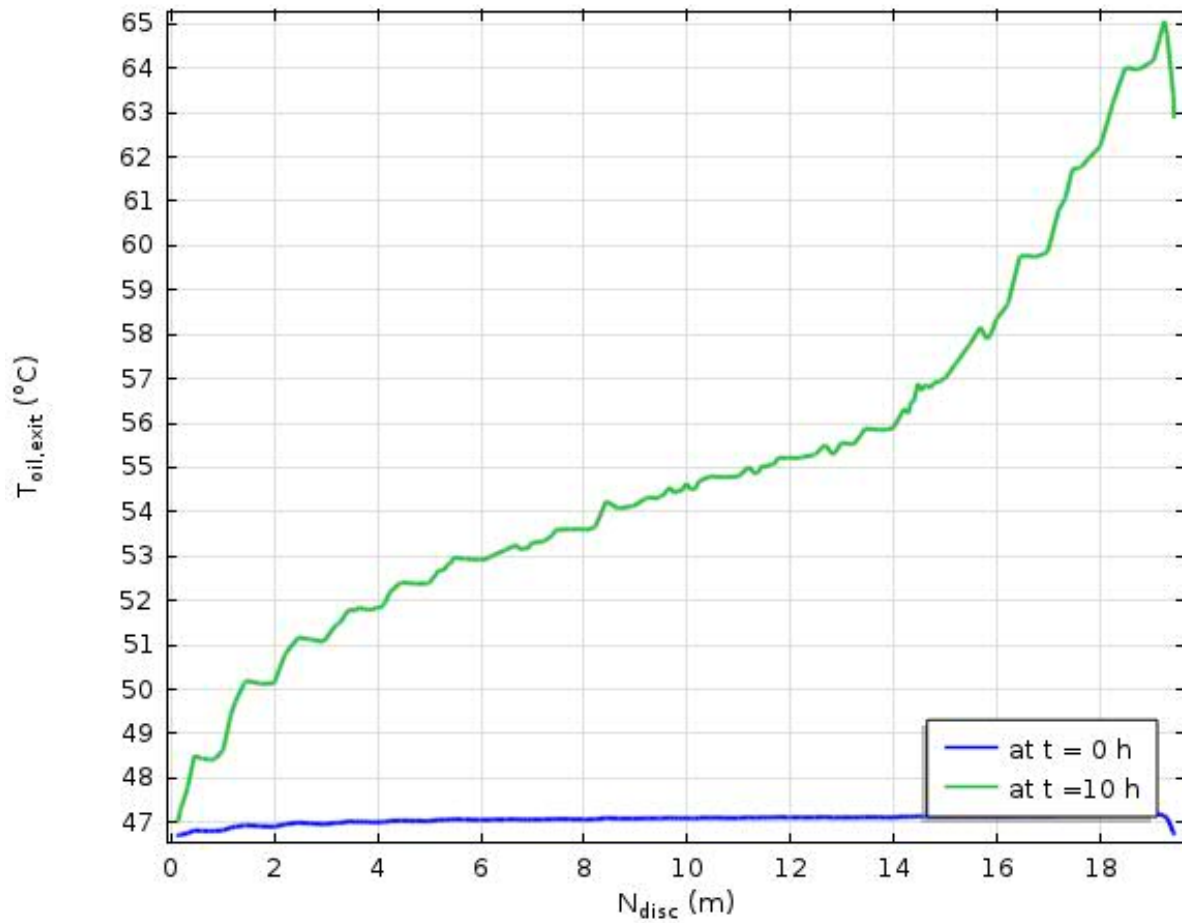
Figure 4.6: Rise in oil temperature immediately near each disc in the exit channel, when the inlet was specified at 46.7°C and 0.0612m/s

Table 4.1: Effect of paper insulation on winding temperature rise

Model	T_{ex}	T_{avg}	T_{hst}	HST-location
CHT with paper	62.5	60.5	64.2	5th from top
CHT without paper	56.71	70.95	81.3	5th from top

4.4 Summary

This chapter discusses the numerical modeling results of the thermal performance of oil-filled power transformers using fundamentals of CFD. It was observed that the
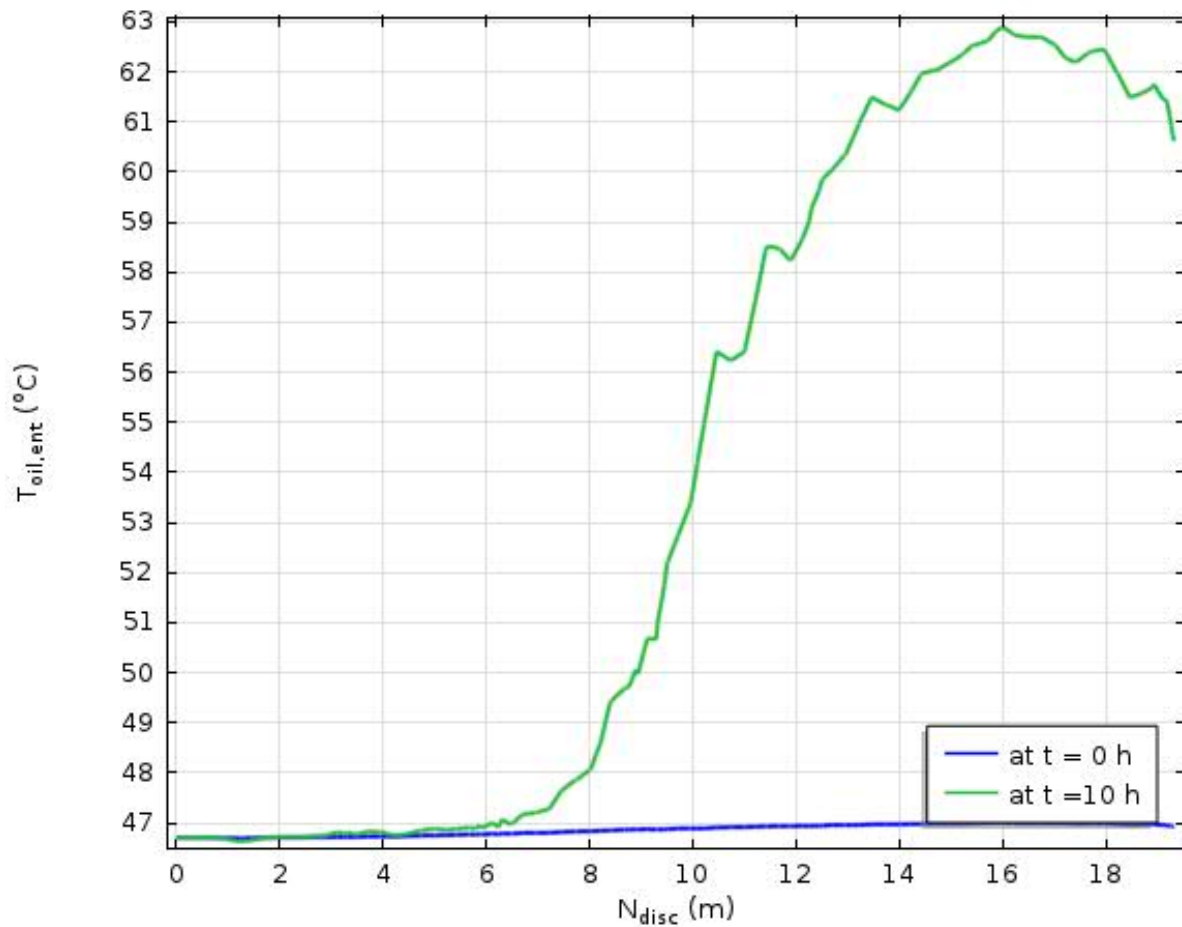
Figure 4.7: Rise in oil temperature immediately near each disc in the exit channel, when the inlet was specified at 46.7°C and 0.0612m/s

convection pattern and structural complexities plays a significant role in determining the thermal performance of transformers. It was also observed that disposition of hot-spot temperature can significant change the thermal profile thereby influencing the oil and winding temperatures. These results suggests that the temperature rise in operating transformers during daily loading cycles changes swiftly thereby indicating a continuous disposition in the so-called equilibrium stage of moisture and temperature interactions. These results hence become a benchmark to observe the temperature influenced transient moisture dynamics in oil-filled power transformers.

Chapter 5

RESULTS OF MOISTURE MODELING

This chapter summarizes the investigations on moisture dynamics in power transformers through mathematical modeling. Section 5.1 deals with the effect of various physical parameters on moisture sorption using drying models. With the help of various operating modes, the elaborate discussion in the respective subsections correlates these parameters with average moisture discretization and its influence on response-time during transient analysis. Section 5.2 provides a closer look at the moisture interactions on the oil-paper interface during variable operating conditions. The fluctuating temperature profile in oil and winding obtained from Chapter 4 has been associated with the moisture changes through relative saturation and shifting equilibrium. These results are the most realistic representation of moisture measurements within a functional transformer without the need for disembarking or intrusive testing and hence are cost-effective and time-efficient.

5.1 Moisture-in-Paper Model

During transformer drying or on-load conditions, the winding temperature is higher than that of the surrounding media and bulk moisture migrates from paper or pressboard to the nearby media contained within the encapsulated unit. While this media is oil in case of an operational transformer, it may be hot air/oil, nitrogen (N_2) or vacuum depending upon the drying requirement.

Generally, water transport through the solid insulation is a slow process, but a transient condition may exist when there is a shift in thermal equilibrium between bulk source and surrounding media. All moisture-in-model results are obtained by solving Eq.3.6 with appropriate boundary conditions as discussed in Chapter 3.

Determination of response time during transient equilibrium condition signifies the time instant whereupon the first change is apparent. Theoretically, it depends on the effective diffusion coefficient, thickness of insulation and exposure sides as given by Eq.5.1 and 5.2 respectively. But various permutations in this study shows that it also depends on initial and equilibrium moisture concentration, surface temperature and impregnation condition of the insulate.

Single sided diffusion (ss):

$$\tau_{ss} = \frac{4d^2}{\pi^2 D_{eff}} \tag{5.1}$$

Double sided diffusion (ds):

$$\tau_{ds} = \frac{d^2}{\pi^2 D_{eff}} \tag{5.2}$$

where,τ is the equilibrium time constant (h), d is the thickness of paper/pressboard (m) and D_{eff} is the effective diffusivity (m^2/s).

Table 5.1 summarizes the available diffusion coefficients from previous studies.These coefficients are obtained by experimental investigations on insulation paper/pressboard of known material properties (i.e.porosity, density, thickness and impregnation state).

Table 5.1: Diffusion coefficients of oil-impregnated (OI), and non oil-impregnated (NOI) Kraft paper (KP), and pressboard (PB) insulation as reported in various literature sources

Author	Insulation condition	$D_0(m^2/s)$	k'	$E_a(K)$
Ast [67]	NOIKP	2.25×10^{-11}	0.1955	8834
Guidi [16]	OIKP	6.44×10^{-14}	0.5	7700
Foss [12]	OIKP	1.34×10^{-13}	0.5	8074
Foss [12]	NOIKP	2.62×10^{-12}	0.5	8140
Du [11]	NOIPB	0.67×10^{-12}	0.45	7646

Besides, some previously published data suggests that the total diffusion time for moisture migration between paper to oil depends on its thickness, concentration and temperature of operation as shown in Table5.2.

Table 5.2: Reported diffusion time constants for oil-impregnated pressboard insulation of 1mm thickness under various temperature

Temperature($^\circ$C)	Diffusion time (days)		
	1mm	2mm	4mm
20	93	373	1493
40	20	79	317
60	4.2	17	67
80	0.9	3.6	14

Table 5.3 provides a basis for future calculations through on-site transformer data, and Table 5.4 shows the various parameters investigated in this work to isolate their effect on moisture-in-paper models.
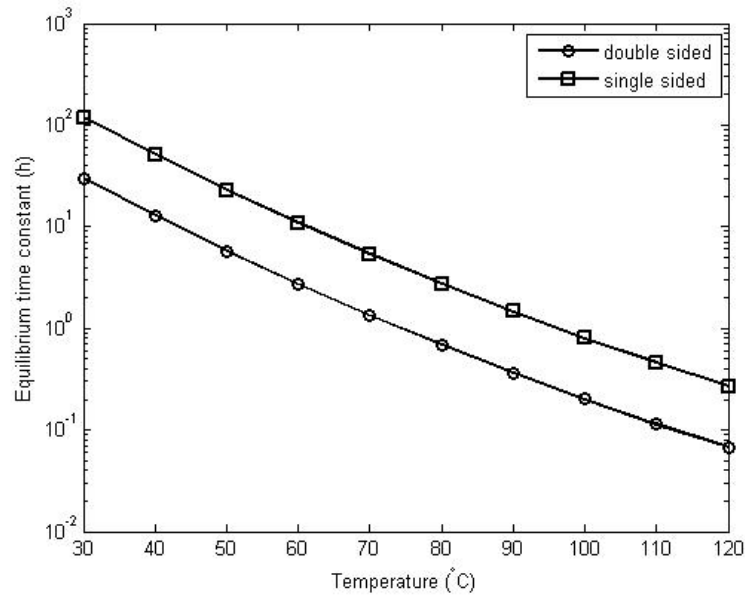
Figure 5.1: Effect of variable temperature on diffusion time constant for 1mm thick oil-impregnated Kraft paper sample with 3% moisture

(a)   (b)
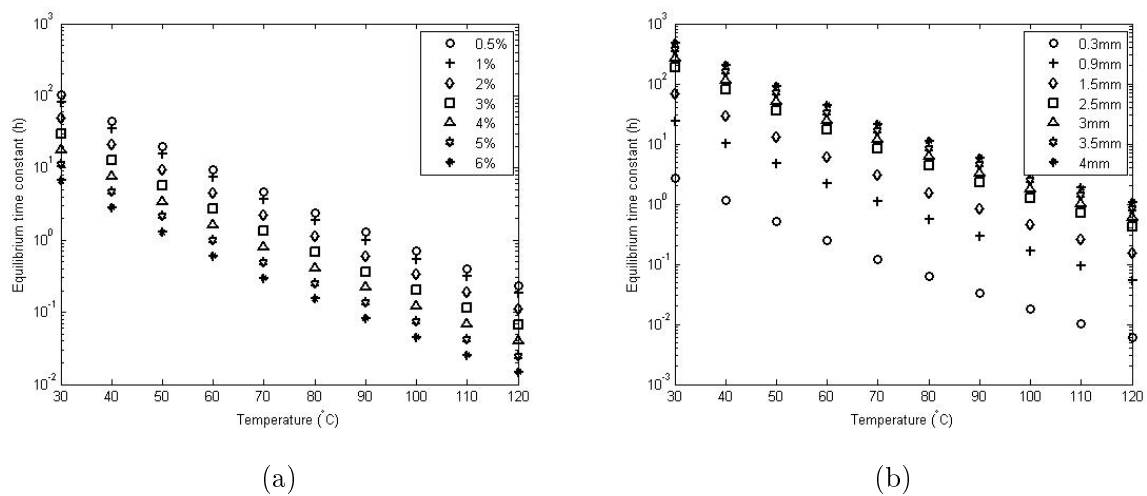
Figure 5.2: Simulated effect of a)variable concentration in paper on equilibrium time constant, b)variable paper thickness on equilibrium time constant

5.1.1   Effect of diffusion coefficient:

Furthermore, Fig.5.3 shows the effect of diffusion coefficients on moisture determination in 1mm thick oil-impregnated Kraft paper samples at the actual average winding

Table 5.3: On-site data recorded for 132/33 kV 50 MVA oil-filled power transformer at
Jaipur, India

	Oil	**Support**	**Spacers**	**Kraft paper**
Mass	22500kg	1125kg	450kg	675kg
Moisture	16 ppm	2.2%	2.2%	1.8%
Temperature	52°C	-	-	48°C

Table 5.4: Investigated parameters for moisture dynamics in oil-filled power transformer

	Thickness (mm)	**Temperature (°C)**	**Density (g/cm^3)**	**Initial Moisture (%)**
Pressboard	1,1.5,3	30,50,70,90	0.95-1.2	0.5
Paper	1,2,3	40,60,80,100,120	0.93	0.5

temperature.

It can be seen from the same figure that the diffusion coefficients proposed by Asem [48] using vacuum drying experiments produce a contradictory picture of saturation time as compared to the other conventional coefficients by [12, 16]. This must because of the presumption that diffusion coefficient is dependent on moisture concentration and independent of temperature.

Despite the allowed tolerance reported in their respective work, an estimated error of 7.14% with Foss's data and 16.57% with Guidi's data was observed upon comparison with Asem's experiments. Although it can be observed that universality on diffusion coefficients does not exist due to variation in experimental techniques, yet Foss' data can be considered more realistic due to lower error and higher extrapolation accuracy.

Similarly, Fig.5.4 shows the comparative average moisture distribution analysis in non-impregnated Kraft paper samples of 1mm thickness at 75°C with 2.2% surface moisture
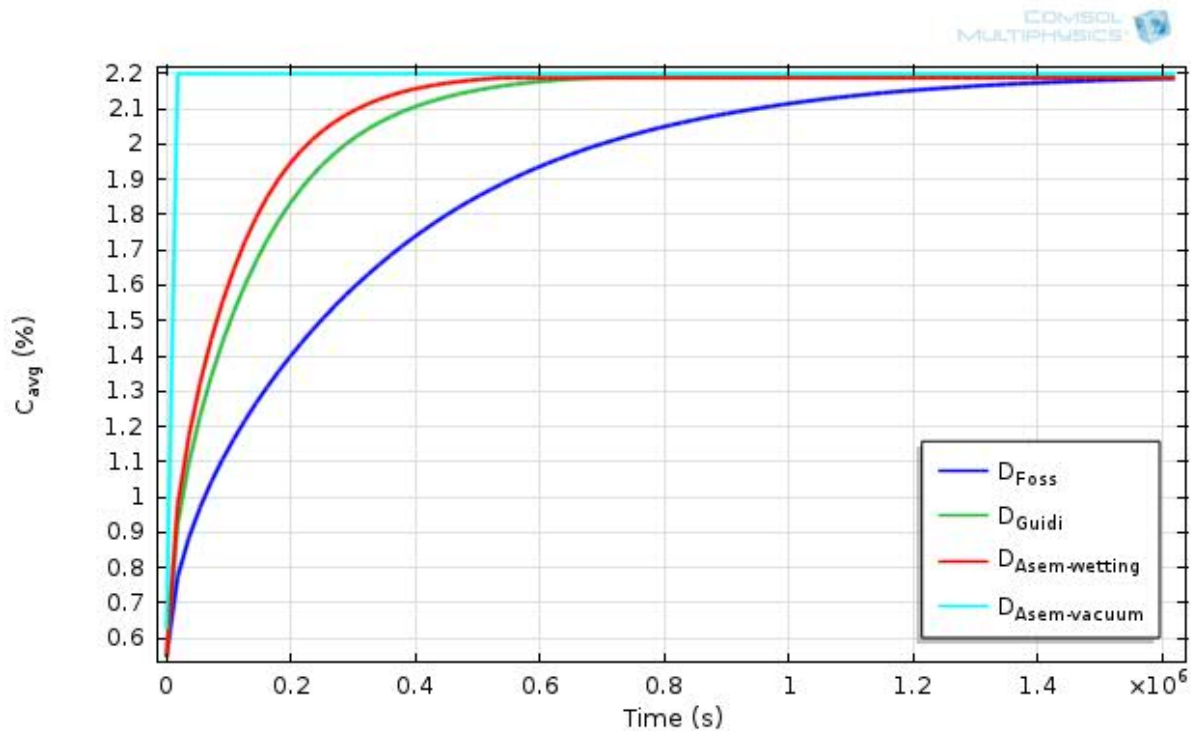
Figure 5.3: Simulated results on effect of diffusion coefficient over average moisture distribution in oil-impregnated Kraft paper sample of thickness 1mm

concentration using coefficient proposed by [11,12,111].

It must be noted that the diffusion coefficients reported by Asem [48] and Ast [67] can not be used in this study due to the vast difference in densities of the investigated materials. Also, due to complex nature of pressboards very few sources have reported coefficients for non-impregnated pressboard samples, where acceptable coefficients for oil-impregnated pressboards are yet to be proposed.

This leads to a conclusive proof that although diffusion coefficient can not be universal value, yet its determination will require exhaustive experimental investigations that are currently beyond the scope of this thesis. In the present work, extrapolation of the data published by various authors have lead to the required diffusion coefficients applicable to solve the proposed model.
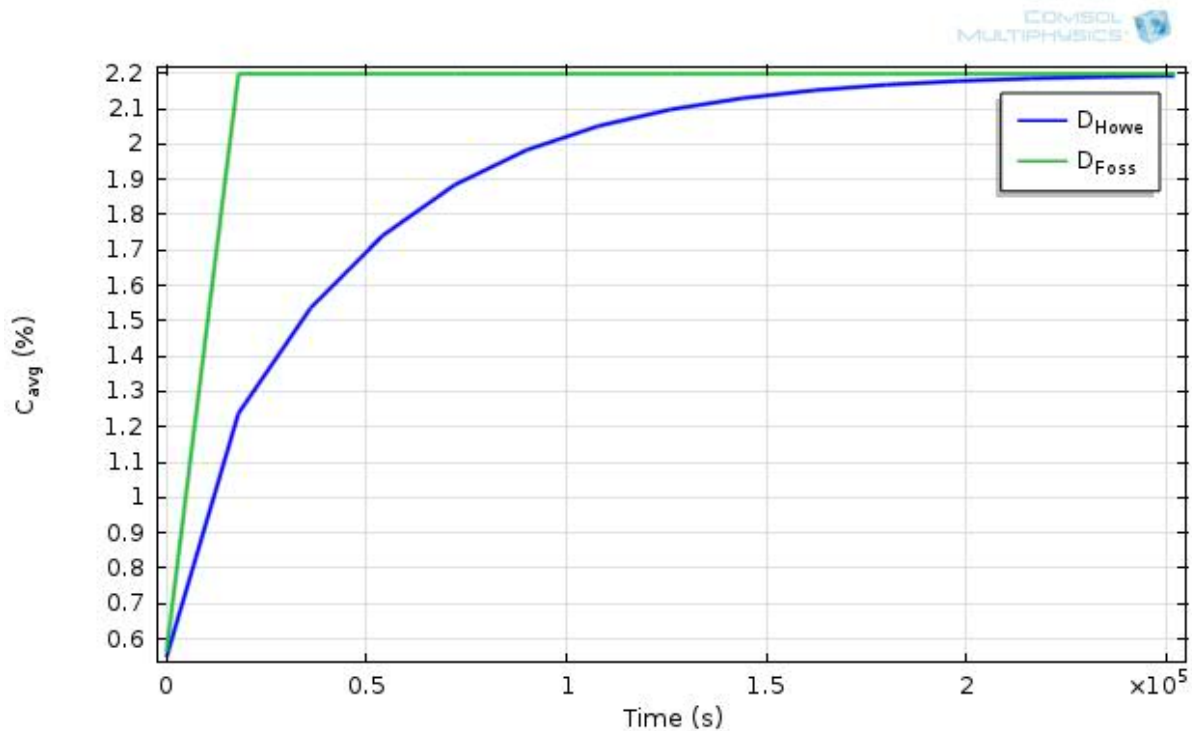
Figure 5.4: Simulated results on effect of diffusion coefficient over average moisture distribution in oil-impregnated Kraft paper sample of thickness 1mm

5.1.2 Effect of material type

To isolate the effect of material type on moisture removal, Fig.5.5 discusses a classic example of a hot-oil drying operation during on-site water removal. Oil-impregnated paper and non-impregnated pressboard sample of variable densities are subjected to moisture removal such that, the equilibrium condition formulated at the boundary of oil-paper interface depends on the partial water vapor pressure and oil temperature.

Fig.5.5a and 5.5b shows the drying curve for oil-impregnated Kraft paper and non-impregnated pressboard samples in accordance with previously published experimental data [11, 12, 48, 111] at a uniform time-stepping of 2 hours.

A conditional reverse is employed when an already dried winding comes in contact with moist oil/air and tries to achieve an equilibrium while adhering to the strictly isothermal
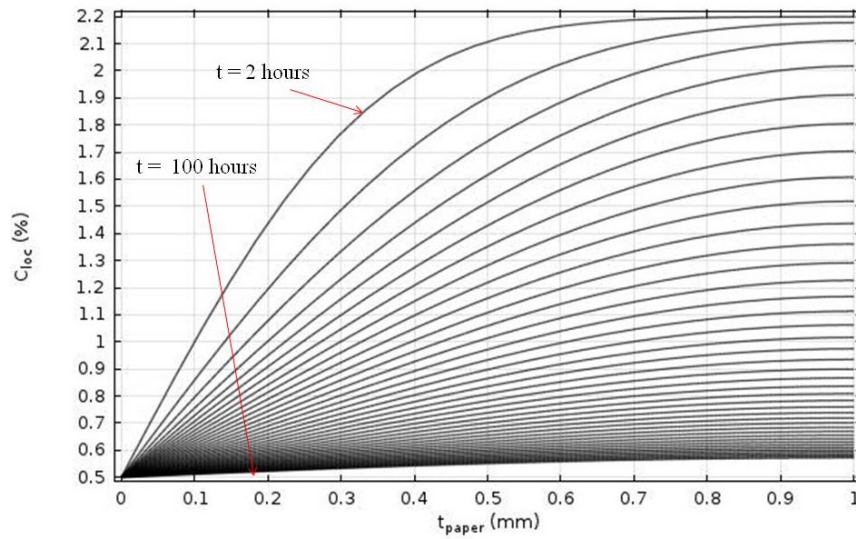
(a) Simulated drying time for oil-impregnated Kraft paper
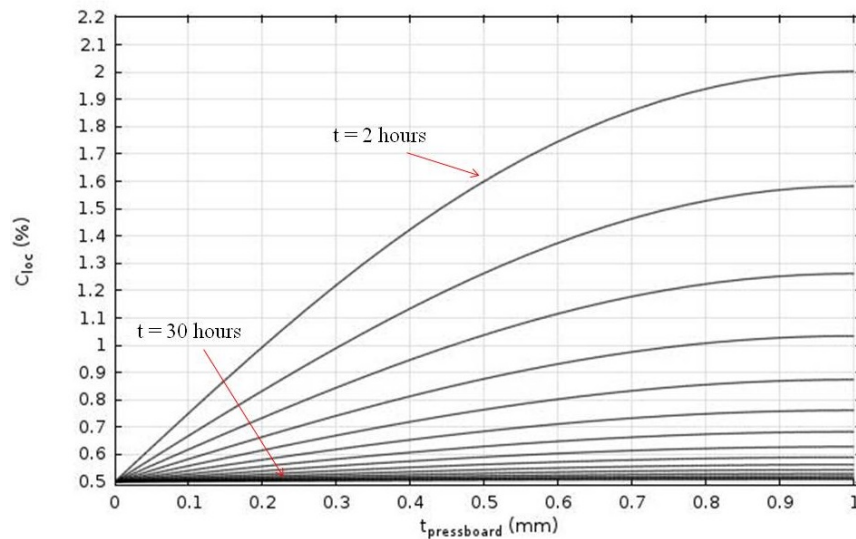
(b) Simulated drying time for non-impregnated pressboard

Figure 5.5: Simulated drying curves for various insulating materials of 1mm thickness using coefficients suggested by [11,12]

conditions. Fig.5.6, shows this reversal in the form of moisture uptake by oil-impregnated paper and non-impregnated pressboards at 75°C using coefficients described in Table.5.5.

The resultant observations from Fig.5.5 suggests that the oil-impregnated Kraft paper sample needs longer exposure periods as compared to the non-impregnated pressboard

Table 5.5: Effective diffusion coefficients obtained from [11, 16] for various insulates

	D_0 (m^2/s)	k'	E_a (K)
Oil-impregnated paper	6.44×10^{-14}	0.5	7700
Non-impregnated pressboard	0.67×10^{-12}	0.45	7646

sample for complete moisture removal. In case of a conditional reverse shown by Fig.5.6, the moisture uptake time is also higher for kraft paper as compared to pressboard.

The disparity in removal/up-take time by the investigated insulates is found to be a strong function of material density and intra-layer proximity of paper and pressboard samples. Kraft paper samples are thinner and posses lower density. The loosely bound multi-layers of paper are much thinner as compared to those in pressboard.

This causes an uneven distribution of moisture within the complex labyrinth of multi-layers thereby requiring higher thermal exposure for moisture removal depending upon the proximity of an active layer from the surface.

The conventional pressboards are pre-compressed insulates with higher density and closely bound multi-layers despite having same thickness. The proximity of active layers to the exposed surface justifies smaller excitation period, ergo the lesser saturation time.

In case of a transient analysis, Fig.5.7 shows the effect of material type on response time for moisture removal by insulate samples as discussed before. It is evident from the same figure that moisture removal is non-zero decay process whose time response should be 37% of the initial value.

Similarly, Fig.5.8 shows the effect of material type on response time for moisture uptake by insulate samples such that the exponential increase in concentration values corresponds to a first-order system whose time response must be 63.2% of the final value.

Furthermore, upon comparing the uptake and removal time of similar insulate materials through Fig.5.9, one can observe that the moisture interaction changes with
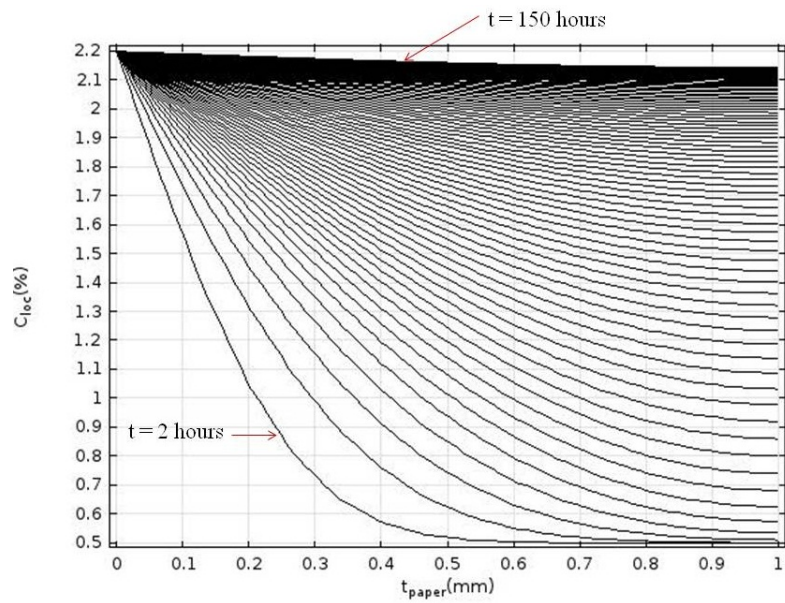
(a) 1mm oil-impregnated Kraft paper sample during drying
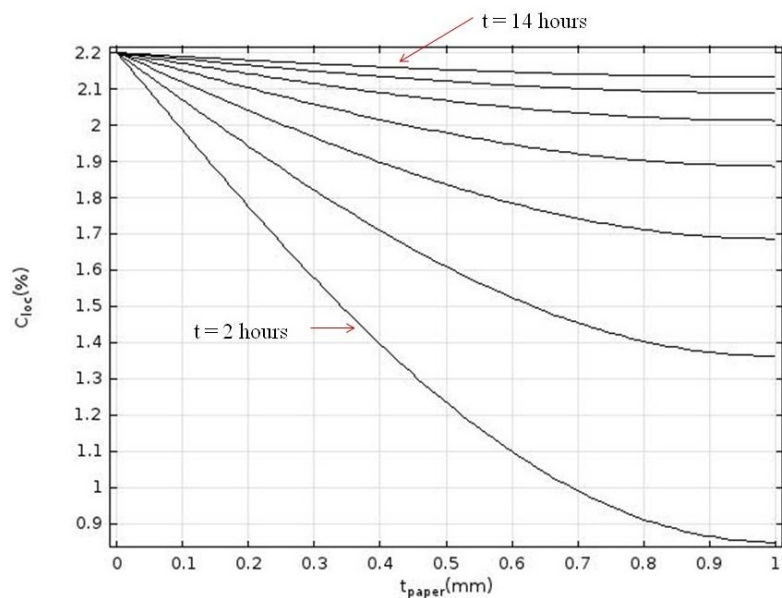
(b) 1mm oil-impregnated pressboard during drying

Figure 5.6: Spatial variation in oil impregnated paper and pressboard samples of 1mm thickness at 75°C and 2.2% surface moisture

impregnation condition of the material. A thorough discussion on the effect of such a conditioning is followed up in the next subsection.
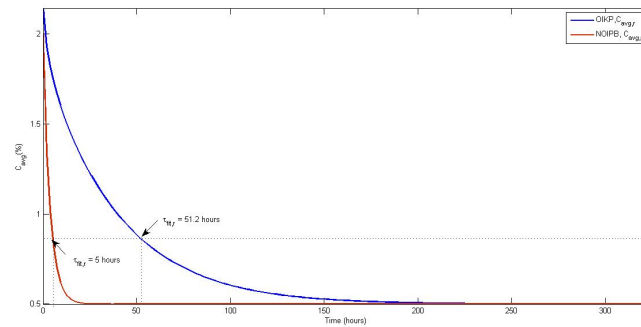
Figure 5.7: Effect of material on moisture removal time response
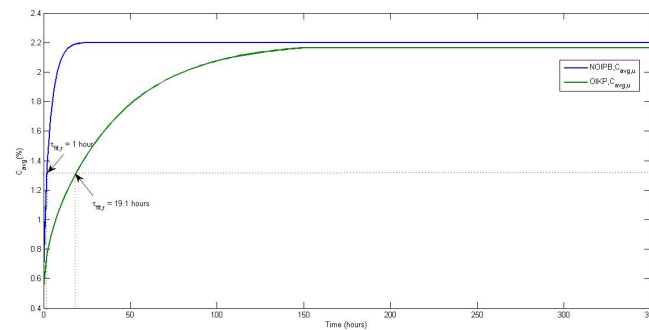
Figure 5.8: Effect of material on moisture uptake time response

5.1.3   Effect of oil impregnation

Based on the previous experiments by [11, 12, 16, 67] and simulated observations from subsection 5.1.1, it is evident that oil impregnation of an insulate can dramatically effect the moisture uptake or removal rate.

Since theses process are regulated by the effective diffusion coefficients, Fig.5.10 shows the behavior of 1mm thick Kraft paper during moisture uptake and removal with variable impregnation condition. Simultaneously, it should be noted that due to the unavailability of acceptable diffusion coefficients for oil-impregnated pressboard, relevant comparisons can not be made.

There are previously available comparisons where the oil-impregnated pressboard is
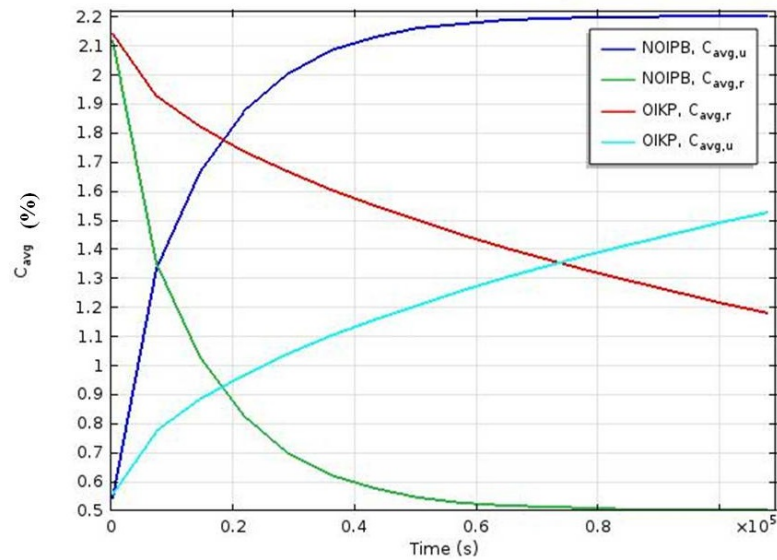
Figure 5.9: Simulated moisture discretization during uptake (u) and removal (r) from 1mm thick samples at 75°C with variable preconditioning

assumed to be behaving in the same manner as that of impregnated paper, but the initial findings in this work clearly indicates that such an assumption can dramatically increase the risk of error during moisture measurement studies.

It is understood that upon drying the hydroxyl groups released from within the cellulose chain causes vacant sites. The consolidate thermal energy now required to break the cellulose bonds is lower and paper/pressboard is more susceptible to physico-chemical damage.

Upon impregnation, the oil molecules are expected to take up the vacant sites available within the cellulose molecule after an initial drying. This doping causes a weaker dipole-dipole interaction between the water molecule and the otherwise hydrophilic cellulose matrix. Therefore, a reluctance is evidently visible during both moisture uptake and removal from oil-impregnated materials.

More interesting results can be obtained upon comparison of the impregnated paper diffusivity during uptake and removal stages. A rough calculation can suggest that the time response for moisture removal using impregnated paper is approximately 3 times
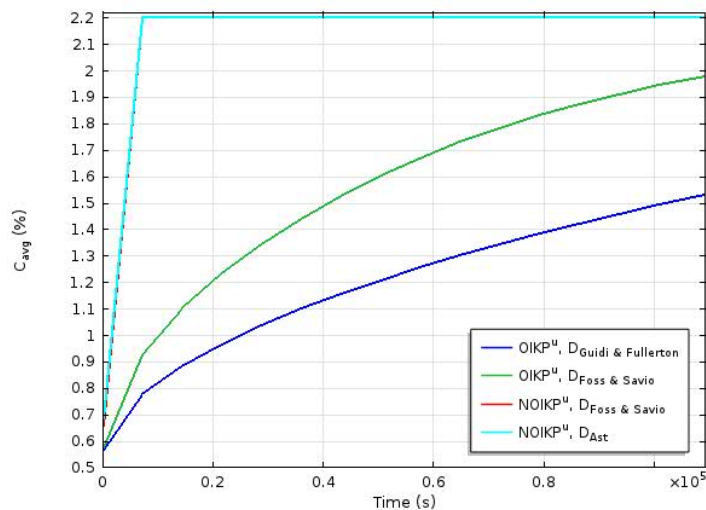
(a) Average moisture distribution in 1mm Kraft paper
with and without impregnation during uptake
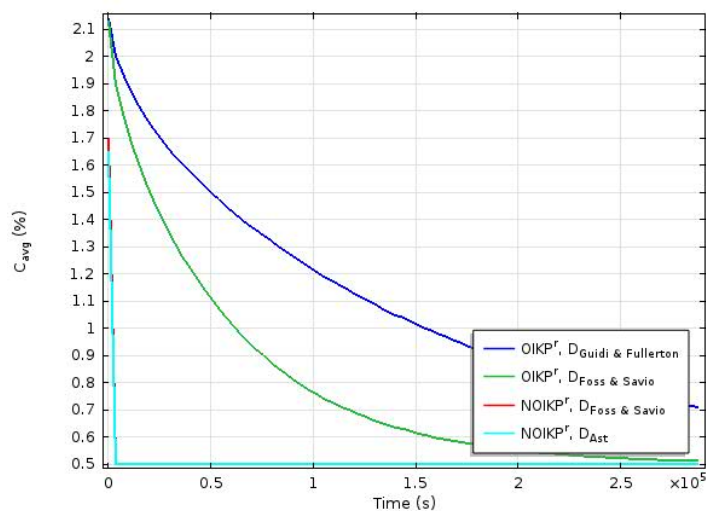
(b) Average moisture distribution in 1mm Kraft paper
with and without impregnation during removal

Figure 5.10: Simulated results on average moisture concentration against effects of oil impregnation in paper and pressboard samples

than the uptake time using Foss' data [12]. Similar trends can be obtained for non-impregnated samples as well, except these responses are much smaller and extend up-to few minutes.

Although a perfect trend is difficult to obtain, yet it can be seen that insulation thickness dominates the experimentally obtained diffusion coefficients. This suggests that material thickness is certainly an important physiological parameter affecting the moisture dynamics within oil-filled transformers. Hence the next subsection will explore the effect of insulation thickness on various moisture distribution methods and their respective time response.

5.1.4 Effect of insulation thickness

The transformer solid insulation can consist of pressboard and paper material of variable thickness at the same time within the same unit. It has been discussed previously that the experimental diffusion coefficients proposed by [12] are one order of magnitude higher than the ones proposed by [16] with the knowledge of insulation thickness unlike the latter.

Therefore, to isolate the effect of insulate thickness on average moisture distribution, Fig.5.11 shows the comparative uptake time by oil-impregnated Kraft paper of variable thickness parameterized in Table5.4.

There is a prominent observation available from Fig.5.11, regarding the saturation time of oil-impregnated kraft paper and non-impregnated pressboard. It can be seen that the time shift for saturation of oil-impregnated paper increases by approximately 3 times when the thickness is less than 2mm. Similarly, for non-impregnated pressboards the saturation time increases by approximately 4 times when the thickness is doubled.

This observation is restricted, but not limited, to thicker materials. This is because the original experimentation by Foss & Savio [12] were carried out on 2.5mm thick, impregnated Kraft paper under strictly controlled laboratory conditions. Similarly those done by Du [11] were carried out on 1 and 1.5mm non-impregnated pressboards.

As discussed earlier, upon thermal excitation the interactive forces between an active layer and surface is already weaker for Kraft paper samples. Now with increasing number
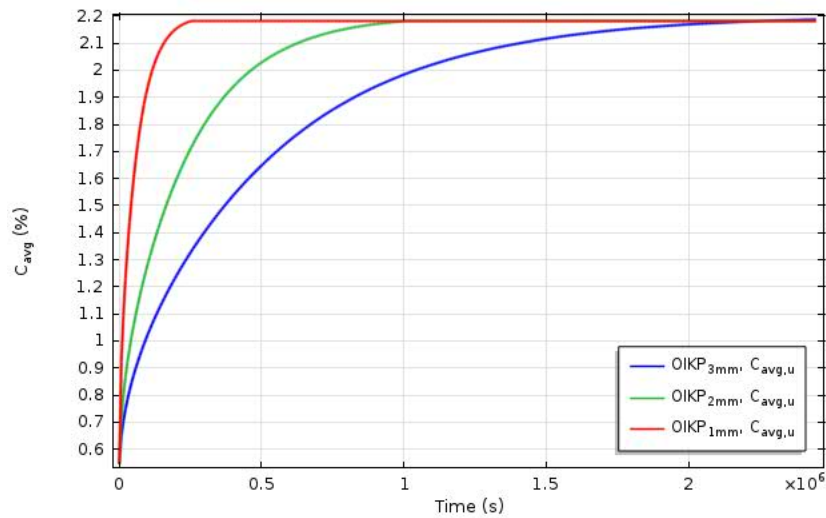
(a) Average moisture in impregnated Kraft paper with variable thickness
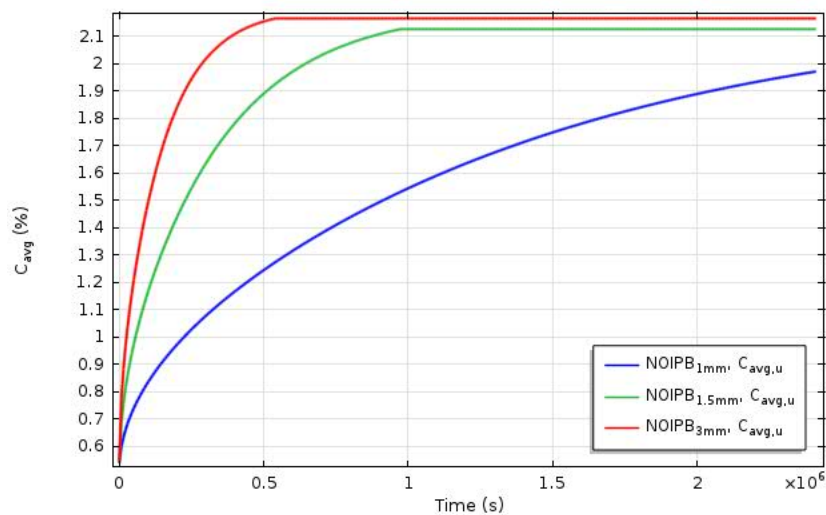
(b) Average moisture in non-impregnated pressboard with variable thickness

Figure 5.11: Effect of variable thickness on moisture uptake capacity of oil-impregnated paper and non-impregnated pressboard samples

of layers the moisture movement through intra-layers of paper becomes more reluctant and hence the saturation time increases.

Similar observations can be made for non-impregnated pressboard samples, where

despite a relatively higher interactive force than Kraft paper, the thermal excitation dampens with constant surface resistance and increasing number of layers, thereby leading to larger saturation times.

This observation is well supported by the difference in equilibrium time constant measurement obtained by comparing Eq.5.1 and Fig.5.12 for impregnated Kraft paper samples of varying thickness. The time response from the proposed figure is obtained by assuming that the moisture uptake is a first-order system whose response can be obtained when the final values reaches its limit by 63.2%.
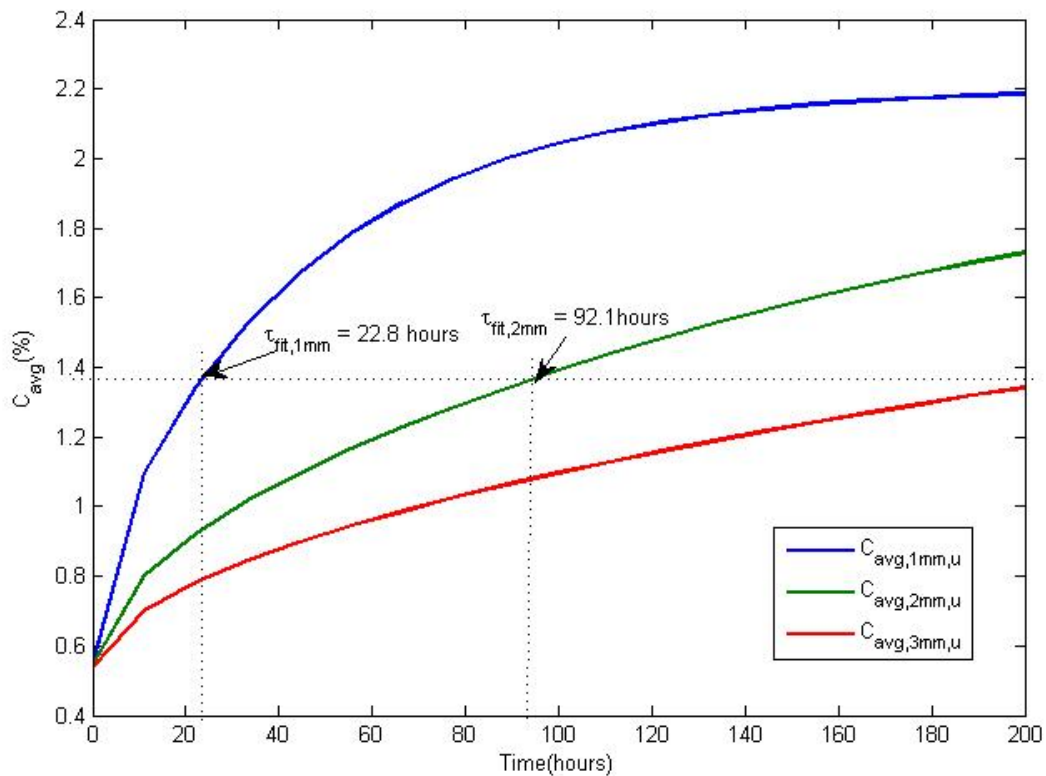
Figure 5.12: Simulated response time for average moisture distribution in impregnated paper samples with variable thickness at 75°C and 2.2% surface concentration

Upon direct substitution in the aforementioned equation, one can observe that there is absolutely no trend to be followed between equilibrium time constant of an impregnated paper sample with consecutive thickness, despite maintaining similar conditions.

$$\tfrac{\tau_2}{\tau_1} = 4.002,\ \tfrac{\tau_3}{\tau_2} = 2.5,\ \tfrac{\tau_4}{\tau_3} = 1.78$$

where $\tau_{1,2,3,4}$ represents the equilibrium time constant for moisture uptake by paper sample with 1, 2, 3, 4mm thickness at 75°C.

A comparative analysis from these sources suggest that a simulated time response for moisture uptake through curve fitting shows 1.36 times higher values for equilibrium response as compared to the theoretically acquired values.

Similar observations can be reported for non-impregnated pressboard materials, where the ratio of theoretical time constant obtained for insulates of variable thickness is shown below and simulated responses are obtained from curve fitting data in Fig.5.13.

$$\tfrac{\tau_2}{\tau_1} = 3.36,\ \tfrac{\tau_3}{\tau_2} = 2.25,\ \tfrac{\tau_4}{\tau_3} = 1.78$$

A similarity in trends of theoretical time constants between oil-impregnated paper and non-impregnated pressboards have been obtained upon comparing the respective geometric progressions. More interestingly, a progression factor of 1.3-1.4 exists upon small (0.5mm) depth increments in pressboards.

Similarly, in order to isolate the effect of insulate thickness on moisture removal rates, Fig.5.14 shows the comparison of simulated response time for non-impregnated pressboard and impregnated paper samples with variable thickness.

It can hence be inferred that not only the density and impregnation of material, its interaction depth also plays a dominating role in moisture removal or uptake during various transformer operations. This inference also points to an interesting question pertaining to moisture interaction behavior i.e. what is the role of exposure sides on moisture release/uptake?

The next subsection shall explore more about such interactions using uptake and removal examples for oil-impregnated paper and non-impregnated pressboard.
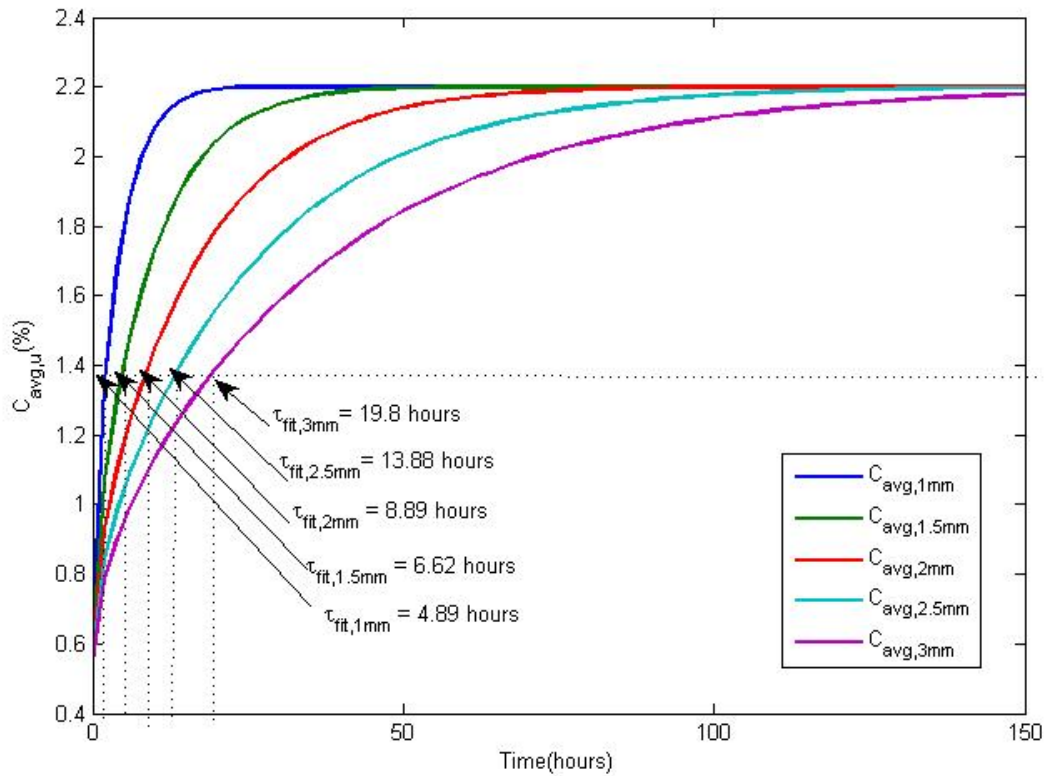
Figure 5.13: Simulated response time for average moisture distribution in impregnated pressboard sample with variable thickness at 75°C and 2.2% surface concentration

5.1.5 Effect of exposure sides

Fig.5.15 and 5.16 shows the effect of variable exposure sides on local moisture distribution in impregnated paper and non-impregnated pressboard sample that is exposed to 75°C.

It can be seen from the same figure that upon dual exposure, the rate of saturation in oil-impregnated kraft paper is 2.5 times faster than single-sided exposure. Similar trends can be obtained for non-impregnated pressboards, where the rate of saturation is approximately 2.8 times faster for dual-sided cases as compared to single-sided interactions.

This also brings us to our previous hypothesis that the time response of any process
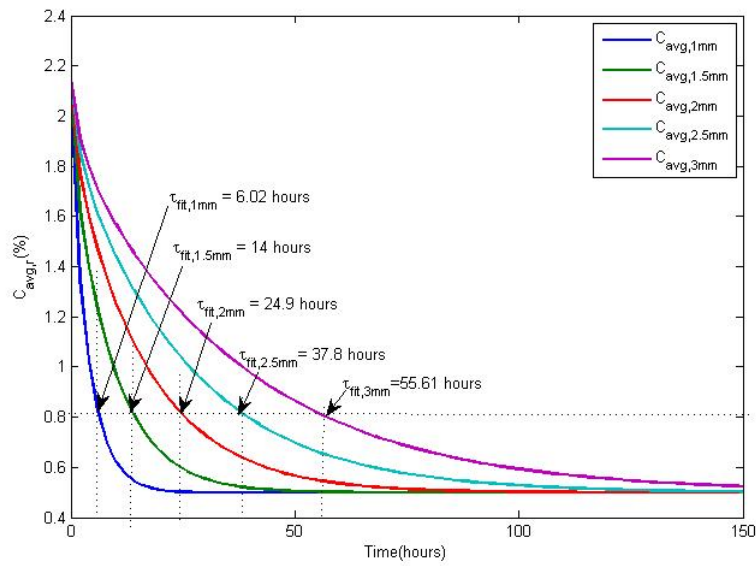
(a) Time response for average moisture removed by non-impregnated pressboards
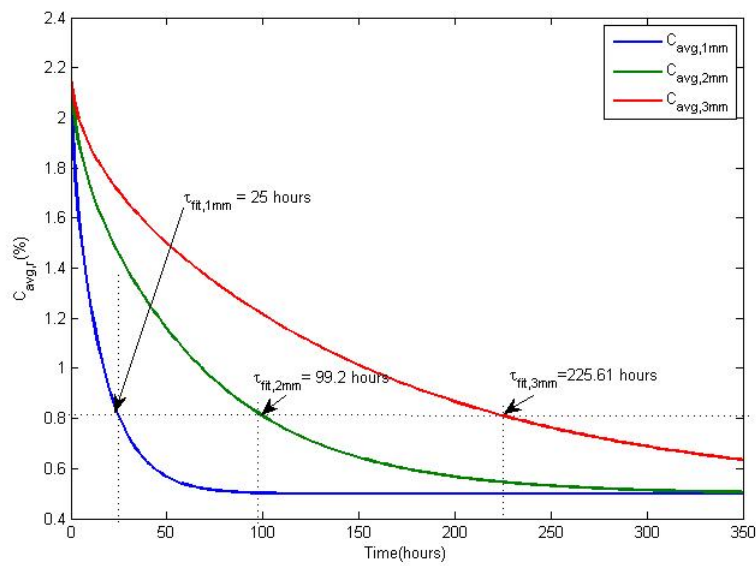
(b) Time response for average moisture removed by oil-impregnated Kraft paper

Figure 5.14: Effect of insulate thickness with variable impregnation condition on time response of moisture removal process

(uptake or removal) must depend on the number of exposure sides along with other physiological aspects of the insulating material. In order to obtain the time response for an average moisture distribution during removal and uptake process, Fig.5.17 can provide several interesting insights.

(a) Simulated spatial moisture discretization during single-sided diffusion

(b) Simulated spatial moisture discretization during double-sided diffusion
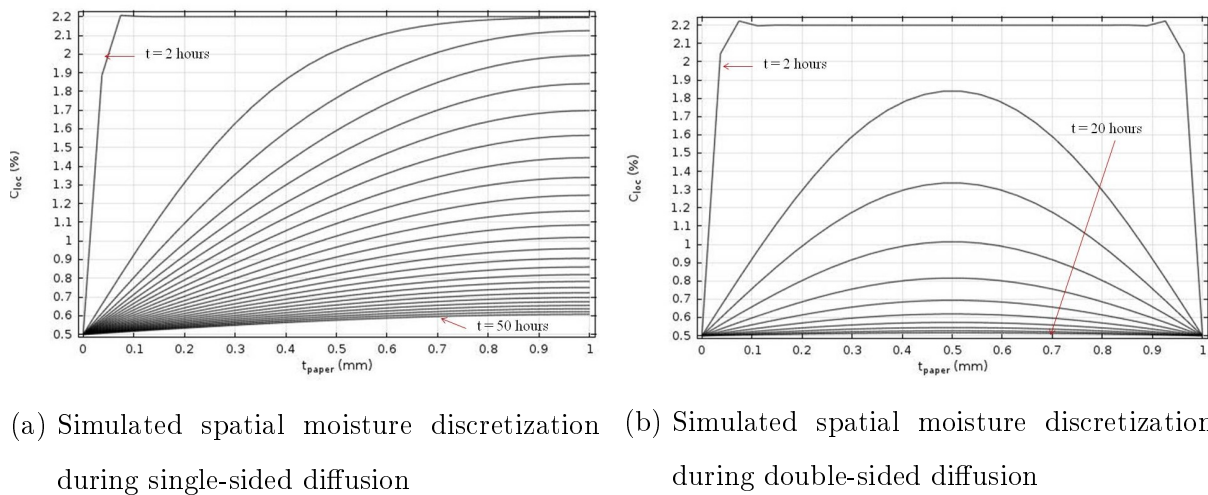
Figure 5.15: Simulated spatial distribution of surface moisture within 1mm oil-impregnated Kraft paper at 75°C during single (ss) and double-sided (ds) exposure

(a) Simulated spatial moisture discretization during single-sided exposure

(b) Simulated spatial moisture discretization during double-sided exposure
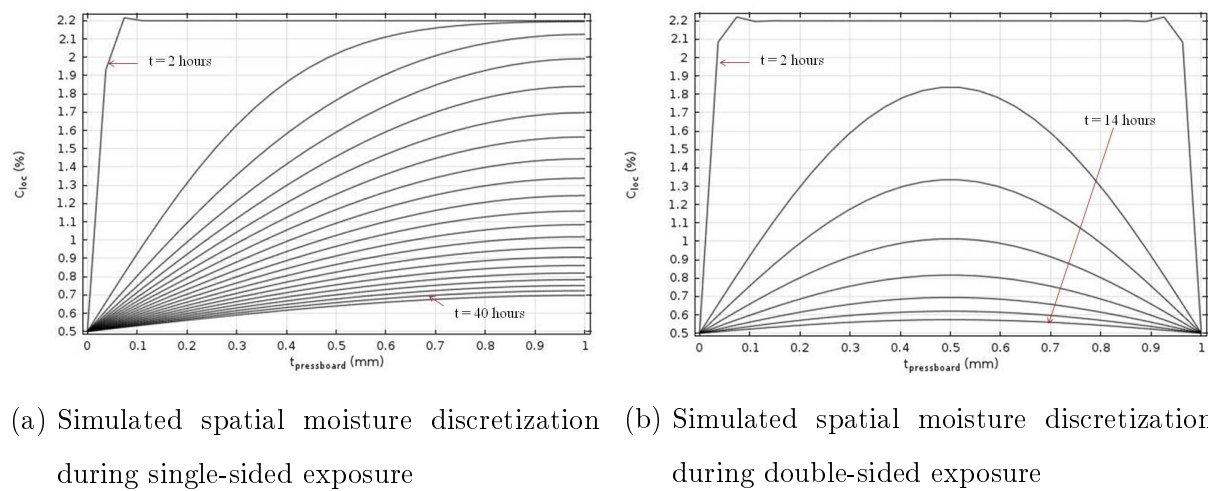
Figure 5.16: Simulated spatial distribution of surface moisture within 1mm non-impregnated pressboard at 75°C during single (ss) and double-sided (ds) exposure

It can be seen from the same figure that the moisture uptake time for oil-impregnated Kraft paper and pressboard increases by approximately three times when the thermal
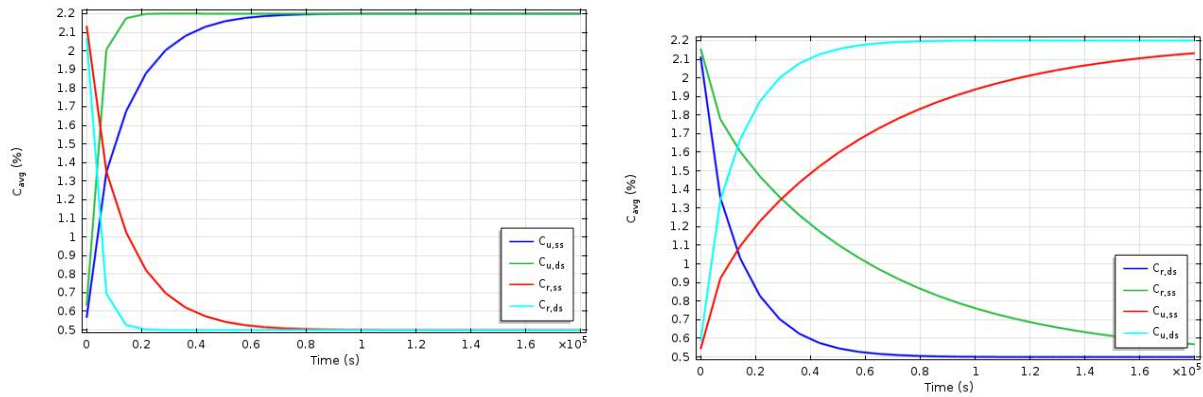
(a) Comparative average distribution in pressboard through variable exposure pattern

(b) Comparative average distribution in Kraft paper through variable exposure pattern

Figure 5.17: Effect of exposure sides on average moisture distribution with 1mm thick impreganted Kraft paper and non-impregnated pressboard sample at 75°C during uptake and removal processes

exposure is restricted to single side only. Similarly, moisture removal rates increase by almost four time upon such restrictions.

Although, clear trends are difficult to obtain within particularly for non-impregnated pressboard samples due to smaller response time ($\lesssim$ 4 hours), it still understandable that the moisture interaction can behave differently if the surface(equilibrium) concentration and temperature is changed. The next subsection discusses in detail about the effect of such parameters on response time for moisture distribution in various insulating materials.

5.1.6 Effect of surface moisture

In order to isolate the effect of surface(equilibrium) moisture concentration on the water interaction, Fig.5.18 shows the change in average distribution of moisture in non-impregnated pressboard material with variable concentration conditions during uptake processes. Similar trends can be obtained for moisture removal rates for the same material under equivalent conditions as shown in Fig.5.19.
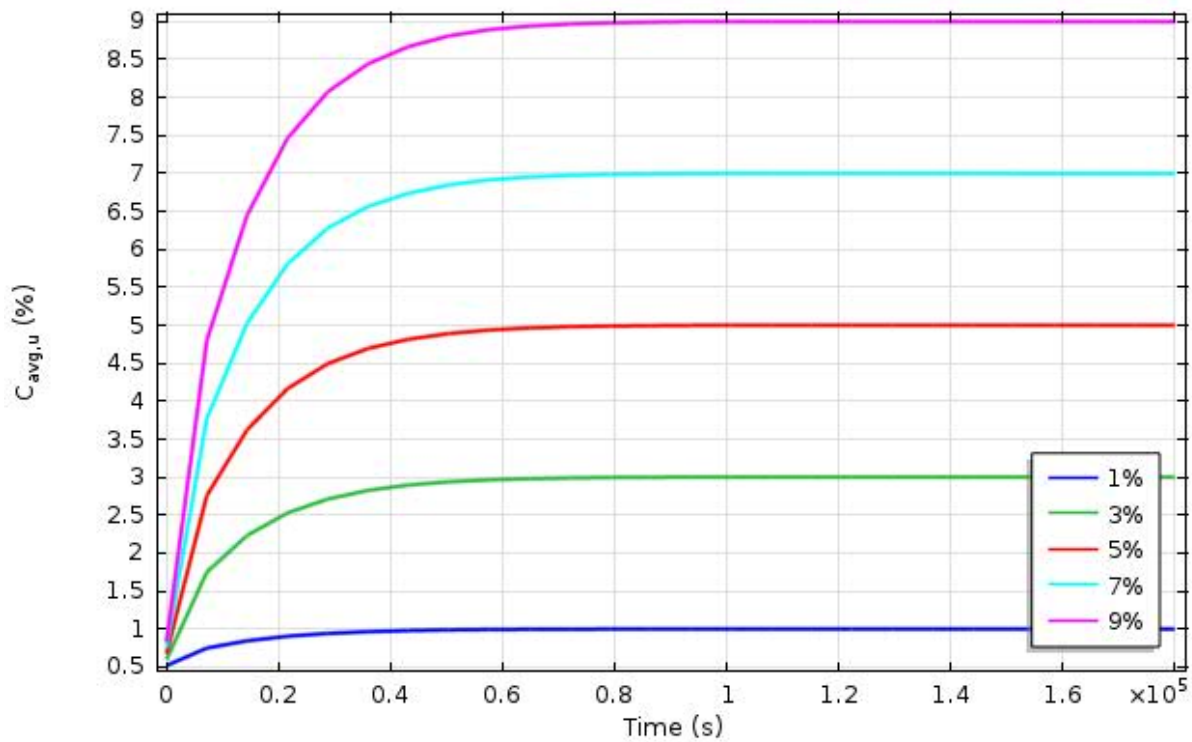
Figure 5.18: Average moisture distribution within non-impregnated pressboards with variable surface concentration during moisture uptake process

From observing Fig.5.18, one can interpret that despite the constantly increasing surface concentration, the theoretical equilibrium time constant varies within 4.04-4.20 hours. Such a small variation is justified by the fact that effective diffusivity varies within a much smaller range of 2.68 - 2.78×10^{-11} m^2/s. Contrary to this evaluation, simulated response time of non-impregnated pressboard samples will vary within a much broader range of 2.8-4.2 hours.

Obviously, similar comparisons can be drawn from the moisture removal process where the simulated time-responses will vary within a range of 0.8 - 4.02 hours, unlike the theoretical time-constant that is fixed at 4.20 hours over a constant diffusivity.

At this stage, rather than a comparative analysis for paper and pressboard material, it is imperative that a proper reasoning must be provided to justify the relevance of diffusion time-constants with increasing surface moisture during any interactive process.
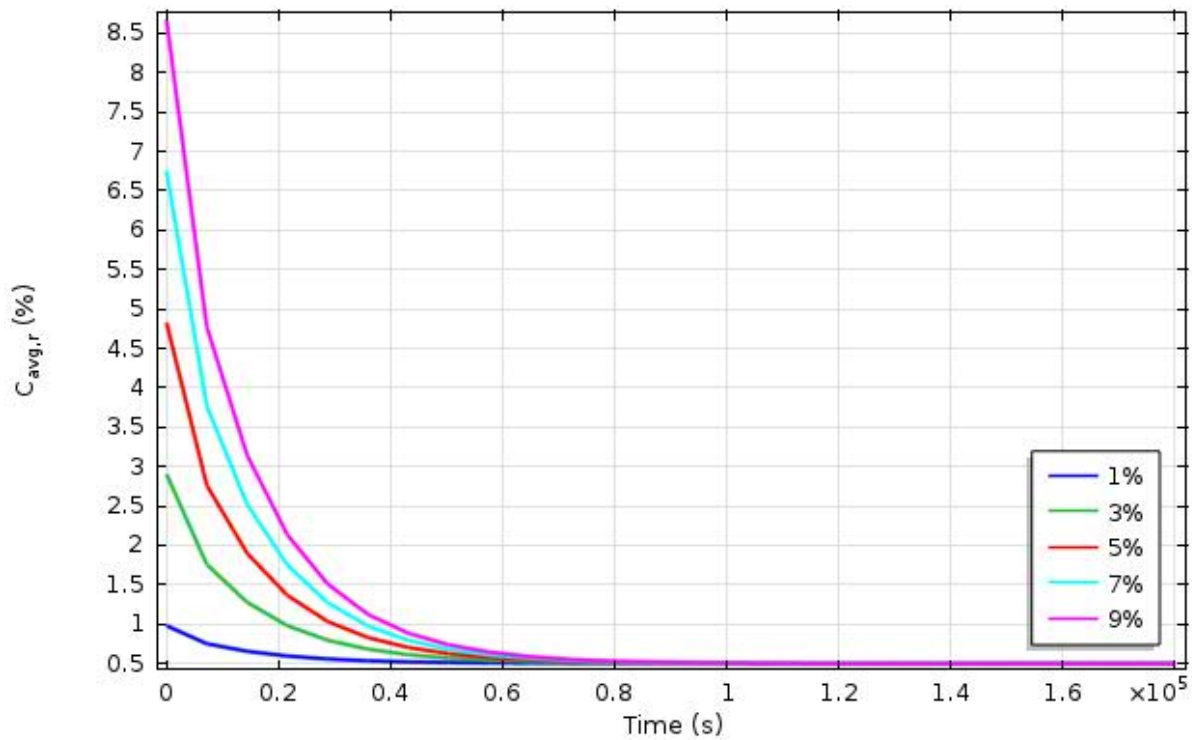
Figure 5.19: Average moisture distribution within non-impregnated pressboards with variable surface concentration during moisture uptake process

This is because the removal processes are a direct representation of the factory drying of wet insulation materials. Whereas, moisture uptake represents the critical and often less-discussed stage of insulation exposure after primary drying but before impregnation/installation.

During factory drying (removal) of extremely wet samples, the saturation time becomes independent of the surface moisture especially at higher concentration level provided the thickness and temperature is maintained. Such a behavior is expected only when a super saturation is achieved by all the active multi-layers of the component (i.e. pressboard or paper) during diffusion through the insulate. Therefore, once this limit is attained, the surface concentration hardly matters.

Hence an inference can be drawn that not just the surface concentration but also the temperature variations shall influence the inherent time responses of the various process

that can provide a reliable moisture-in-paper model.

5.1.7   Effect of temperature

At this point one must understand that in order to isolate the effect of insulation properties including initial water retention, all studies were strictly restricted to an average winding temperature that was obtained from the stationary thermal modeling of the relevant transformer. However, as seen in the previous section, an unwanted super saturation will occur within the multi-layers of pressboard (and paper) material with very high concentration exposures that is independent of its impregnation behavior. When such a case exists, it becomes imperative that the operation temperature is changed accordingly suitably to accommodate the moisture removal or uptake process along with relevant material property, surface moisture concentration and available exposure sides.

Fig.5.20 shows change in moisture uptake behavior of oil-impregnated paper and non-impregnated pressboard of 1mm thickness when the surface concentration is relatively high (say 6%) against a temperature range of 30-110°C. Similar results can be obtained for moisture removal from paper and pressboard materials under high humidity level and variable temperature. The boundary conditions are modified to suit the classic hot-oil drying method

The rate of moisture uptake or removal is a strong function of temperature. The dissociation energy of a single bond hydrocarbon (C-H) is much lower than the hydroxyl (O-H) bonds. This causes the initiation of bond cleavage at those prime locations where hydrocarbon bonds are followed by hydroxyl bonds. As the operation proceeds, a constant thermal exposure will allow maximum bond cleavage thus resulting in both complete removal as well as a decrease in mechanical strength of the material. It is therefore imperative that the material is not bone dried and some moisture is allowed within the insulate to maintain the dielectric and mechanical strength without compromising its
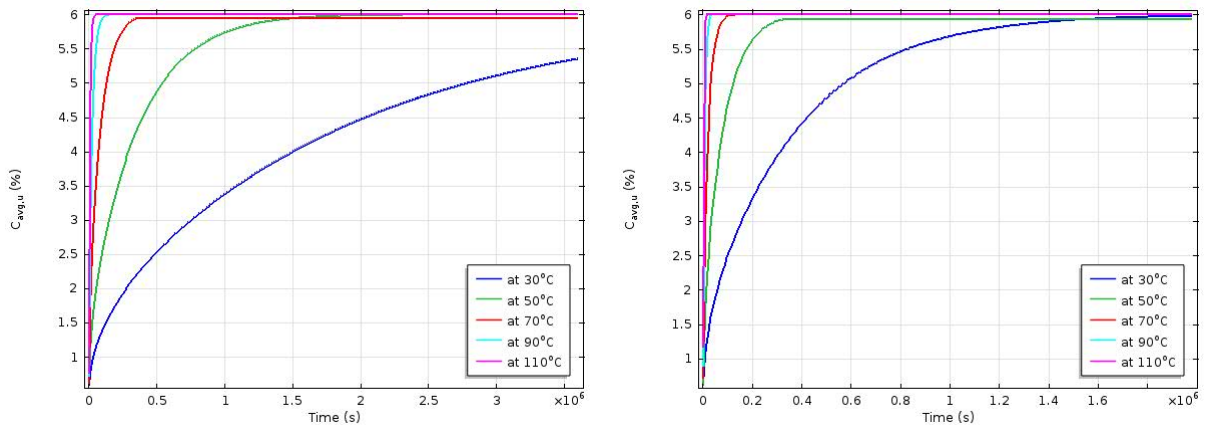
(a) Average moisture distribution in oil-impregnated Kraft paper during uptake

(b) Average moisture distribution in non-impregnated pressboard during uptake

Figure 5.20: Effect of temperature on average moisture distribution in paper and pressboard samples during moisture uptake process under varying isotherms
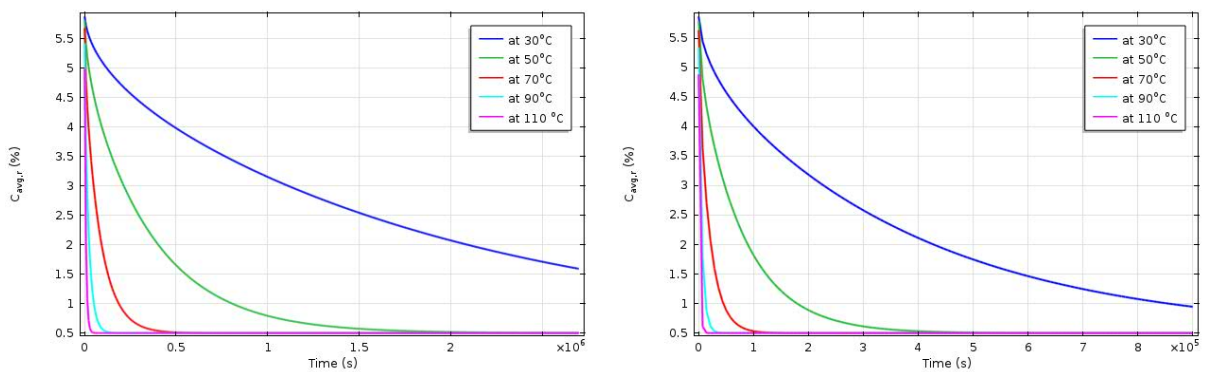
(a) Average moisture distribution in oil-impregnated Kraft paper during uptake

(b) Average moisture distribution in non-impregnated pressboard during uptake

Figure 5.21: Effect of temperature on average moisture distribution in paper and pressboard samples during moisture removal process under varying isotherms

insulating properties.

On the hand, during a moisture uptake process, the surrounding air is allowed to posses higher relative humidity as compared to the original insulating material. For a

non-impregnated material, the high concentration difference allows the moisture to easily seep through the multi-layers of the insulate.

However, for an impregnated sample a moisture resistance can be expected within the insulate multi-layers due to an uneven (practical) oil impregnation. The resistance will cause a slower rate of moisture uptake without completely depriving of the unavoidable interaction.

Hence, it can be assumed safely that a moisture-in-paper model will depend on the operating condition including the insulate properties and a universality is utmost challenging since manufacturers can prefer any permissible permutation. The equilibrium time constant for moisture-in-paper models will change exponentially with material type, thickness, exposure sides, temperature and concentration.

For the sake of providing a definite solution, an empirically fitted data has been obtained to calculate the equilibrium time constant correlation as shown in Eq.3.19 as discussed in Chapter 3. It is generated by curve fitting of equilibrium time constant data against variable parameters discussed above. This corrected time response (τ_{corr}) has been used in the further studies.

The following analysis on oil moisture determination with the help of a CFD-based thermal model is capable of estimating the moisture distribution in oil, paper, pressboard and at the interactive surface. More importantly, unlike the previous attempts of moisture predictions using top or bottom oil temperature, our thermal model is capable of determining the active temperature ranges for paper and pressboard material separately, thus increasing the degree of accuracy for future use.

5.2 Moisture-in-oil Model

In order to create reliable models for moisture migrations through oil, it is imperative that the load variations and water vapor pressure changes are properly tracked. The

temperature rise in oil has been studied by the proposed thermal model in the present work. Since all calculations in the previous chapter were confined to natural cooling pattern, few assumptions have been made prior to proposing the necessary moisture-in-oil model.

1. Upon transfer of moisture from paper to oil, instantaneous solubility is following the applied temperature trend.

2. In accordance with field information, the sensor is either located at the bottom or separately in a bypass line which is far away from the winding.

3. Since natural cooling prevails, moisture in oil that is closer to the windings will respond faster as compared to other locations.

4. Since the thermal responses were found smaller than the moisture responses, small investigations periods are applied to estimate the moisture-in-oil response with variable condition.

With reference to the aforementioned assumptions, there are two most important cases that one must be looking into. Firstly, the classic no load case and secondly an average daily loading cycle. The first case shows a classic no-load condition to show the absence of heating source on temperature distribution. The second case shows a combination of conditions that are actually endured by the transformer daily over shorted period of time.

5.2.1 No-Loading

A classic no-loading condition is very common in transformers. In this case, no heat was supplied to the transformer and by the virtue of natural cooling, only flow fields were detected. The oil dissolved in this oil moves slower than it is anticipated thereby creating perfectly equilibrium conditions for an oil-paper insulation complex.
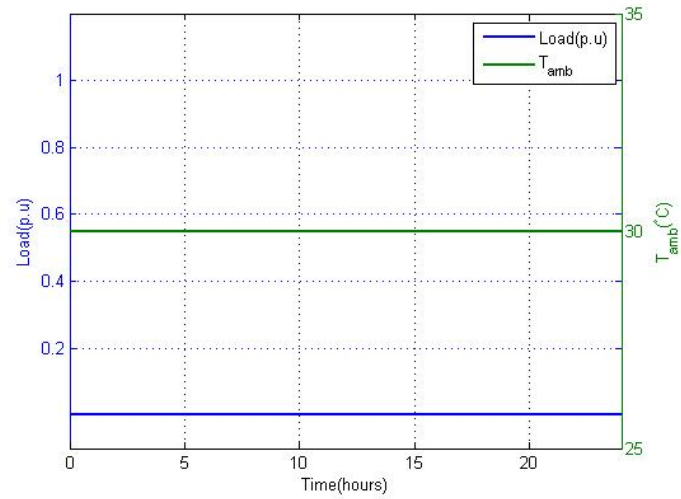
(a) Simulated no-load temperature conditions where K=0 and T_{amb} is constant
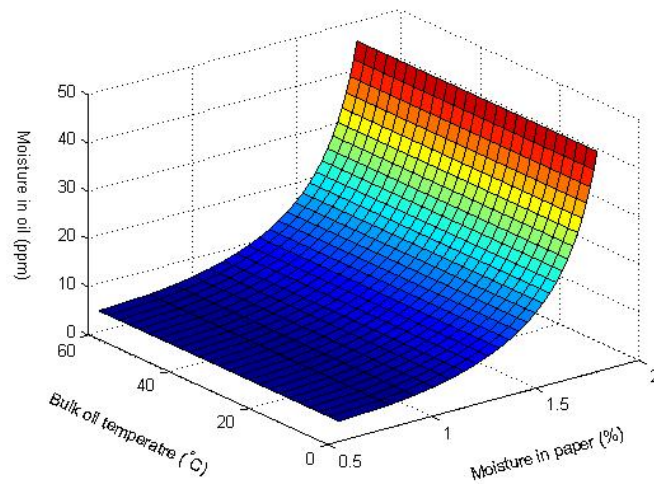
(b) Simulated no-load moisture conditions where K=0 and T_{amb} is constant. This is an ideal case of equilibrium moisture in oil-paper insulation system

Figure 5.22: Simulated temperature and moisture predictions in oil-paper insulation complex under no-load conditions

5.2.2 Daily-Loading

As mentioned earlier, since transformer thermal transients are achieved quite early, smaller investigation periods are applied herein to replicate the typical daily load pattern with mixed loading conditions. Moreover, it is extremely difficult to replicate such conditions purely based on simulated assumptions. Therefore, the reported pattern in [13, 108] has been taken as a reference.

Fig.5.23 shows an average loading cycle applicable in a 225/26.4 kV feeder line on a daily basis. The data for average loading and top-oil temperature has been extracted using an open source digitizer to convert into a usable form.
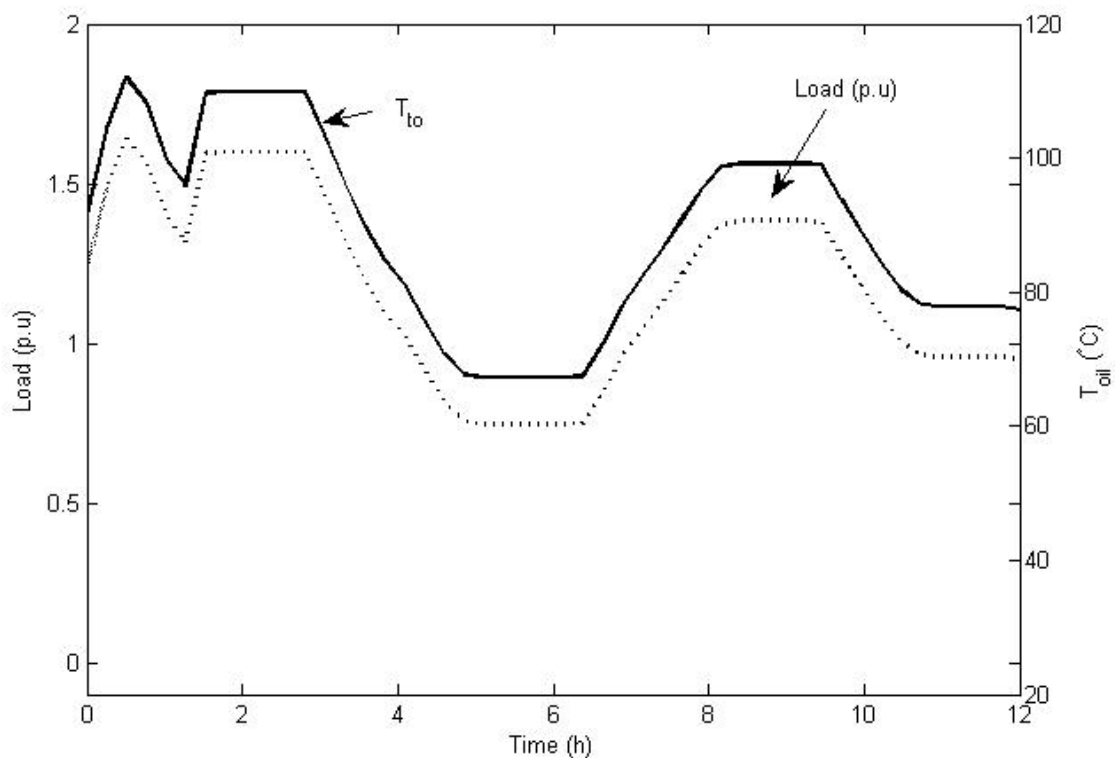
Figure 5.23: A typical daily loading pattern with expected top-oil temperature in oil filled transformers with natural cooling [13]

Similarly, Fig.5.24 shows the average temperature in oil with respect to top and

bottom locations. Since the transformer investigated was relatively new, a lower relative saturation of around 18-20% was expected. Hence, the dissolved moisture is calculated at the average oil temperature reported in this data.
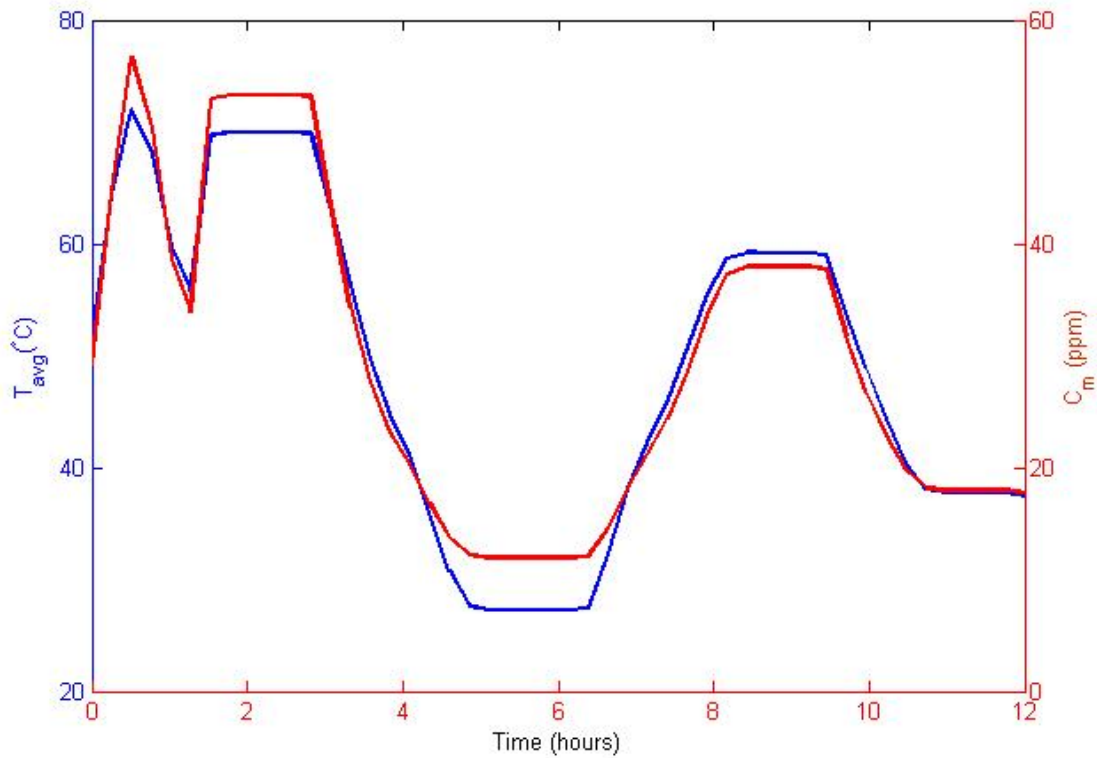
Figure 5.24: Measured moisture obtained against average temperature data obtained from [13]

In order to evaluate the measured dissolved water in oil at average temperature, the equation obtained from moisture-in-oil model discussed in Chapter 3 has been applied with appropriate constants.

It can be seen from Fig.5.25 that deviation in actual moisture when the time response of moisture-equilibrium in paper is assumed as an exponentially changing value as discussed previously. It is perhaps because when the time constant of paper (source) was changing continuously with temperature, there was a significant affect on the total dissolved moisture which was ignored as an initial lag by the sensor. This
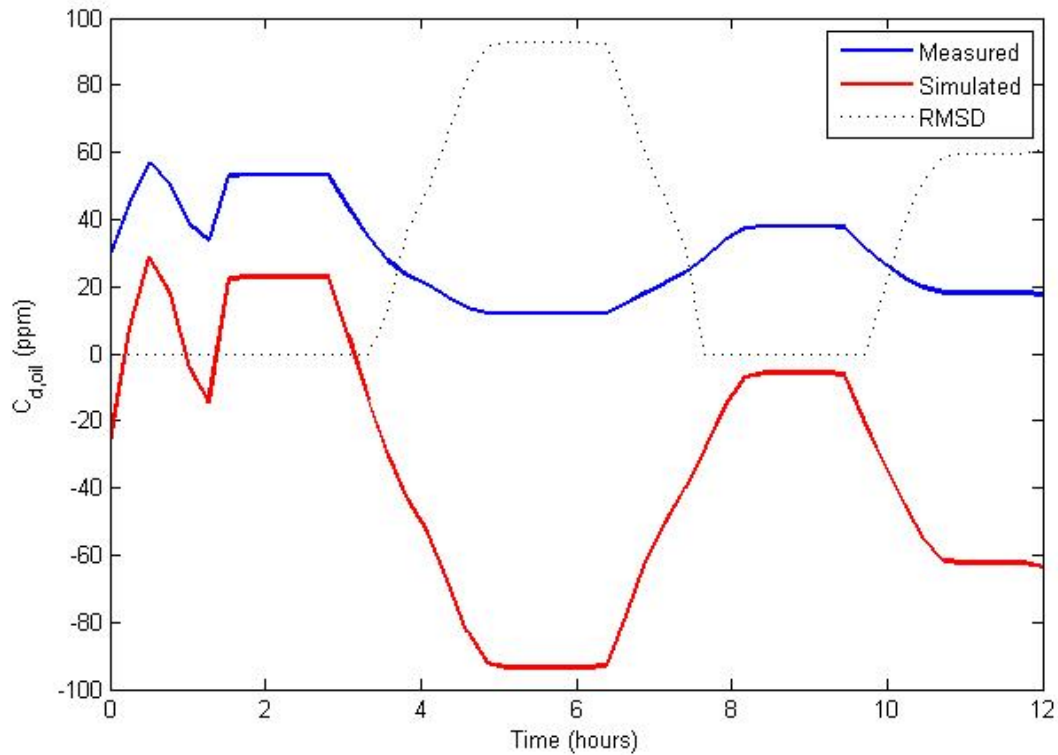
Figure 5.25: Instantaneous moisture measurement in transformer oil with respect of the daily load pattern, compared against the measured moisture to obtain the effect of moisture-in-paper time response

suggests that the moisture measured by sensor at the bottom of the tank can significantly improve its value if its location can be changed.

Based on the above observation, a single model for water distribution in transformer is proposed using the mass balance equation discussed in Chapter 3. Fig.5.26 is the final rated moisture in paper with respect to the rated moisture in oil at every time instant with regard to the changing load pattern.

It must be noted form the above figure that, when a combined load is applied to the transformer, the oil temperature rises in a pattern similar to that of the loading behavior. It is logical because loading is nothing but the variation of harmonics to interpret variable current and voltage combinations. These combinations in-turn acts as the heating source
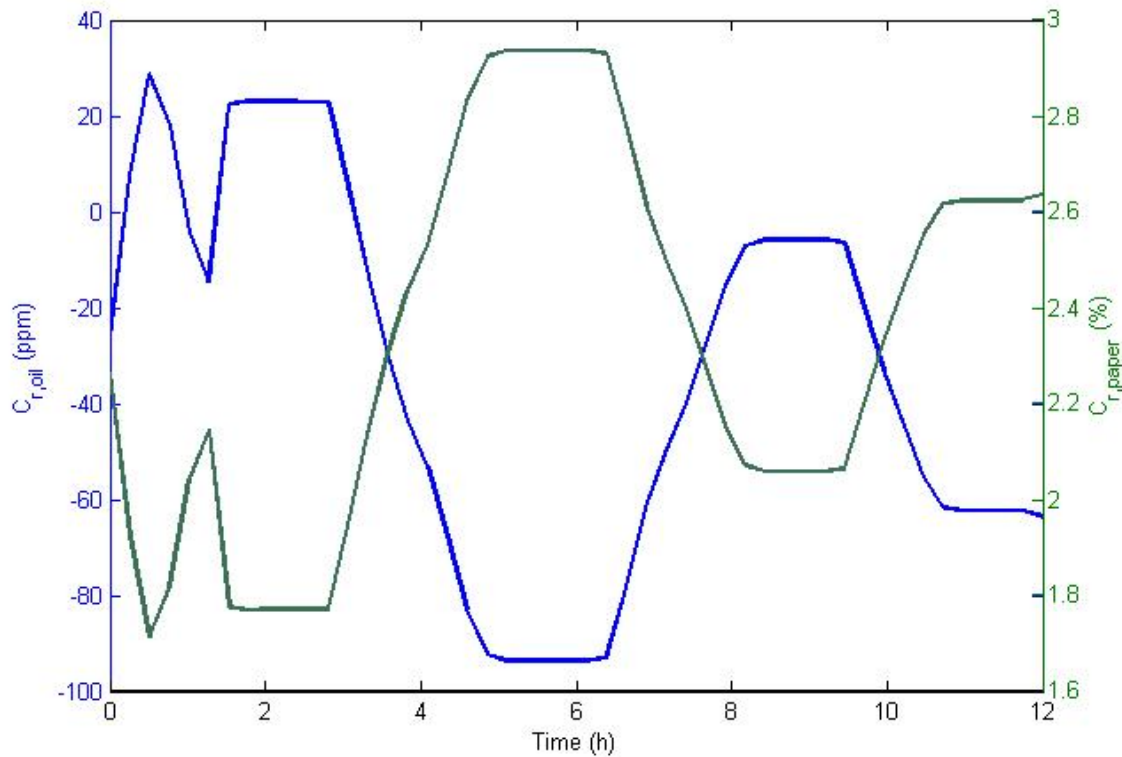
Figure 5.26: Instanteneous change in moisture concentration of oil and paper with respect to the rated (r) temperature

of the winding thus imparting the change in instantaneous oil and winding temperature.

In case of a moisture-in-oil model, the winding temperature is neglected, because at this point the oil has to be hotter than the winding in order to allow reverse moisture diffusion. Naturally, by the laws of mass conservation, the total water in the system needs to be conserved despite its uneven distribution.

In this particular case, the expected mass of water in the tank was known from the field-survey of the electrical unit and manufacturer information. It became easier now to implant the proposed model of moisture balance as per the changing oil-moisture values. In essence, it can be said that the Fig.5.26 is the final pattern of moisture migration and distribution that one can expect within transformer when the load is tripped off.

Another aspect of this finding was to evaluate the accuracy of sensor location in transformers. Since conventionally they are installed at the bottom and far away from the winding, Fig.5.23 proved significant in ascertaining the same. It was visible from this assessment that in case of naturally-cooled transformer, a homogeneity of oil-temperature does not exist everywhere within a tank. This explanation is logical and in agreement with our proposed thermal models. Due to lower temperature in sensor line and non-homogeneity, this lag in measurement is obtained.

By manipulating the sensor temperature to replicate conditions near the winding, a comparative graph was obtained to ascertain the accuracy in measurements of oil-moisture in power transformer as shown in fig.5.27. Here, an unwanted deviation occurs at the beginning of loading cycle later leading to time lag. Since the load pattern suggests that at the beginning of cycle the temperature rise was minimum and oil was almost passive, it is highly probable that the actual (dissolved) moisture remained stagnant.

Practically speaking the oil flow is never zero in transformers and therefore this non-zero velocity field identified in the bypass line shows an inflated value because of the previously traveled oil. Therefore, an error is easily identified despite such precision in sensor mounting and transformer step loading.

This hypothesis is strictly theoretical and is not recommended without prior information about the transformer thermal profile and geometrical specification. Unfortunately, there is no way to test the accuracy of this hypothesis without continuous field measurements, that can be opted for future work.

Hence it can be said that, unlike the previous claims this is by far the most complete model for moisture dynamics in oil-filled power transformers with respect to the thermal behavior near winding as a virtue of load change.
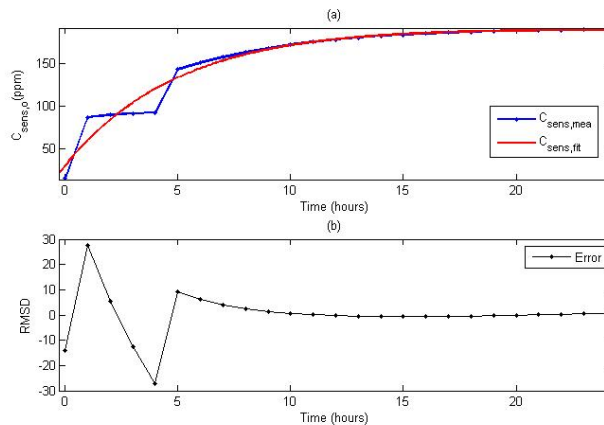
Figure 5.27: Error estimation in sensor location during step rise in moisture and temperature of oil

5.3   Summary

This chapter indicates the coupling of temperature induced moisture distribution profiles in oil-filled transformer insulating materials. There are two critical observations in insulation management. Firstly, even during the so-called equilibrium stage, moisture distribution on the oil-paper interface is dominated by the nature of material, thickness, initial moisture concentration, operating temperature. These factors influence the moisture uptake and removal rate and thus influences the time response of these phenomena during transient interactions. Secondly, the time response thus obtained is an important parameter for obtaining the moisture dissolution in oil and retained concentrations in paper insulation (along with interface distribution) during on-load conditions in operational equipments. These results also discusses the apparent error in moisture concentration measurement using sensor and traditional equations and their potential reasons. These results are extremely important in improving the existing understanding of moisture distribution in oil-filled transformers under various conditions.

Chapter 6

CONCLUSIONS

This chapter presents the general conclusion of the proposed research. It can be observed as the keystone towards understanding the moisture migrations in oil-filled transformers. In the present chapter, major contributions from this work has been summarized that can be later used guidelines as future improvements in moisture evaluations.

6.1   Model Discussions

Although moisture dynamics in power transformers has been reported several times in the available literature, a complete mathematical model to evaluate the dynamics within individual media and interactive interface has been reported for the first time.To determine the dynamics of moisture in prominent zones within the transformer, proper understanding of the temperature is crucial.   Existing technologies for moisture measurement in transformers are mostly based on equilibrium assumptions which leads to a considerable research gap.

In the present work, moisture migration behavior in oil-filled power transformers is studied with reference to the dynamic thermal migrations. The regulating parameter in a thermal model besides oil flow and geometrical constraints, is the internal heat

generation. Since the heat is generated by the virtue of power losses within windings, it was possible to introduce various function to isolate the effect of loading pattern on oil-winding temperature rise. The temperature statistics obtained from this model was very helpful in predicting the moisture migration behavior in oil-paper complex by distinguishing the direction of water transfer.

In case of a moisture-in-paper model, exhaustive studies on the effect of various parameters on the time response of migration has been studied. This observation was necessary to prove that the time response for moisture sorption in paper is not constant as reported by various resources [2, 7, 11, 68, 95, 108]. The typical equilibrium moisture prediction was also challenged in the present by proposing its co-dependency on the rated oil-moisture and temperature.

It is indeed possible to create a thermal equilibrium condition within the insulation complex if the transformer is maintained at a constant temperature for a fairly long period of time. Despite being theoretically correct, it is not possible to achieve this condition within an active transformer that is facing fluctuating loads during an uninterrupted operational cycle. Therefore, the moisture-in-paper model strictly works under isothermal conditions to mimic the drying operations (i.e., factory and on-line) with regard to the consecutive non-equilibrium conditions created between each steady state. In order to simulate the moisture-in-paper model in accordance with the drying conditions, it is imperative to isolate the effect of the parameters that will influence this model.

It was observed that various factors such as, density, orientation, degree of polymerization and crystalline structure of glucopyranose, dominates the moisture saturation time and response to uptake or removal processes. It was possible to obtain a rudimentary correlation between the effective parameters and equilibrium time response.

Another aspect of the thermal modeling was to obtain the hot-spot temperature that is an indicator of the transformer life. Since the data available to simulate the proposed

model was that for a new transformer, an ageing limit could not be found. It will be however, interesting to see the effect of such variations on relative insulation ageing. It was therefore proposed that the hot-spot temperature obtained from the thermal model is nothing but the indicator of temperature rise limits and cooling capacity of the applied oil. In an essence, it was observed that there is limited scope for the paper to achieve an equilibrium during fluctuating load conditions. It was however possible to model this hypothesis based on the assumption that the transformer has not been disturbed for a very long time. At this stage, it is noteworthy that such a condition will rarely exist in an operational transformer.

Besides, moisture migration from oil to paper and vice-versa is highly affected by the winding axial temperature distribution. Due to the non-uniform temperature distribution profile in oil and within windings, it was possible to obtain the instantaneous moisture dissolved in oil as a strong function of this temperature. Two separate cases were discussed where not only the equilibrium condition was established successfully for no-load conditions, but also the average moisture distribution was obtained for a typical daily loading cycle.

Some interesting results were obtained from moisture-in-oil models during typical cycles. In this case, it was obtained that besides the temperature distribution, sensor location is the most dominating aspect. The tested bottom-location for sensors was challenged in this study from the prospect of naturally cooled transformers. With regard to the loading behavior and temperature obtained, it was visible that an evident error will occur between the measured and simulated values. It is however still unclear as to where this sensor must be located without interfering with the daily operations of the equipment.

In the end, it is necessary to address the previously posted objectives and explore the applicability of the proposed solutions:

- **Mechanism of moisture migrations** was understood through thorough

investigations of the various transformer operations. Additionally, a parametric investigation on drying operations was done to segregate the moisture-uptake and removal processes to prove that all correlations are not universal.

- **Physics behing thermal profiles** was thoroughly investigated with the help of cfd-based thermal analysis models. Since low-voltage windings are closer to the core and posses higher heat density, the results were restricted, but not limited to low-voltage windings only.

- **Reliable thermal models** were developed using the proposed thermal model. The effect of a moving heat source was introduced for the first-time and its influence on the temperature distribution scheme was discusses. Simultaneously, it was also found that oil moisture near the winding will always be higher than the sensor location by the virtue of these thermal models.

- **Failure prone-zones** were identified with the help of this thermal model. The hottest-spot was identified mostly near the top of the winding.

- **Predictive models** were used to determine the effect of axial temperature rise on overall moisture changes in transformers. It was observed that although they do not influence the moisture-in-paper models, yet their influence on the oil moisture distribution near and away from the windings can not be ignored.

- **Quantitative** models were proposed for moisture in paper distribution by the virtue of changing time response during uptake or removal processes. These models are highly material specific and may not be universal, yet their applicability is not restricted.

- **Quantitative** models were proposed for moisture in oil distribution with respect to the variable loading pattern and temperature rise. It was observed that the average oil temperature near the winding will be higher as compared to that away from it, just justifying the effect of axial winding temperature.

6.2 Future Work

It is expected that the framework designed in this study can help in improving the basic understanding of moisture distribution in transformer. Future work may include refining of this model to improve the sensor location for oil-moisture measurements and identify probe-based techniques to determine the paper-moisture directly.

This completes the basic proposal about moisture dynamics on oil-filled power transformers and its related features.

Bio-data of Author

Sruti Chakraborty was born in 1989, near Bhilai, Chhattisgarh. She grew up in a small town at the outskirts of the city before eventually moving out to Gwalior, Madhya Pradesh for her higher education.

She holds a Bachelor's and Master's degree in Chemical Engineering from Jiwaji University (2010) and North Maharashtra University (2012) respectively. She was selected to work at Global R&D Center, Crompton Greaves Ltd in 2011 where she first came in contact with the topic of moisture related faults in power transformers.

Since then, she has successfully managed to publish various research articles on this topic in conferences and journals of international and national repute. She has also actively participated in various round-table conferences dedicated to transformer condition management and diagnostic research.

In 2013, she entered the PhD program at Malaviya National Institute of Technology, Jaipur. While studying at MNIT-J she published two paper in international conference of very high repute on diffusion mechanisms and drying mathematics respectively. She was also invited to write for Transformer Magazines, an international journal of very high repute on the same topic.

Besides her core research interest, she has participated actively in mathematical modeling of complex chemical problems and has successfully published two papers on alternate energy resources. She has also contributed to one international journal publication on production management scheme of urea fertilizer and diffusion mechanism of coated urea respectively.

Her main research interests are transformer management, thermal modeling, moisture dynamics, condition monitoring, alternate dielectrics, mathematical modeling and computational fluid dynamics.

Bibliography

[1] H. Gasser, C. Krause, and T. Prevost, "Water absorption of cellulosic insulating materials used in power transformers," in *Solid Dielectrics, 2007. ICSD'07. IEEE International Conference on*, pp. 289–293, IEEE, 2007.

[2] R. Rodriguez, *Moisture dynamics in transformers insulated with natural esters.* PhD Thesis, University Carlos III de Madrid, 2011.

[3] D. F. García, B. García, and J. C. Burgos, "Modeling power transformer field drying processes," *Drying Technology*, vol. 29, no. 8, pp. 896–909, 2011.

[4] T. A. Prevost and T. V. Oommen, "Cellulose insulation in oil-filled power transformers: Part i-history and development," *IEEE electrical insulation magazine*, vol. 22, no. 1, pp. 28–35, 2006.

[5] R. J. Liao, M. Z. Zhu, L. J. Yang, X. Zhou, and C. Y. Gong, "Molecular dynamics study of water molecule diffusion in oil–paper insulation materials," *Physica B: Condensed Matter*, vol. 406, no. 5, pp. 1162–1168, 2011.

[6] "Guide for installation and maintenance of oil-immersed power transformers," *IEEE Standard C 57.93*, no. 1, 2007.

[7] T. Oommen, "Moisture equilibrium in paper-oil insulation systems," in *Electrical/Electronical Insulation Conference, 1983 EIC 6th*, pp. 162–166, IEEE, 1983.

[8] M. Koch, *Reliable moisture determination in power transformers*. PhD Thesis, University of Stuttgart, 2008.

[9] P. Picher, F. Torriano, M. Chaaban, S. Gravel, C. Rajotte, and B. Girard, "Optimization of transformer overload using advanced thermal modelling," in *CIGRE conference, Paris, A2-305*, 2010.

[10] F. Torriano, M. Chaaban, and P. Picher, "Numerical study of parameters affecting the temperature distribution in a disc-type transformer winding," *Applied Thermal Engineering*, vol. 30, no. 14, pp. 2034–2044, 2010.

[11] Y. Du, *Measurement and modeling of moisture diffusion processes in transformer insulation using interdigital dielectrometery sensors*. PhD Thesis, Massachusetts Institute of Technology, 1999.

[12] S. Foss and L. Savio, "Mathematical and experimental analysis of the field drying of power transformer insulation," *IEEE Transactions on Power Delivery*, vol. 8, no. 4, pp. 1820–1828, 1993.

[13] L. Zhou, G. Wu, and J. Liu, "Modeling of transient moisture equilibrium in oil-paper insulation," *IEEE Transactions on Dielectrics and Electrical Insulation*, vol. 15, no. 3, 2008.

[14] J. Wijaya, W. Guo, T. Czaszejko, D. Martin, N. Lelekakis, and D. Susa, "Temperature distribution in a disc-type transformer winding," in *Industrial Electronics and Applications (ICIEA), 2012 7th IEEE Conference on*, pp. 838–843, IEEE, 2012.

[15] A. Skillen, A. Revell, H. Iacovides, and W. Wu, "Numerical prediction of local hot-spot phenomena in transformer windings," *Applied Thermal Engineering*, vol. 36, pp. 96–105, 2012.

[16] W. Guidi and H. Fullerton, "Mathematical methods for prediction of moisture take-up and removal in large power transformers," in *Proceedings of IEEE Winter Power Meeting*, vol. 100, pp. 242–244, 1974.

[17] S. V. Kulkarni and S. Khaparde, *Transformer engineering: design and practice*, vol. 25. CRC Press, 2004.

[18] R. M. Del Vecchio, B. Poulin, P. T. Feghali, D. M. Shah, and R. Ahuja, *Transformer design principles: with applications to core-form power transformers*. CRC press, 2010.

[19] J. H. Harlow, *Electric power transformer engineering*. CRC press, 2012.

[20] R. M. Marko, *Thermal modeling of a natural-convection cooled oil-immersed distribution transformer*. M.Sc Thesis, University of Manitoba, 1997.

[21] W. H. Tang and Q. Wu, *Condition monitoring and assessment of power transformers using computational intelligence*. Springer Science & Business Media, 2011.

[22] V. Kogan, J. Fleeman, J. Provanzana, and C. Shih, "Failure analysis of ehv transformers," *IEEE Transactions on Power Delivery*, vol. 3, no. 2, pp. 672–683, 1988.

[23] L. Lundgard, W. Hansen, D. Linhjell, and T. Painter, "Ageing of oil impregnated paper in power transformers," *IEEE Transactions on Power Delivery*, vol. 19, no. 2, pp. 230–239, 2004.

[24] P. Transformers—Part, "7: loading guide for oil-immersed power transformers," *IEC standard*, vol. 60076, no. 7, 2005.

[25] P. Griffin, V. Sokolov, and B. Vanin, "Moisture equilibrium and moisture migration within transformer insulation systems,"

[26] P. Griffin, C. Bruce, and J. Christie, "Comparison of water equilibrium in silicone and mineral oil transformers," in *Minutes of the Fifty-Fifth Annual International Conference of Doble Clients*, pp. 10–9, 1988.

[27] C. W. 05, "An international survery on failures in large power transformers in service," *Electrica*, vol. 88, 1983.

[28] V. Sokolov and B. Vanin, "Experience with in-field assessment of water contamination of large power transformers," in *Proceedings of EPRI Substation Equipment Diagnostics Conference VII, New Orleans*, Citeseer, 1999.

[29] D. Susa, *Dynamic thermal modeling of transformer*. PhD Thesis, Helsinki Institute of Technology, 2005.

[30] S. Tenbohlen, M. Stach, T. Lainck, G. Gunkel, J. Altmann, G. Darmisch, and E. Brasel, "New concepts for prevention of ageing by means of on-line degassing and drying and hearmatically sealing power transformers," *CIGRE A2 204*, 2004.

[31] M. Ariffin and P. Ghosh, "Estimating the age of paper insulation in 33/11 kv distribution power transformers using mathematical modelling," in *19th International Conference on Electricity Distribution*, pp. 1–4, 2007.

[32] D. H. Shroff and A. W. Stannett, "A review of paper aging in power transformers," in *IEE Proceedings C (Generation, Transmission and Distribution)*, vol. 132, pp. 312–319, IET, 1985.

[33] R. Jeffries, "The sorption of water by cellulose and eight other textile polymers," *Journal of the Textile Institute Transactions*, vol. 51, no. 9, pp. T339–T340, 1960.

[34] A. M. Emsley, X. Xiao, R. J. Heywood, and M. Ali, "Degradation of cellulosic insulation in power transformers. part 3: Effects of oxygen and water on ageing in oil," *IEE Proceedings-Science, Measurement and Technology*, vol. 147, no. 3, pp. 115–119, 2000.

[35] A. Emsley and G. Stevens, "Review of chemical indicators of degradation of cellulosic electrical paper insulation in oil-filled transformers," *IEE Proceedings-Science, Measurement and Technology*, vol. 141, no. 5, pp. 324–334, 1994.

[36] Y. Du, A. V. Mamishev, B. C. Lesieutre, M. Zahn, and S.-H. Kang, "Moisture solubility for differently conditioned transformer oils," *IEEE transactions on Dielectrics and Electrical Insulation*, vol. 8, no. 5, pp. 805–811, 2001.

[37] T. Rouse, "Mineral insulating oil in transformers," *IEEE Electrical Insulation Magazine*, vol. 14, no. 3, pp. 6–16, 1998.

[38] T. Oommen, "On-line moisture sensing in transformers," in *Electrical Electronics Insulation Conference, 1991. Boston'91 EEIC/ICWA Exposition., Proceedings of the 20th*, pp. 236–240, IEEE, 1991.

[39] M. Koch, "Improved determination of moisture in oil-paper-insulation by specialised moisture equilibrium charts,"

[40] W. Wu, *CFD callibrated thermal network modeling for oil cooled power transformers*. PhD Thesis, University of Manchester, 2011.

[41] B. Sparling and J. Aubin, "Assessing water content in insulating paper of power transformers," *Electr. Energy T&D Mag.*, vol. 11, no. 3, pp. 30–34, 2007.

[42] P. Thomas, A. Shukla, *et al.*, "Ageing studies on paper and oil to assess the condition of solid insulation used in power transformers," in *Solid Dielectrics, 2001. ICSD'01. Proceedings of the 2001 IEEE 7th International Conference on*, pp. 69–72, IEEE, 2001.

[43] A. Standard—C57.92, "Guide for loading mineral-oil immersed power transformers," *IEEE standard*, vol. 57, pp. 1–100, 1981.

[44] D. Susa and H. Nordman, "Iec 60076–7 loading guide thermal model constants estimation," *International Transactions on Electrical Energy Systems*, vol. 23, no. 7, pp. 946–960, 2013.

[45] P. Allen, O. Szpiro, and E. Campero, "Thermal analysis of power transformer windings," *Electric Machines and Electromechanics*, vol. 6, no. 1, pp. 1–11, 1981.

[46] A. Oliver, "Estimation of transformer winding temperatures and coolant flows using a general network method," in *IEE Proceedings C (Generation, Transmission and Distribution)*, vol. 127, pp. 395–405, IET, 1980.

[47] Y. Du, B. Lesiuetre, A. Mamishev, and S. Lindgren, "Moisture equilibrium in transformer paper-oil system," *IEEE Electrical Insulation Magazine*, vol. 15, no. 1, pp. 11–20, 1999.

[48] A. Asem and A. Howe, "Drying of power-transformer insulation," in *IEE Proceedings C (Generation, Transmission and Distribution)*, vol. 129, pp. 228–232, IET, 1982.

[49] J. Fabre and A. Pichon, "Deteriorating processes and products of paper in oil. application to transformers," *CIGRÉ paper*, vol. 137, p. 18, 1960.

[50] A. Emsley and G. Stevens, "Kinetics and mechanisms of the low-temperature degradation of cellulose," *Cellulose*, vol. 1, no. 1, pp. 26–56, 1994.

[51] T. Leibfried, A. J. Kachler, W. S. Zaengl, V. Der Houhanessian, A. Küchler, and B. Breitenbauch, "Ageing and moisture analysis of power transformer insulation systems," *CIGRÉ Session, Paris*, pp. 1–6, 2002.

[52] J. M. Mufuta and E. Van den Bulck, "Modelling of the mixed convection in the windings of a disc-type power transformer," *Applied Thermal Engineering*, vol. 20, no. 5, pp. 417–437, 2000.

[53] F. M. Clark, "Factors affecting the mechanical deterioration of cellulose insulation," *Transactions of the American Institute of Electrical Engineers*, vol. 61, no. 10, pp. 742–749, 1942.

[54] M. Saravolac, "The use of optic fibres for temperature monitoring in power transformers," in *Condition Monitoring and Remanent Life Assessment in Power Transformers, IEE Colloquium on*, pp. 7–1, IET, 1994.

[55] M. Pradhan and T. Ramu, "Diagnostic testing of oil-impregnated paper insulation in prorated power transformers under accelerated stress," in *Electrical Insulation, 2004. Conference Record of the 2004 IEEE International Symposium on*, pp. 66–69, IEEE, 2004.

[56] J. Unsworth and F. Mitchell, "Degradation of electrical insulating paper monitored with high performance liquid chromatography," *IEEE transactions on electrical insulation*, vol. 25, no. 4, pp. 737–746, 1990.

[57] W. Lampe and E. Spicar, "The oxygen-free transformer: Reduced ageing by continuous degassing," *Cigre paper*, vol. 12, no. 0, 1976.

[58] V. Sokolov, "Experience with the refurbishment and life extension of large power transformers," in *Minutes of the Sixty-First Annual International Conference of Doble Clients*, pp. 6–4, 1994.

[59] IEC641, "3-1: Specifications for pressboard and presspaper for electrical purposes, part3: specification for individual materials," *IEC standard*, vol. 64131, no. 7, 1992.

[60] C57.106, "Guide for acceptance and maintanance of insulating oil equipments," *IEEE standard*, vol. 57, pp. 1–100, 2002.

[61] R. Eberhardt, C. Sumereder, and M. Muhr, "Determination of humidity in oil impregnated cellulose insulation system," in *International colloquium Transformer Research and Asset Management*, pp. 1–6, CIGRÉ, 2009.

[62] M. Koch, S. Tenbohlen, and T. Stirl, "Advanced online moisture measurements in power transformers," *Proc. CMD*, pp. 1–6, 2006.

[63] J. D. Piper, "Moisture equilibrium between gas space and fibrous materials in enclosed electric equipment," *Electrical Engineering*, vol. 65, no. 12, pp. 791–797, 1946.

[64] G. Beer, G. Gasparani, F. Osimo, and F. Ross, "Experimental data on the drying-out of insulation samples and test coil for transformers," *CIGRÉ*, no. 135, 1966.

[65] T. Oommen, "Moisture equilibrium charts for transformer insulation drying practice," *IEEE transactions on power apparatus and systems*, no. 10, pp. 3062–3067, 1984.

[66] W. Fessler, T. Rouse, W. McNutt, and O. Compton, "A refined mathematical model for prediction of bubble evolution in transformers," *IEEE Transactions on Power delivery*, vol. 4, no. 1, pp. 391–404, 1989.

[67] P. Ast, "Movement of moisture through a50p281 kraft paper (dry and oil impregnated)," *General Electric, Test Report HV-ER-66-41*, 1966.

[68] R. Villarroel, D. Garcia, B. Garcia, and J. Burgos, "Diffusion coefficient in transformer pressboard insulation part 1: non impregnated pressboard," *IEEE Transactions on Dielectrics and Electrical Insulation*, vol. 21, no. 1, pp. 360–368, 2014.

[69] J. Crank, *The mathematics of diffusion*. Oxford university press, 1979.

[70] J. A. Thompson, "A moisture diffusion model for transformer oil and paper," in *Power and Energy Society General Meeting, 2011 IEEE*, pp. 1–3, IEEE, 2011.

[71] D. Garcia, B. Garcia, and J. Burgos, "A review of moisture diffusion coefficients in transformer solid insulation-part 1: coefficients for paper and pressboard," *IEEE Electrical Insulation Magazine*, vol. 29, no. 1, pp. 46–54, 2013.

[72] D. Garcia, R. Villarroel, B. Garcia, and J. Burgos, "A review of moisture diffusion coefficients in transformer solid insulation-part 2: Experimental validation of the coefficients," *IEEE Electrical Insulation Magazine*, vol. 29, no. 2, pp. 40–49, 2013.

[73] R. Hosseini, M. Nourolahi, and G. B. Gharehpetian, "Determination of od cooling system parameters based on thermal modeling of power transformer winding," *Simulation Modelling Practice and Theory*, vol. 16, no. 6, pp. 585–596, 2008.

[74] V. V. S. S. Haritha, *Thermal modeling of electrical utility transformers*. MS Thesis, Indian Institute of Information Technology, 2011.

[75] G. Bertotti, "General properties of power losses in soft ferromagnetic materials," *IEEE Transactions on magnetics*, vol. 24, no. 1, pp. 621–630, 1988.

[76] R. M. Del Vecchio and P. Feghali, "Thermal model of a disk coil with directed oil flow," in *Transmission and Distribution Conference, 1999 IEEE*, vol. 2, pp. 914–919, IEEE, 1999.

[77] J.-M. Mufuta and E. Van den Bulck, "Modelling of the mass flow distribution around an array of rectangular blocks in-line arranged and simulating the cross-section of a winding disc-type transformer," *Applied Thermal Engineering*, vol. 21, no. 7, pp. 731–749, 2001.

[78] J. Gastelurrutia, J. C. Ramos, G. S. Larraona, A. Rivas, J. Izagirre, and L. Del Río, "Numerical modelling of natural convection of oil inside distribution transformers," *Applied thermal engineering*, vol. 31, no. 4, pp. 493–505, 2011.

[79] N. El Wakil, N. C. Chereches, and J. Padet, "Numerical study of heat transfer and fluid flow in a power transformer," *International Journal of Thermal Sciences*, vol. 45, no. 6, pp. 615–626, 2006.

[80] T. Hammon and A. Stokes, "Optical fibre bragg grating temperature sensor measurements in an electrical power transformer using a temperature compensated optical fibre bragg grating as a reference," in *Optical Fiber Sensors*, p. Th337, Optical Society of America, 1996.

[81] A. L. Ribeiro, N. Eira, J. Sousa, P. Guerreiro, and J. Salcedo, "Multipoint fiber-optic hot-spot sensing network integrated into high power transformer for continuous monitoring," *IEEE Sensors Journal*, vol. 8, no. 7, pp. 1264–1267, 2008.

[82] H. Nordman and M. Lahtinen, "Thermal overload tests on a 400-mva power transformer with a special 2.5-pu short time loading capability," *IEEE Transactions on Power Delivery*, vol. 18, no. 1, pp. 107–112, 2003.

[83] D. Martin, J. Wijaya, N. Lelekakis, D. Susa, and N. Heyward, "Thermal analysis of two transformers filled with different oils," *IEEE Electrical Insulation Magazine*, vol. 30, no. 1, pp. 39–45, 2014.

[84] J. Zhang, X. Li, and M. Vance, "Experiments and modeling of heat transfer in oil transformer winding with zigzag cooling ducts," *Applied Thermal Engineering*, vol. 28, no. 1, pp. 36–48, 2008.

[85] E. Childs, "Flow maldistribution in disc-type power transformer windings," in *ASME, Heat Transfer Division*, vol. 75, pp. 137–143, 1987.

[86] J. Zhang and X. Li, "Coolant flow distribution and pressure loss in onan transformer windings part i: Theory and model development," *IEEE Transactions on Power Delivery*, vol. 19, no. 1, pp. 186–193, 2004.

[87] J. Zhang and X. Li, "Coolant flow distribution and pressure loss in onan transformer windings. part ii: Optimization of design parameters," *IEEE transactions on power delivery*, vol. 19, no. 1, pp. 194–199, 2004.

[88] O. Gouda, G. Amer, and W. Salem, "Predicting transformer temperature rise and loss of life in the presence of harmonic load currents," *Ain Shams Engineering Journal*, vol. 3, no. 2, pp. 113–121, 2012.

[89] G. Alegi and W. Black, "Real-time thermal model for an oil-immersed, forced-air cooled transformer," *IEEE transactions on power delivery*, vol. 5, no. 2, pp. 991–999, 1990.

[90] L. W. Pierce, "An investigation of the thermal performance of an oil filled transformer winding," *IEEE Transactions on Power Delivery*, vol. 7, no. 3, pp. 1347–1358, 1992.

[91] G. Swift, T. S. Molinski, and W. Lehn, "A fundamental approach to transformer thermal modeling. i. theory and equivalent circuit," *IEEE Transactions on Power Delivery*, vol. 16, no. 2, pp. 171–175, 2001.

[92] C. Weigen, P. Chong, and Y. Yuxin, "Power transformer top-oil temperature model based on thermal–electric analogy theory," *European Transactions on Electrical Power*, vol. 19, no. 3, pp. 341–354, 2009.

[93] G. Swift, T. S. Molinski, R. Bray, and R. Menzies, "A fundamental approach to transformer thermal modeling. ii. field verification," *IEEE Transactions on Power Delivery*, vol. 16, no. 2, pp. 176–180, 2001.

[94] E. Kranenborg, C. Olsson, B. Samuelsson, L. Lundin, and R. Missing, "Numerical study on mixed convection and thermal streaking in power transformer windings," in *Fifth European Thermal-Sciences Conf., The Netherlands*, 2008.

[95] J. Aubin, R. Bergeron, and R. Morin, "Distribution transformer overloading capability under cold-load pickup conditions," *IEEE Transactions on Power Delivery*, vol. 5, no. 4, pp. 1883–1891, 1990.

[96] R. Radakovic and K. Feser, "A new method for calculation of hot-spot temperature in power transformer with onan cooling," *IEEE Transactions on Power Delivery*, vol. 8, no. 4, pp. 1284–1292, 2003.

[97] R. Lewis, K. Morgan, and B. Schrefler, "A general method for predicting the flows and temperature in a network of interconnecting ducts," in *Numerical Methods in Thermal Problems: Proc. 2nd Int. Conf.*, vol. 2, pp. 623–635.

[98] M. Yamaguchi, T. Kumasaka, Y. Inui, and S. Ono, "The flow rate in a self-cooled transformer," *IEEE transactions on power apparatus and systems*, no. 3, pp. 956–963, 1981.

[99] E. Simonson and J. Lapworth, "Thermal capability assessment for transformers," in *Reliability of Transmission and Distribution Equipment, 1995., Second International Conference on the*, pp. 103–108, IET, 1995.

[100] E. Rahimpour, M. Barati, and M. Schäfer, "An investigation of parameters affecting the temperature rise in windings with zigzag cooling flow path," *Applied Thermal Engineering*, vol. 27, no. 11, pp. 1923–1930, 2007.

[101] Y.-H. Oh, K.-D. Song, J.-H. Sun, K.-Y. Park, and B.-H. Lee, "The thermal analysis of natural convection cooling type transformer," in *Electrical Machines and Systems, 2003. ICEMS 2003. Sixth International Conference on*, vol. 1, pp. 358–360, IEEE, 2003.

[102] H. Yamazaki, T. Sakamoto, and I. Takagi, "Basic cooling characteristics of perfluorocarbon liquid immersed windings for nonflammable transformers; disk coil cooling for large-capacity forced circulating transformers. part 1," *Heat Transfer-Japanese Research;(United States)*, vol. 20, no. 7, 1991.

[103] A. Weinläder and S. Tenbohlen, "Thermal-hydraulic investigation of transformer windings by cfd-modelling and measurements," in *Proceedings of the 16th International Symposium on High Voltage Engineering*, 2009.

[104] K.-J. Oh and S.-S. Ha, "Numerical calculation of turbulent natural convection in a cylindrical transformer enclosure," *Heat Transfer—Asian Research*, vol. 28, no. 6, pp. 429–441, 1999.

[105] R. W. Pryor, *Multiphysics modeling using COMSOL: a first principles approach*. Jones & Bartlett Publishers, 2009.

[106] C. M. Version, "4.3 user guide," *Released October 1st*, 2012.

[107] B. A. Finlayson, *Introduction to chemical engineering computing*. John Wiley & Sons, 2012.

[108] B. García, J. C. Burgos, A. M. Alonso, and J. Sanz, "A moisture-in-oil model for power transformer monitoring-part i: Theoretical foundation," *IEEE Transactions on Power Delivery*, vol. 20, no. 2, pp. 1417–1422, 2005.

[109] V. Davydov and O. Roizman, "Moisture assessment in power transformers," *Vaisala news*, vol. 160, pp. 18–21, 2002.

[110] J. A. Almendros-Ibanez, J. C. Burgos, and B. Garcia, "Transformer field drying procedures: A theoretical analysis," *IEEE Transactions on Power Delivery*, vol. 24, no. 4, pp. 1978–1986, 2009.

[111] A. Howe, "Diffusion of moisture through power-transformer insulation," in *Proceedings of the Institution of Electrical Engineers*, vol. 125, pp. 978–986, IET, 1978.

[112] B. Ramarao, A. Massoquete, S. Lavrykov, and S. Ramaswamy, "Moisture diffusion inside paper materials in the hygroscopic range and characteristics of diffusivity parameters," *Drying technology*, vol. 21, no. 10, pp. 2007–2056, 2003.

[113] J. Zhang and A. Datta, "Some considerations in modeling of moisture transport in heating of hygroscopic materials," *Drying Technology*, vol. 22, no. 8, pp. 1983–2008, 2004.

[114] J. Li, Z. Zhang, S. Grzybowski, and Y. Liu, "Characteristics of moisture diffusion in vegetable oil-paper insulation," *IEEE Transactions on Dielectrics and Electrical Insulation*, vol. 19, no. 5, 2012.

[115] M. C. Zaretsky, J. R. Melcher, and C. M. Cooke, "Moisture sensing in transformer oil using thin-film microdielectrometry," *IEEE Transactions on Electrical Insulation*, vol. 24, no. 6, pp. 1167–1176, 1989.

[116] R. Grubb, M. Hudis, and A. Traut, "A transformer thermal duct study fo various insulating fluids," *IEEE Transactions on Power Apparatus and Systems*, vol. PAS-100, no. 2, pp. 466–473, 1981.

[117] G. Kömürgöz, İ. Özkol, and N. Güzelbeyoğlu, "Temperature distribution in the disc-type coil of transformer winding," in *Second International Conference on Electrical and Electronics Engineering*, pp. 64–65, Citeseer, 2001.

[118] M. Pradhan and T. Ramu, "Estimation of the hottest spot temperature (hst) in power transformers considering thermal inhomogeniety of the windings," *IEEE transactions on power delivery*, vol. 19, no. 4, pp. 1704–1712, 2004.

PUBLICATIONS FROM THIS WORK

Simulation-based fluid-thermal analysis of power transformers

Critical reviews on advanced thermal assessment
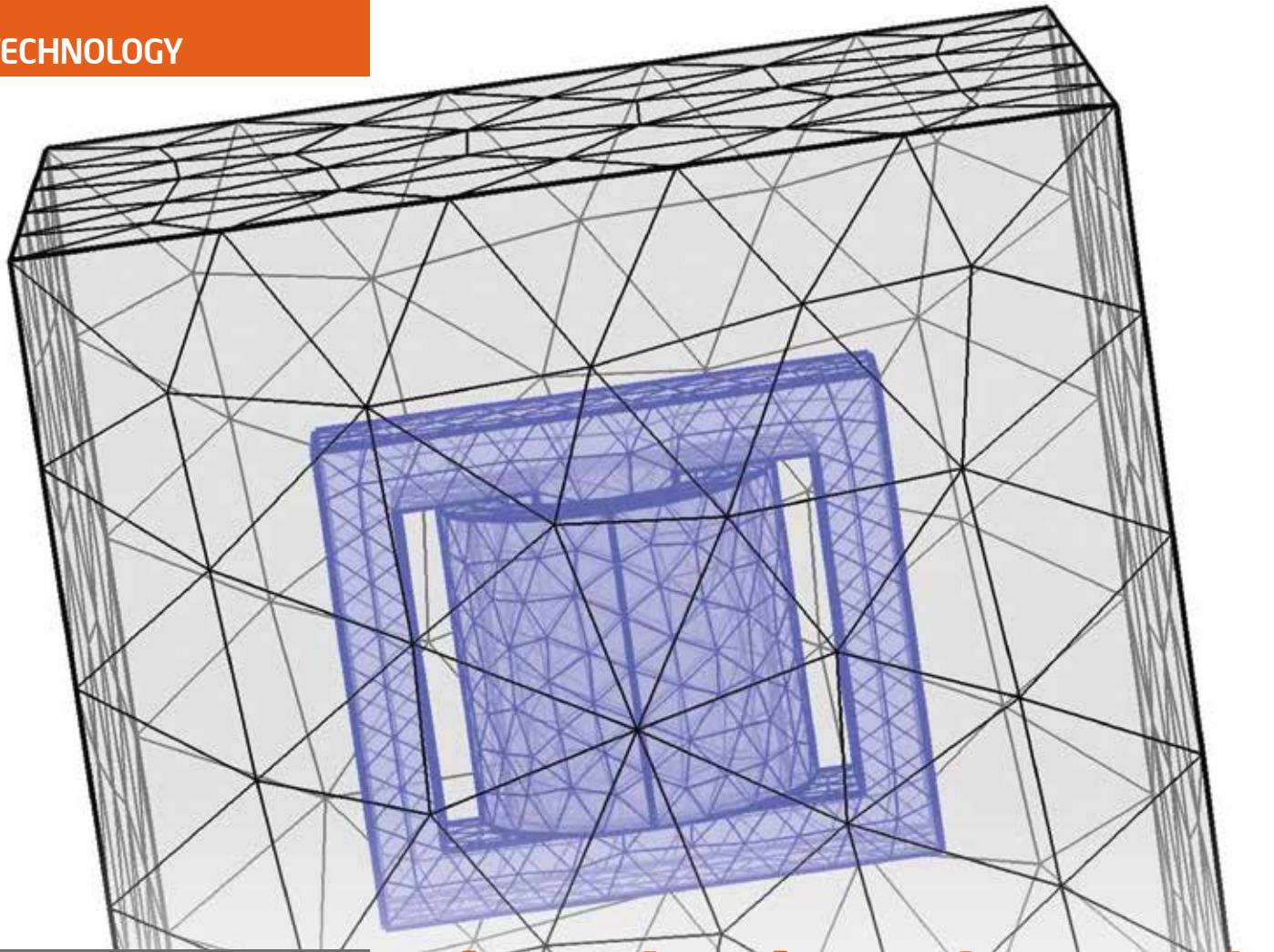
ABSTRACT

The transformer life and performance strongly depend on winding hot-spot temperature (HST). Various alternative techniques for HST prediction are gaining popularity over the conventional direct-measurement methods. In this context, the application of Computational Fluid Dynamics (CFD) based thermal models is particularly interesting because of their accurate assessment, higher precision and low cost. Besides, it can remarkably evaluate and improve the design efficiency of transformer without overshooting the capital cost. In the present work, a comprehensive understanding of CFD-based fluid-thermal assessment is attempted to encourage the readers to review transformer thermal models. It is also expected that these attempts will progressively assist in correlating various economical and operational parameters of transformer manufacturing and asset management.

KEYWORDS

oil-filled transformers, cooling, hot-spot, thermal assessment, Computational Fluid Dynamics

1. Introduction

The economic reliability of power transformer changes dramatically with its thermal performance. Renewed interests in improving the heat-induced failure models have steered the manufacturers and researchers towards application of advanced thermal modelling techniques that use highly efficient numerical approximation and visually-aided simulation-based solution approach. Two widely acclaimed methods for transformer thermal assessment are Thermal-Hydraulic Network Modelling (THNM) and Computational Fluid Dynamics (CFD). Their sole objective is to predict the oil-winding temperature rise and improve the winding-HST displacement predictions without compromising the capital cost.

These methods are realistic, cost-effective, scientifically accurate, and efficient in improving transformer performance through real-time simulations of multiple interdependent physical phenomena,

Thermal simulations are a step forward in comprehensive understanding of temperature rise phenomena within transformers with respect to localized heating and buoyancy-driven flows

which ultimately affects the temperature rise and HST evaluation. The attractive aspects of such methods include reliable estimation of the magnitude of internal heat, effect of coolant oil pattern and transformer configuration, and most significantly, its solution technique. Figure 1 is a representation of key aspects in CFD-based thermal modelling of any transformer.
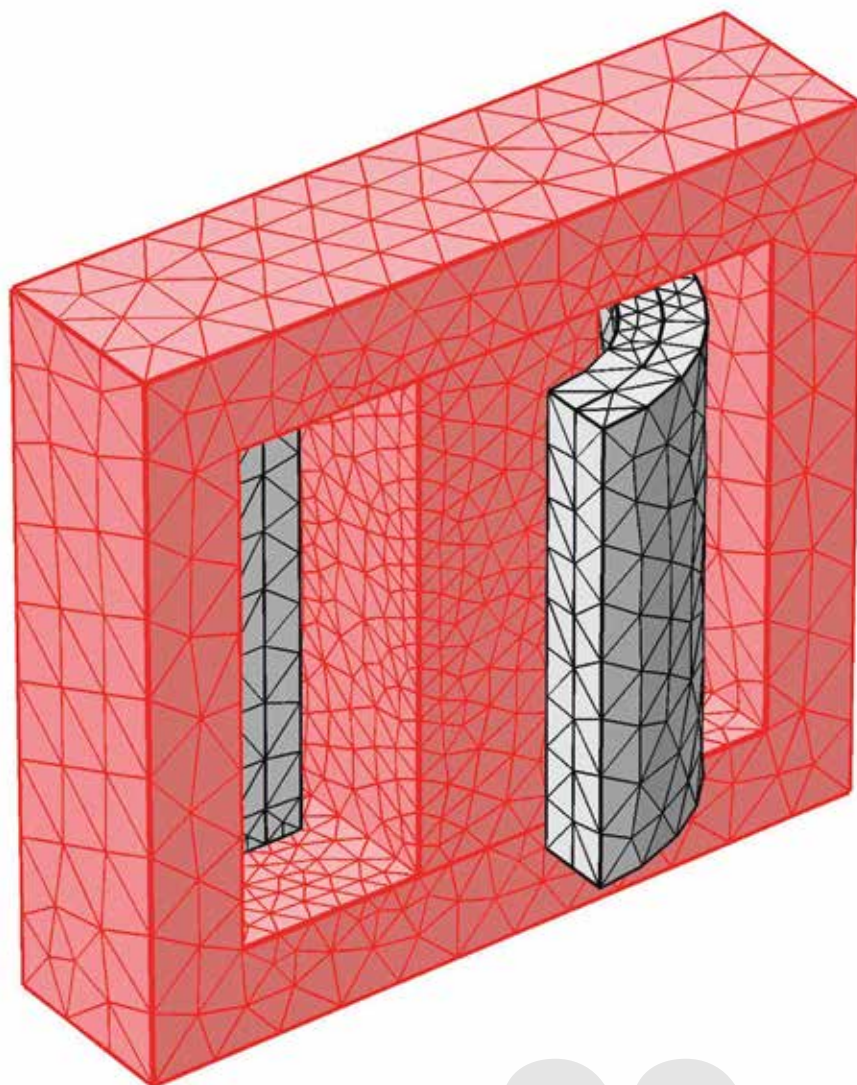
The upcoming sections of this article will assist the reader to gain a comprehensive understanding about CFD-based thermal modelling of an oil-filled transformer through an in-depth analysis of the concomitant multiphysics, application and limitations.

2. CFD-based thermal modelling: Key aspects

The accuracy of any CFD-based assessment improves inherently with proper understanding of governing physics and a potential solution technique. Therefore, pertinent information about the key aspects propelling a CFD-based assessment includes: calculation domain, governing physics and meshing scheme [1]. As we move forward, we will understand the physical significance of each of these aspects in detail.

2.1 Calculation domain

A 3D investigation of the equipment's thermal behaviour is undoubtedly the best incentive to assess, optimize and improve its functionality and in-service life. However, such an assessment not only requires pertinent information about

The transformer life and performance strongly depend on winding hot-spot temperature

a) Precise meshing of interactive area;
b) Analyzing the governing physics;
c) Evaluating the effect of winding configuration;
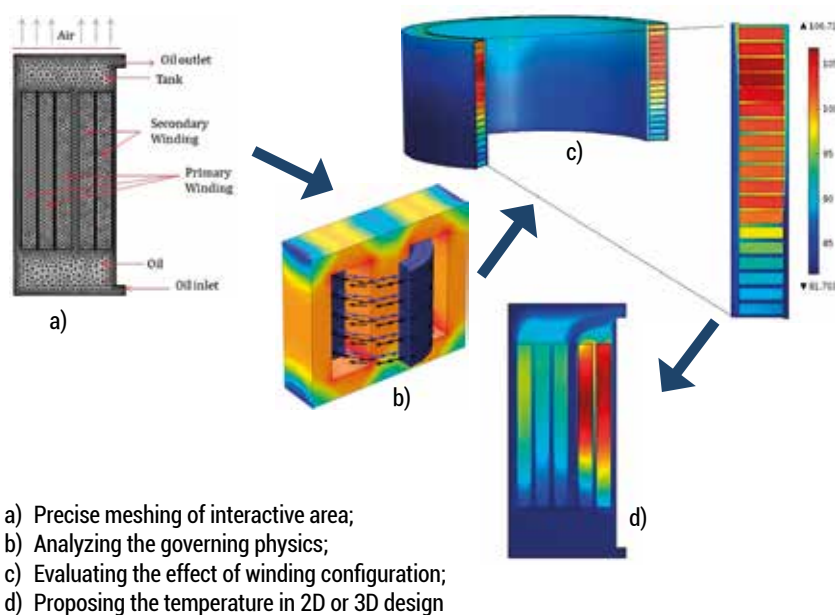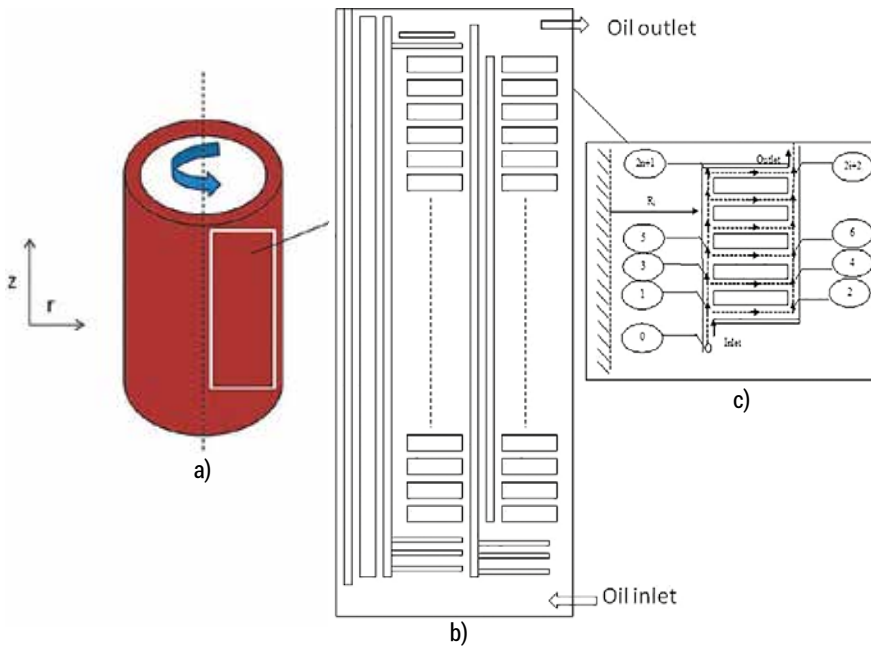d) Proposing the temperature in 2D or 3D design

Figure 1. Representation of key aspects of CFD-based thermal modelling of transformers

a) 3D winding;
b) 2D axisymmetric model;
c) 2D slice model

Figure 2. Simplification of the winding domain for CFD applications by schematic representation of 3D winding, 2D axisymmetric model, and 2D slice model

Apart from the transformer construction and operating conditions, interactive winding geometry strongly influences the transformer thermal behaviour

transformer construction, but also becomes tiresome if one is solely interested in examining the winding thermal performance as shown in Figure 2.

In the present work, exclusive discussions are presented on the CFD applications in improving the design of core-type transformers containing disc windings. Previous CFD-based attempts on estimating the impact of winding geometry on flow distribution reveals that the complex labyrinth of radial and axial channels in disc windings is responsible for mixed convection, thermal streaking and HST disposition with respect to buoyancy changes [1, 2, 5, 6, 8, 9]. This clearly indicates that apart from the transformer construction and operating conditions, interactive winding geometry strongly influences the transformer thermal behaviour.

2.2 Governing equations and boundary conditions

Classical combination of Navier-Stokes with energy conservation equations governs the fluid-thermal assessment of transformers by conservation of mass, momentum and energy, as shown below:

$$[\partial\rho/\partial t+((u.\nabla).\rho)]+\rho.(\nabla.u)=0 \qquad (1)$$

$$\rho.[\partial u/\partial t+((u.\nabla).u)]-\nabla.\sigma=F_v \qquad (2)$$

$$\rho.[\partial E/\partial t+((u.\nabla E)]-\nabla.(k_s.\Delta T_s)+p.\nabla u-Q_s=0^* \qquad (3)$$

Since oil is weakly-compressible, despite an infinitesimally small density variation ($\beta.\Delta T_f \ll 1$), the viscous flow will become strong enough to allow desired fluid-thermal interactions. This is known as the Boussinesq approximation and expressed mathematically as follows [4]:

$$F_v = \rho(T).g \qquad (4)$$

$$\rho(T) = \rho_0.[1-\beta.\Delta T_f] \qquad (5)$$

These governing equations require an inlet flow rate and hydrostatic pressure of oil as primary boundary conditions. In this context, oil inlet velocity can be obtained from an energy balance equation, whereas the inlet pressure of oil can be obtained by evaluating the hydrostatic pressure difference between the top and bottom of windings as shown below [7]:

$$u_0 = Q_s/(A_c.C_p.\rho.\Delta T_f) \qquad (6)$$

$$p_0 = \rho(T).g.H.\Delta T_f \qquad (7)$$

Where:
$\partial\rho/\partial t$ = rate of mass change (kg/m³·s)
$\partial u/\partial t$ = rate of momentum change (m/s²)
$\partial E/\partial t$ = rate of energy change (W/s)
u = vector representing velocity (m/s)
ρ = temperature dependent oil density (kg/m³)
ρ_0 = temperature dependent oil density at average ambient (kg/m³)
σ = viscosity tensor (Pa·s)
F_v = viscous body force (N/m³)
E = internal energy (W)
k_s = thermal conductivity of winding material (W/m·K)
T_s = winding thermal gradient (K)
Q_s = volumetric heat source (W/m³)
p = hydrostatic pressure (Pa)
T_f = oil temperature (K)
g = gravitational acceleration (m/s²)
u_0 = inlet oil velocity (m/s)
p_0 = inlet pressure (Pa)
A_c = cross sectional area of inlet channel (m²)
H = height of winding (m)

2.3 Meshing and grid analysis

The accuracy of any CFD-based assessment depends on its meshing precision. Meshing is the spatial discretization of the investigated domain into smaller blocks or cells of definite shapes (e.g. triangular or quadrilateral for 2D geometries, and tetrahedral, hexahedral, pyramids, or prisms for 3D geometries). Figure 3 shows a meshing scheme using 2D triangular elements of the investigated winding domain.

Previously, Finite Difference Method (FDM) based assessment produces false-time stepping over structured meshes, whereas FDM-based iterative approaches

The equations are in vector representation, where the dot "." represents multiplication of a scalar with a vector having spatially changing values.

show divergent patterns while analyzing buoyancy-driven flows. Unlike such loose and oversimplified grids, Finite Volume Method (FVM) not only incorporates a tighter grid, but also refines it continuously to ascertain the independence of physical properties over mesh complexities thereby increasing the solution accuracy, otherwise known as grid analysis [1]. Similar approaches exist within the Finite Element Method (FEM) based CFD environments, namely, COMSOL Multiphysics, Code_Saturne, etc. Both FVM and FEM apply various iterative solvers with suitable algorithms to analyze the proposed problems. Therefore, the solver continues to operate until the solution converges and the truncation error minimizes. The relative tolerance and convergence of FDM and FVM/FEM is approximately 10^{-3} and 10^{-6}, respectively, thus suggesting relatively tightly-controlled grid.

## 3. CFD analysis: Parametric investigations

The CFD-based fluid-thermal assessment of transformers, especially windings, depends on winding configuration and flow parameters besides the obvious transformer operating conditions. In this context, we investigate the effects of various parameters on oil-winding temperature rise and HST disposition on a 2D slice model of disc windings. Torriano et al. [9] provide the configuration details for a potential case-study on disc windings with various boundary conditions.

3.1 Effect of inflow: Location, magnitude, and pattern

Winding thermal performance strongly depends on flow distribution behaviour within the immediate vicinity of conducting discs. In fact, IEC 60076-2 (1993) suggests that the temperature rise limits and HST can be significantly improved through suitable analysis of oil-flow patterns [10]. In this context, analysis of oil inlet location, width of inlet, inflow velocity and flow pattern are prominent.

Figure 4(a) shows that upon changing the inlet location, the temperature rise limits can vary significantly. The effect of location is proposed by observing the inlet at inner (Ch_{in}) and outer (Ch_{out}) channels respectively, such that oil enters from bottom and exits from top of the winding. If the inlet channel width is

The application of CFD-based thermal models is particularly interesting because of their accurate assessment, higher precision and low cost
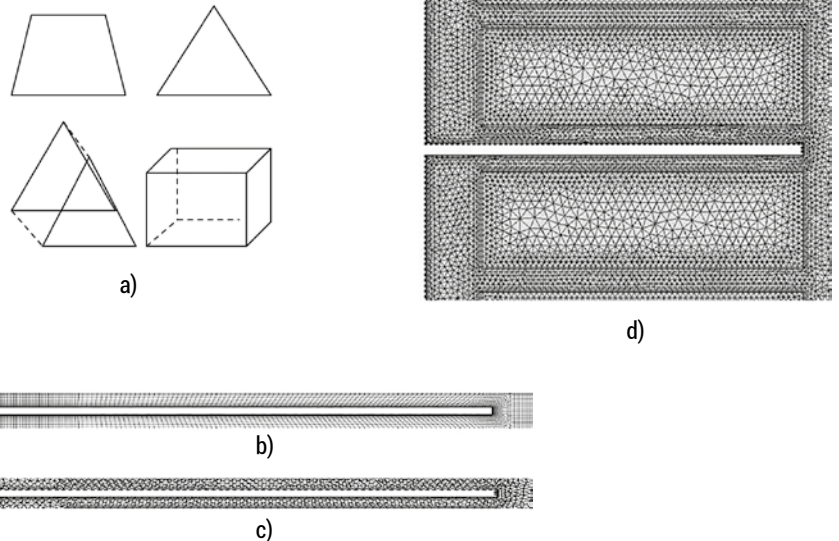
a) 2D and 3D mesh elements in FVM and FEM packages;
b) Structured meshing near washer;
c) Unstructured meshing near washer;
d) Free meshing of solid-fluid domain in FEM

Figure 3. Various meshing aspects of simulation-based fluid-thermal assessment of windings

small, then there is a homogeneous mixing of oil near the entrance of winding which decays with increasing entry length, thereby accumulating excess heat near the centre of the winding. This is also why HST exists somewhere in the middle or near the top, if not on the top most disc on the winding.

Figure 4(b) shows a sort of a parabolic temperature profile over a finite number of conducting discs, which is due to the parabolic velocity profile and fully developed hydrodynamic boundary layers near the conducting surfaces. The blue line depicts the surface temperature behaviour of conductors when the oil inlet is positioned at the outer channel given by the bottom contour of Figure 4(a). Similarly, the green curve depicts the surface temperature rise behaviour when inlet is located within the inner channel of winding as given by top contour of Figure 4(a). Hence, a complete "bathtub" temperature curve can be expected from such simulations.

Moreover, while a wider inlet channel

(Ch_{in} = 8.9 mm) allows lower temperature rise limits (HST at 89.92 °C) unlike narrow channels (Ch_{in} = 6.4 mm, HST at 92.702 °C), its application is also dominated by the flow calculations. In this particular case, the inner channel is 1.4 times the width of the outer channel as reported elsewhere [9]. At this point, one can easily observe that suitability of the inlet channel width and location depends entirely on the inflow conditions.

It is understood that if upstream oil circulation is extremely slow, then buoyancy decreases due to the overwhelming conduction. The resultant low oil velocities are rendered useless and winding heat dissipation fails. Hence, minimum oil velocity must be known to optimize and improve the transformer thermal design. The parametric investigation shown in Figure 5(a) reveals that average oil temperature rises rapidly beyond a certain value. Similar results can be expected to portray average conductor temperature.

a)

b)
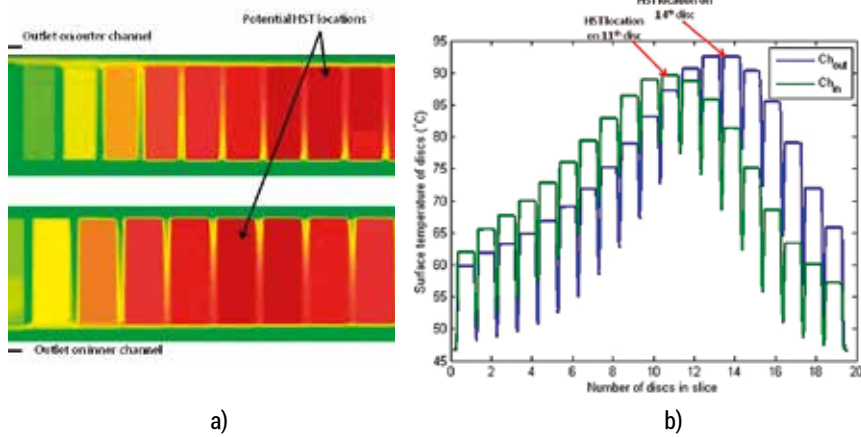
a) 2D plots depicting the effect of inlet location;
b) 1D plots depicting the effect of inlet location

Figure 4. Effect of inlet location and inlet channel width on temperature rise limits and HST
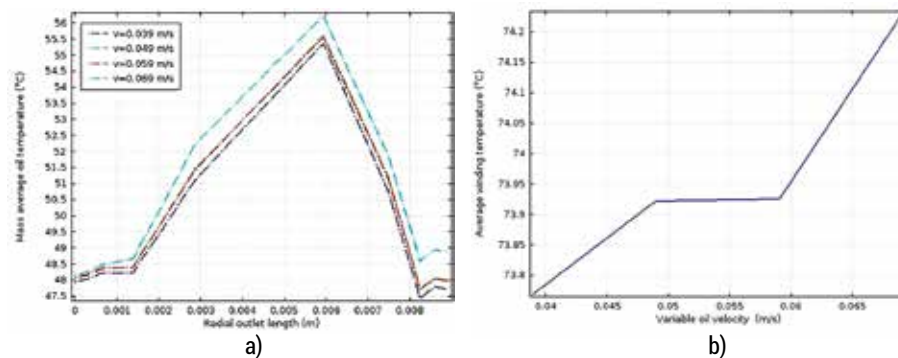
If upstream oil circulation is extremely slow, then buoyancy decreases due to the over-whelming conduction

It is evident from Figure 5 that without attaining the desired minimum velocity, efficient heat dissipation cannot be achieved. For example, if we apply very high velocity (u > 0.059 m/s) to a relatively thinner inlet channel, the average surface temperature will increase due to non-uniform mixing throughout the entry length. Maintaining uniform oil velocity across the winding height is equally significant, without which local heat accumulation and "heat-pool" formation can occur. To overcome this, pressboard washers (in the form of sticks and blocks) are strategically placed within the axial and radial channels of windings. Washer assisted oil flow is referred to as directed cooling, where washer location depends largely on radial duct height, number of discs, oil inlet velocity and transformer cooling pattern.

Figure 6(a) shows the application of various blocks and stick washers for improving transformer thermal design. Figure 6(b) shows the effect of stick spacers on winding thermal behaviour using 2D contour plots.

The strategic placement of these washers can dramatically reduce the HST magnitude. For example, when three passes are created within the single slice of winding by introducing washers near the 6th and 12th disc from the bottom, the magnitude of HST decreases by almost 5.8 °C when compared to two-pass structure. Washers alter the oil interaction pattern, thereby causing sudden change in temperature of conductor and the oil surrounding it. It is also obvious that despite better cooling efficiency, application of directed cooling is restricted by winding configuration and thus requires further improvement during the thermal assessment.

3.2 Effect of winding design: disc and layer

Figure 6 suggests that the transformers are not only distinguished on the basis of core configuration, but also by winding construction. Therefore, accurate information pertaining to winding configuration can influence the accuracy of any simulated assessment. Although a comparison between the disc and layer winding thermal profile is not possible because of obvious reasons, we still will try to objectify some of the critical outcomes that may support our hypothesis.

The thermal conductivity of copper and insulates is highly anisotropic [9], which varies for disc and layer arrangement even within the same transformer. This not only affects the heat source and resultant temperature calculations, but also affects the magnitude and location of HST formation on the assembly. Specific simulations reveal that while a hot-spot is expected somewhere near the top in case of disc windings, it is always encountered at the top in case of layer windings [12, 13]. However, the accuracy of this observation is yet to be established by further investigations using CFD-based techniques.

Although the scientific literature is abundant with various aspects of simulation-based thermal assessment of disc and layer type windings, suitable CFD calibrations to improve such models using modern day FVM and FEM solvers remain to be seen.

3.3 Effect of approximation approach

Any discussion on CFD-based assessment will remain incomplete without analysing the competency of the nume-

a)

b)

a) Rise in average oil temperature over outlet length;
b) Rise in average winding surface temperature

Figure 5. Effect of variable oil velocity on temperature rise behaviour

rical approximation technique. A CFD software package comprises three components: pre-processor, post-processor and solver. Basically, this solver acts as the brain of applied software package and hence one can navigate between packages based on solver operation. There are two basic solvers commercially available on the market: direct solvers and iterative solvers for analysing stationary, non-linear partial differential equations. As the name suggests, direct solvers apply matrix solution techniques such as Lower-Upper (LU) decomposition or Gauss elimination method, whereas iterative solvers apply numerical iteration techniques until the solution converges and the truncation error is minimized. This is also known as the convergence of applied solver as discussed earlier.

Since solvers apply a wide variety of algorithms to analyse and solve the posed problem, robustness and accuracy becomes intertwined. Over the years, FVM-based packages have acquired more than three quarters of the CFD market due to their easy implementation and wide range of applicability. Various researchers have implemented popular FVM packages such as ANSYS Fluent, Gambit, etc. to analyse the thermal behaviour of transformers. However, structured meshing and need for an alternate meshing interface adds to the overall computation cost of such packages.

On the other hand, FEM-based software packages are slowly gaining popularity among CFD users due to the high precision and ease of handling complex problems [12]. It is true that both FVM and FEM provide more-or-less the same geometric flexibility, unlike FDM packages which are strictly restricted to structured girds despite any curvature. However, FEM packages are exceptional due to their peculiar use of continuous Galerkin methods to generate weighed residual functions within the partial differential equations. Such an approach not only helps in reducing the domain complexity, but also simplifies the applied boundary conditions, thereby increasing the accuracy of solutions. This particular feature makes FEM superior to FVM despite its somewhat disadvantageous feature – domain dependence. Currently researchers are feverishly trying to improve such pitfalls of FEM-based packages and improved versions;
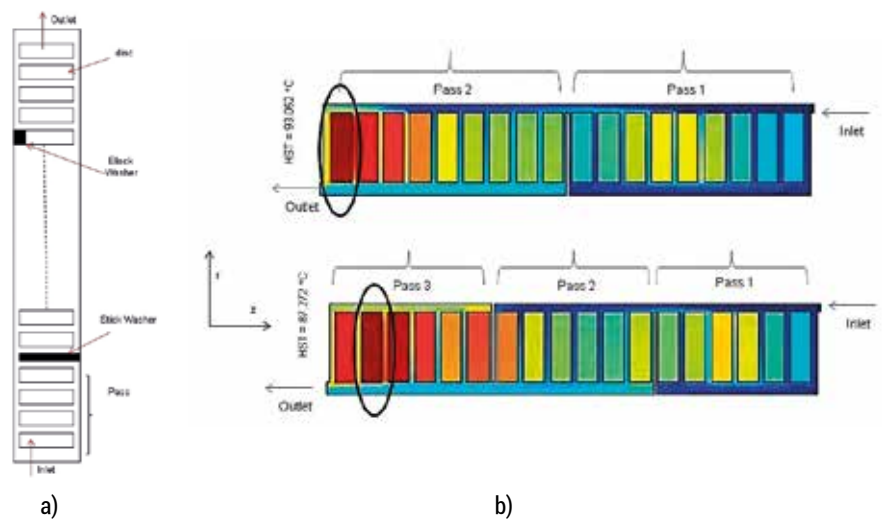
a) Type of washers in disc windings;
b) Effect of stick washer on winding temperature rise

Figure 6. Effect of washers on winding temperature rise and HST behaviour

Minimum oil velocity must be known to optimize and improve the transformer thermal design

namely, COMSOL Multiphysics, Code_Saturne, etc. are beginning to float in the commercial market.

4. Result verification

One of the persistent questions with simulation-based assessments is verification of the CFD results. Currently, the simulated results are either compared against on-site heat-run tests, verified by gas analysis or applying continuously evolving standards such as IEC60354, IEC60076-2, etc. [10, 11]. At this point, one has to understand that the essence of simulation-based assessments is to inform the researcher/manufacturer about several manifolds of coupled multiphysics that ultimately govern the fluid-thermal behaviour of transformer under variable conditions. We hope to reach a point in the future where more advanced technologies could assist the researcher in analysing and verifying the CFD analysis without overshooting the recurring experimental costs.
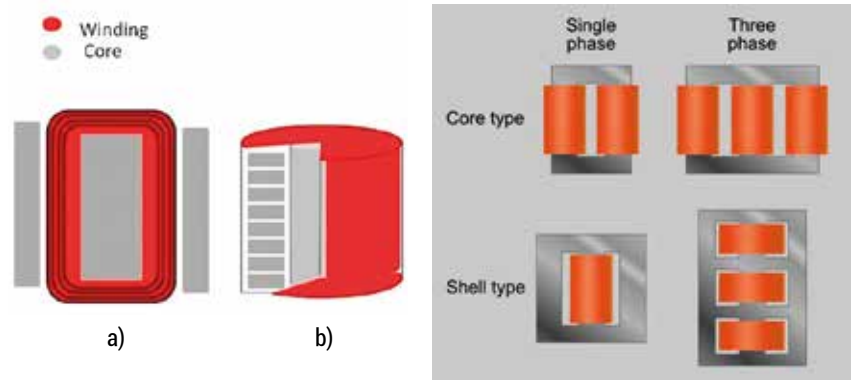

Figure 7. Various core and winding constructions in transformers: a) layer winding; b) disc winding

The accuracy of any CFD-based transformer thermal assessment depends on the accurate information on winding design, operational parameters, loading behaviour and its meshing precision

Conclusion

The accuracy of any CFD-based transformer thermal assessment depends on accurate information on winding design, operational parameters and loading behaviour. It is a unique step forward towards comprehensive understanding of temperature rise phenomena within transformers with respect to localized heating and buoyancy driven flows. Such methods are immensely popular for determining design efficiency of transformers regardless of their operational stage. However, the sole limitation of this alternative is its accuracy restriction on oversimplified 2D models. In case of 3D systems, the computational time significantly increases, thereby increasing the cost of assessment. This suggests future scope of method improvement whether by software upgrading or mathematical simplification.

Bibliography

[1] J Mufuta, E. Van den Bulck, *Modelling of the mixed convection in thewindings of a disc-type power transformer*, Applied Thermal Engineering, Vol. 20, no. 5, pp. 417-437, 2000

[2] J Kranenborg, C O. Olsson, B Samuelsson, L Å.Lundin, R M.Missing, *Numerical study on mixed convection and thermal streaking in power transformer windings*, 5th European Conference on Thermal Sciences, Eindhoven (Netherlands), 2008

[3] R Hosseini, M Nourolahi, G B. Gharehpetian, *Determination of OD cooling system parameters based on thermal modelling of power transformer winding*, Simulation Modelling Practice and Theory, Vol. 16, no.8, pp. 585-596, 2008

[4] F Torriano, M Chaaban, P Picher, *Numerical investigation of 3D flow and thermal effects in a disc-type transformer winding*, Applied Thermal Engineering, Vol. 40, no.1, pp. 121-131, 2010

[5] P H G Allen, O Szpiro, E Campero, *Thermal analysis of power transformer windings*, Electrical Machines and Power Systems, Vol. 6, no.1, pp. 6- 11, 1981

[6] A Skillen, A Revell, H Iacovides, W Wu, *Numerical prediction of local hot-spot phenomena in transformer windings,* Applied Thermal Engineering, Vol. 36, no.1, pp. 96-105, 2012

[7] J Wijaya, W Guo, T Czaszejko, D. Susa, *Temperature distribution of disc type windings in transformers*, 7th IEEE Conferece on Industrial Electronics and Applications, Singapore, 2012

[8] X Zhang, Z Wang, Q Liu, *Prediction of pressure drop and flow distribution in disc type transformer windings in an OD-cooling mode,* IEEE Transactions on Power Delivery, TPWRD-01247-2015, pp. 1-9, 2016

[9] F Torriano, M Chaaban, P Picher, *Numerical study of parameters affecting the temperature distribution in disc-type transformer winding*, Applied Thermal Engineering, Vol. 30, no.1, pp. 2034-2044, 2010

[10] IEC Standard Publications, Temperature rise in oil-filled transformers, IEC 60076-7, 2005

[11] IEC Standard Publications, Temperature rise in oil-filled transformers, IEC 60076-2, 2011

[12] E. Dick, *Computational Fluid Dynamics: An Introduction*, 3rd edition, Springer, 1995

[13] M K Pradhan, T S Ramu, *Estimation of hottest spot temperature in power transformers considering thermal inhomegeniety of windings*, IEEE Transactions on Power Delivery, Vol. 19, no.4, pp.1704-1712, 2004

Authors

Sruti Chakraborty is a doctoral candidate at the Department of Chemical Engineering, Malaviya National Institute of Technology, India. She is currently working on improving transformer diagnostics through dynamic moisture migration models. Her research interests include transformer thermal modelling, condition monitoring, alternative fluids, mathematical modelling, and CFD. She has published 15 papers in various journals and conferences of high repute and is winner of two academic awards.

Manish Vashishtha is an assistant professor at the Department of Chemical Engineering, Malaviya National Institute of Technology, India. He obtained his PhD on Interface Engineering from Indian Institute of Technology, New Delhi in 2010. He has more than 15 years of teaching and research experience with 40 research publications to his name. His research interests are mathematical modelling, fluid dynamics, thin-films, and equipment design.

Sushil E. Chaudhari is an Assistant General Manager (AGM) at Raj Petro Specialties Pvt. Ltd., Mumbai, India. He obtained his PhD from Baroda University, India in 2007. He has previously worked with Crompton Greaves Ltd. and actively participated in the field of liquid dielectrics, new manufacturing process development and existing process enhancement and condition monitoring and diagnostics of power transformers and reactors. He is an active member of CIGRE Working Group and an IEEE reviewer with 17 patents and 12 publications to his name.

A novel approach to determine moisture migration through pressboard insulation using FEM

Sruti Chakraborty and Manish Vashishtha

A Novel Approach to Determine Moisture Migration Through Pressboard Insulation Using FEM

Sruti Chakraborty[1,a] and Manish Vashishtha[1,b]

[1]*Department of Chemical Engineering, Malaviya National Institute of Technology, JLN-Marg, Jaipur-302017, India*

[a]Corresponding author: 2012rch9520@mnit.ac.in
[b]mvashishtha.chem@mnit.ac.in

Abstract. Moisture measurement in transformer pressboard is an integral part of monitoring mechanical and dielectric strength of insulation. The existing correlations for pressboard moisture mostly considers non-impregnated and steady state (equilibrium) conditions at oil and pressboard interface. In this paper, we discuss the transient moisture migration in oil impregnated pressboard insulation between two consecutive equilibrium conditions with due emphasis on insulation properties. This study is helpful in determining the insulation drying time and moisture retention in impregnated pressboards without conducting extensive experimentation.

INTRODUCTION

Cellulosic insulation (paper, pressboard, wood etc.) plays a significant role in providing structural and dielectric support to an electrical transformer for its safe operation under fluctuating loading cycles (Prevost and Oommen, 2006). It is economic and highly accepted way to insulate windings of oil filled electrical transformers operating at high and extra high voltage levels. It contains multiple layers of anhydrous-beta-D-Glucose links with high tensile strength, dielectric stability and moisture adherence. The minimum moisture retention within the microfibrils of thick and thin insulation can be up to 0.5-1% (dry basis) in new transformer and 2-4% (dry basis) in old transformers (>20years).

Due to difficult accessibility, Oommen (1984) suggested an indirect method to calculate moisture in paper/pressboard by moisture in oil assuming a so-called equilibrium between moisture in oil and paper. The moisture in pressboard is a ration of mass of moisture in pressboard to mass of pressboard (on dry-basis).In simpler terms, it is the ration of partial vapor pressure (P_v) of moisture to saturated water vapor pressure (P_{sat}) for known temperature (otherwise known as relative humidity) :

$$R.H_{air} = R.H_{paper} = \frac{P_v}{P_{sat}} \tag{1}$$

During equilibrium conditions in an air-pressboard system, the relative humidity pf (RH_{air}) is equal to that of pressboard (RH_{PB}). Saturated moisture vapor pressure is easily estimated using Magnus correlation, where P_{sat} is expressed in hPa and air temperature is expressed in ^0C:

$$P_{sat} = 6.10 \times 10^{\frac{A_1 T}{B_1 + T}} \tag{2}$$

The constants in Magnus formulae i.e. A_1 and B_1 are 1.5 and 235 respectively and are experimentally determined. Further, the moisture in pressboard sample on achieving equilibrium is calculated from Fessler's formulae correlating P_v (mmHg) and equilibrium moisture content (C_{eq}) during a local thermal equilibrium:

$$C_{eq} = 2.173 \times 10^{-7} \times P_v^{0.6685} \times \exp\left(\frac{4725.6}{T + 273.15}\right)$$

(3)

All these equations strongly suggest equilibrium between pressboard, air and surrounding oil so-as to determine the moisture concentration in one system or the other. Most of these equations are empirical correlations with little to no information about the actual experimentation. Some common correlations as discussed in forthcoming sections allow the usage of these equations for oil impregnated Kraft paper and non-impregnated pressboards of variable thickness. However, information on moisture migration from oil-impregnated pressboard is still scarce.

MATHEMATICAL MODEL

During temperature transients between pressboard and oil, moisture migrates from cellulosic insulation into oil through a coupled heat and moisture transport process. Equations (1-3) are applicable during isothermal conditions only when the temperature of pressboard is higher than that of oil. With sudden drop in pressboard temperature the migration may change direction and thus move from oil to pressboard. It is evident by now that small temperature transients can change the direction of moisture migration and therefore Fick's second law of diffusion in one dimension can explain moisture migration from pressboard to oil in an insulation system during unsteady "transient" state:

$$\frac{\partial C(x,t)}{\partial t} = \frac{\partial}{\partial x}\left(D(C,T)\frac{\partial C(x,t)}{\partial x}\right)$$

(4)

Where $C(x,t)$ is the local moisture concentration in pressboard sample of thickness, x and at any given time, t and D is the diffusion coefficient of moisture in pressboard that depends on the local moisture concentration (C) and temperature (T). Du et al.(1999) reported some experimentally determined diffusion coefficients (D) using Arrhenius analogy for impregnated and non-impregnated paper:

$$D(C,T) = D_0\left\{\exp\left(k \times C(x,t) + E_a\left(\frac{1}{T_0} - \frac{1}{T}\right)\right)\right\}$$

(5)

The constants D_0, k and Ea depend on the nature of material and can be experimentally determined; T_0 is a reference temperature (298 K) and T is absolute temperature. For this research the values of coefficients, D_0, k and Ea are 0.67E-12 (m^2/s), 0.5 and 7046 (K) respectively. Equation (5) is a one-dimensional partial differential equation (PDE) and Fourier series shows the general solution on the interface boundary:

$$C(x,t) = C_{eq}\left(1 + \frac{4}{\pi}\exp\left\{Dt\left(\frac{-\pi^2}{L^2}\right)\right\}\sin\left(\frac{\pi x}{L}\right)\right)$$

(6)

Analytical solution is tough to obtain when the number of oil-pressboard interfaces increases and therefore, the exact solution of equation (5) using Finite Element Method (FEM) that requires discretization of moisture in pressboard $C(x,t)$ over spatial and temporal scales as shown below [3]:

$$C_{i,j+1} = C_{i,j} + D_0\left\{\exp\left(Ea\left(\frac{1}{T_0} - \frac{1}{T}\right) + kC_{i,j}\right) \times \frac{\Delta t}{(\Delta x)^2}\right\}$$

$$\times \left[\frac{k}{4}\left(C_{i+1,j} - C_{i,j}\right) + \left(C_{i+1,j} + C_{i-1,j} - 2C_{i,j}\right)\right]$$

(7)

Where, i×j is shows the moisture concentration matrix over space (i) and time (j) separated by small space (Δx) and time steps (Δt) respectively. The boundary conditions to solve equation (7) are:

$$C_{(i=0,j)} = 0, \ C_{(i=L,j)} = C_{eq}, \frac{dC_{(x,t=0)}}{dx} = 0 \tag{8}$$

RESULTS

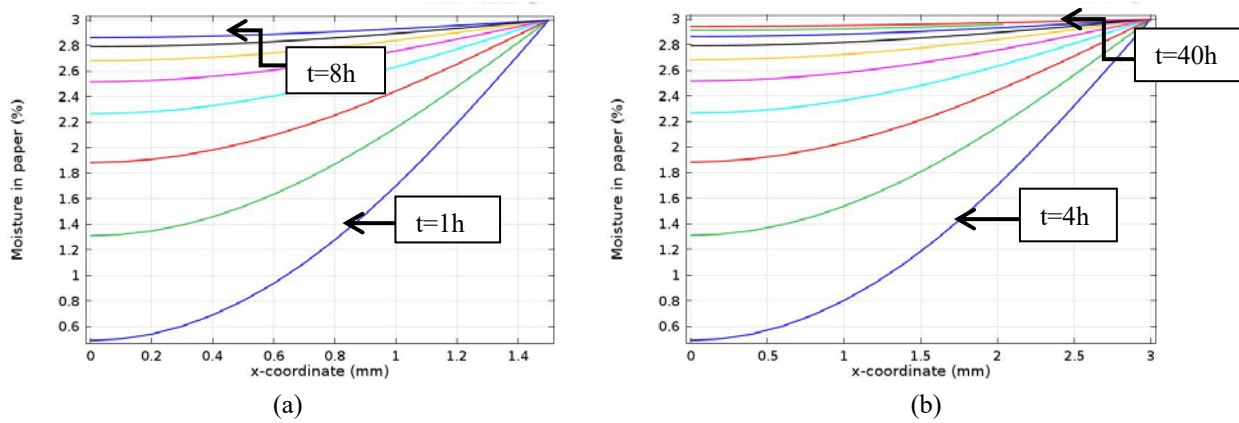Fig. 1 and 2 shows single-sided diffusion from 1.5 and 3 mm oil impregnated pressboard at different temperatures.

(a)

(b)

FIGURE 1. Single-sided diffusion of moisture in pressboard of (a) 1.5mm, (b) 3mm at 3% equilibrium moisture under 80^0C

(a)

(b)

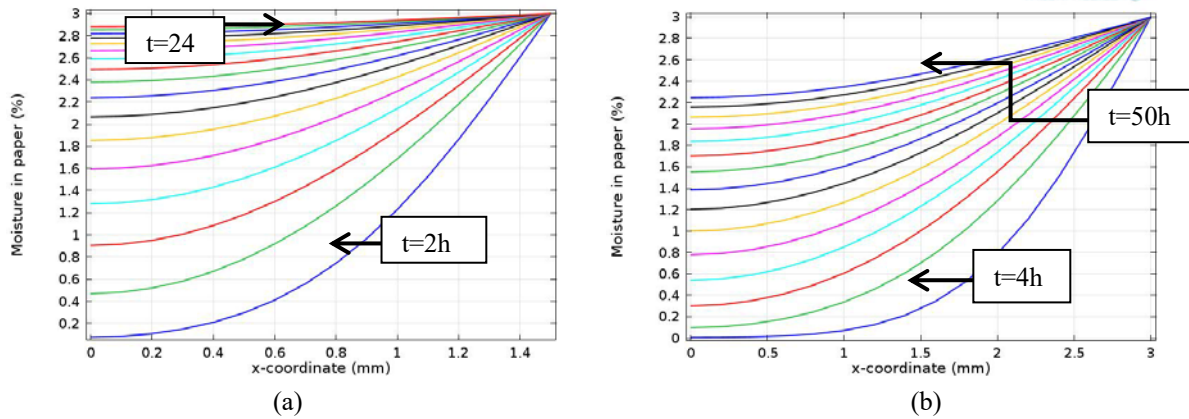**FIGURE 2.** Single-sided diffusion of moisture in pressboard of (a) 1.5mm, (b) 3mm at 3% equilibrium moisture under 60^0C

Table 1 shows interesting data on equilibrium time constant for moisture diffusion in pressboard insulation based on simulated diffusion data. It emphasizes that as the thickness of insulation doubles, the equilibrium time constant quadruples at same temperature and initial moisture concentration.

TABLE 1. Calculated equilibrium time constants for oil impregnated pressboards

PB thickness (mm)	Temperature (^{0}C)	Equilibrium time constant (h)
1.5	60	1.74
	80	0.527
3	60	6.97
	80	2.110

CONCLUSIONS

This paper discusses a simple method to develop moisture in oil-pressboard insulation system of transformers using finite element approach. Diffusion coefficient of moisture in pressboard is an influential parameter in determining moisture at oil-pressboard interface, which is of utmost importance during transformer monitoring. The general solution of moisture diffusion equation using Fick's second law is similar to Fourier series solution of 1-dimensional PDE. In this work, separate solution for moisture in oil-pressboard interface of insulation system with variable insulation thickness suggests strong correlation of moisture thickness on equilibrium time constant for oil-impregnated pressboards. Due to scarcity of diffusion coefficients for oil-impregnated pressboards, the applicability of these solutions is still under consideration. Future work involves developing strong empirical relations to fit the simulated curves for moisture behavior in oil-impregnated pressboards for non-isothermal cases.

ACKNOWLEDGMENTS

REFERENCES

1. T. A. Prevost, and T. V. Oommen, IEEE Electr. Insul. Mag. **1**, 28-35 (2006).
2. Y. Du, M. Zahn, B. C. Lesieutre and A.V. Mamishev, IEEE Electr. Insul. Mag. **15**, 11-20 (1999).
3. T. V. Oommen, IEEE Trans. Power App. Sys. **PAS 103**, 3063-3067 (1984).
4. L. J. Zhou, G. N. Wu and J. Liu, IEEE Trans. Dielec. Electr. Insul. **15**, 872-878 (2008).
5. W. Hribernik, W. Kubicek, G. Pascoli, and K. Frohlich, "Verification of a model-based diagnostic system for on-line detection of the mositure content of power transformer insulation using finite element calculation," in IEEE Condition Monitoring and Diagnostics Conference Proceedings (Beijing, CN, 2008), pp. 475-478.
6. J. Li, Z. Zhang, S. Grzybowski, and M. Zahn, IEEE Trans. Dielec. Electr. Insul. **19**, 1615-1622 (2012).

International Conference of
Numerical Analysis and Applied Mathematics 2016
(ICNAAM 2016)
Rodos Palace-Conference Center, Rhodes, Greece,
19-25 September 2016

CERTIFICATION

We certify that **Dr. Manish Vashishtha** has participated in the International Conference of Numerical Analysis and Applied Mathematics 2016 (ICNAAM 2016) with presentation of a scientific paper entitled "*A novel approach to determine moisture migration through pressboard insulation using FEM*" by *Sruti Chakraborty* and *Manish Vashishtha*.

ICNAAM 2016

On behalf of the
Organizing Committee

Prof. T.E. Simos
Academician of the EASA, EAS, EAASL
President of the European Society of Computational Methods
in Sciences and Engineering(ESCMSE)
Chair ICNAAM 2016

A novel approach to determine moisture migration through pressboard insulation using FEM

Sruti Chakraborty[1,a] and Manish Vashishtha[1,b]

[1]*Department of Chemical Engineering, Malaviya National Institute of Technology, JLN-Marg, Jaipur-302017, India*

[a]Corresponding author: 2012rch9520@mnit.ac.in
[b]mvashishtha.chem@mnit.ac.in

Abstract. Moisture measurement in transformer pressboard is an integral part of monitoring mechanical and dielectric strength of insulation. The existing correlations for pressboard moisture mostly considers non-impregnated and steady state (equilibrium) conditions at oil and pressboard interface. In this paper, we discuss the transient moisture migration in oil impregnated pressboard insulation between two consecutive equilibrium conditions with due emphasis on insulation properties. This study is helpful in determining the insulation drying time and moisture retention in impregnated pressboards without conducting extensive experimentation.

INTRODUCTION

Cellulosic insulation (paper, pressboard, wood etc.) plays a significant role in providing structural and dielectric support to an electrical transformer for its safe operation under fluctuating loading cycles (Prevost and Oommen, 2006). It is economic and highly accepted way to insulate windings of oil filled electrical transformers operating at high and extra high voltage levels. It contains multiple layers of anhydrous-beta-D-Glucose links with high tensile strength, dielectric stability and moisture adherence. The minimum moisture retention within the microfibrils of thick and thin insulation can be up to 0.5-1% (dry basis) in new transformer and 2-4% (dry basis) in old transformers (>20years).

Due to difficult accessibility, Oommen (1984) suggested an indirect method to calculate moisture in paper/pressboard by moisture in oil assuming a so-called equilibrium between moisture in oil and paper. The moisture in pressboard is a ration of mass of moisture in pressboard to mass of pressboard (on dry-basis).In simpler terms, it is the ration of partial vapor pressure (P_v) of moisture to saturated water vapor pressure (P_{sat}) for known temperature (otherwise known as relative humidity) :

$$R.H_{air} = R.H_{paper} = \frac{P_v}{P_{sat}}$$

1

During equilibrium conditions in an air-pressboard system, the relative humidity pf (RH_{air}) is equal to that of pressboard (RH_{PB}). Saturated moisture vapor pressure is easily estimated using Magnus correlation, where P_{sat} is expressed in hPa and air temperature is expressed in ^{0}C:

1

$$P_{sat} = 6.10 \times 10^{\frac{A_1 T}{B_1 + T}} \qquad\qquad 2$$

The constants in Magnus formulae i.e. A_1 and B_1 are 1.5 and 235 respectively and are experimentally determined. Further, the moisture in pressboard sample on achieving equilibrium is calculated from Fessler's formulae correlating P_v (mmHg) and equilibrium moisture content (C_{eq}) during a local thermal equilibrium:

$$C_{eq} = 2.173 \times 10^{-7} \times P_v^{0.6685} \times \exp\left(\frac{4725.6}{T + 273.15}\right) \qquad\qquad 3$$

All these equations strongly suggest equilibrium between pressboard, air and surrounding oil so-as to determine the moisture concentration in one system or the other. Most of these equations are empirical correlations with little to no information about the actual experimentation. Some common correlations as discussed in forthcoming sections allow the usage of these equations for oil impregnated Kraft paper and non-impregnated pressboards of variable thickness. However, information on moisture migration from oil-impregnated pressboard is still scarce.

MATHEMATICAL MODEL

During temperature transients between pressboard and oil, moisture migrates from cellulosic insulation into oil through a coupled heat and moisture transport process. Equations (1-3) are applicable during isothermal conditions only when the temperature of pressboard is higher than that of oil. With sudden drop in pressboard temperature the migration may change direction and thus move from oil to pressboard. It is evident by now that small temperature transients can change the direction of moisture migration and therefore Fick's second law of diffusion in one dimension can explain moisture migration from pressboard to oil in an insulation system during unsteady "transient" state:

$$\frac{\partial C(x,t)}{\partial t} = \frac{\partial}{\partial x}\left(D(C,T)\frac{\partial C(x,t)}{\partial x}\right) \qquad\qquad 4$$

Where C(x,t) is the local moisture concentration in pressboard sample of thickness, x and at any given time, t and D is the diffusion coefficient of moisture in pressboard that depends on the local moisture concentration (C) and temperature (T). Du et al.(1999) reported some experimentally determined diffusion coefficients (D) using Arrhenius analogy for impregnated and non-impregnated paper:

$$D(C,T) = D_0\left\{\exp\left(k \times C(x,t) + E_a\left(\frac{1}{T_0} - \frac{1}{T}\right)\right)\right\} \qquad\qquad 5$$

The constants D_0, k and Ea depend on the nature of material and can be experimentally determined; T_0 is a reference temperature (298 K) and T is absolute temperature. For this research the values of coefficients, D_0, k and Ea are 0.67E-12 (m²/s), 0.5 and 7046 (K) respectively. Equation (5) is a one-dimensional partial differential equation (PDE) and Fourier series shows the general solution on the interface boundary:

$$C(x,t) = C_{eq}\left(1 + \frac{4}{\pi}\exp\left\{Dt\left(\frac{-\pi^2}{L^2}\right)\right\}\sin\left(\frac{\pi x}{L}\right)\right) \qquad\qquad 6$$

Analytical solution is tough to obtain when the number of oil-pressboard interfaces increases and therefore, the exact solution of equation (5) using Finite Element Method (FEM) that requires discretization of moisture in pressboard C(x,t) over spatial and temporal scales as shown below [3]:

$$C_{i,j+1} = C_{i,j} + D_0 \left\{ \exp\left(Ea\left(\frac{1}{T_0} - \frac{1}{T} \right) + kC_{i,j} \right) \times \frac{\Delta t}{(\Delta x)^2} \right\}$$

$$\times \left[\frac{k}{4}\left(C_{i+1,j} - C_{i,j} \right) + \left(C_{i+1,j} + C_{i-1,j} - 2C_{i,j} \right) \right]$$

7

Where, i×j is shows the moisture concentration matrix over space (i) and time (j) separated by small space (Δx) and time steps (Δt) respectively. The boundary conditions to solve equation (7) are:

$$C_{(i=0,j)} = 0, \, C_{(i=L,j)} = C_{eq}, \, \frac{dC_{(x,t=0)}}{dx} = 0$$

8

RESULTS

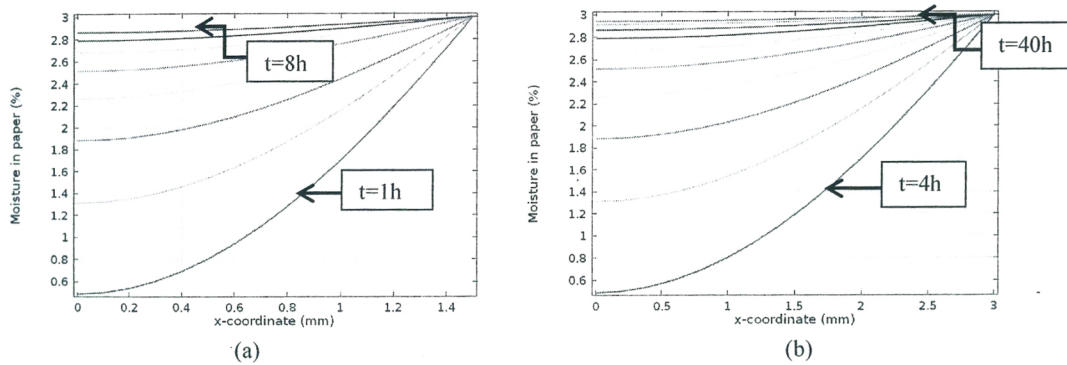Fig. 2 and 3 shows single-sided diffusion from 1.5 and 3 mm oil impregnated pressboard at different temperatures.

FIGURE 2. Single-sided diffusion of moisture in pressboard of (a) 1.5mm, (b) 3mm at 3% equilibrium moisture under 80⁰C
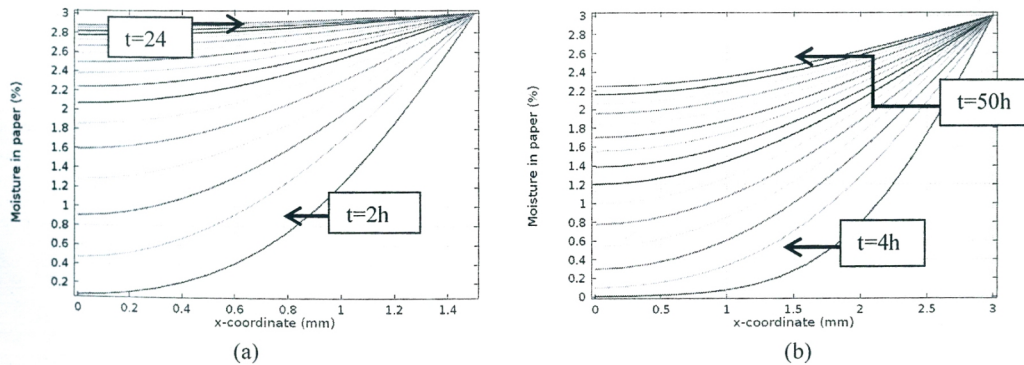

FIGURE 3. Single-sided diffusion of moisture in pressboard of (a) 1.5mm, (b) 3mm at 3% equilibrium moisture under 60⁰C

3

Table 1 shows interesting data on equilibrium time constant for moisture diffusion in pressboard insulation based on simulated diffusion data. It emphasizes that as the thickness of insulation doubles, the equilibrium time constant quadruples at same temperature and initial moisture concentration.

TABLE 1. Calculated equilibrium time constants for oil impregnated pressboards

PB thickness (mm)	Temperature (^{0}C)	Equilibrium time constant (h)
1.5	60	1.74
	80	0.527
3	60	6.97
	80	2.110

CONCLUSIONS

This paper discusses a simple method to develop moisture in oil-pressboard insulation system of transformers using finite element approach. Diffusion coefficient of moisture in pressboard is an influential parameter in determining moisture at oil-pressboard interface, which is of utmost importance during transformer monitoring. The general solution of moisture diffusion equation using Fick's second law is similar to Fourier series solution of 1-dimensional PDE. In this work, separate solution for moisture in oil-pressboard interface of insulation system with variable insulation thickness suggests strong correlation of moisture thickness on equilibrium time constant for oil-impregnated pressboards. Due to scarcity of diffusion coefficients for oil-impregnated pressboards, the applicability of these solutions is still under consideration. Future work involves developing strong empirical relations to fit the simulated curves for moisture behavior in oil-impregnated pressboards for non-isothermal cases.

ACKNOWLEDGMENTS

REFERENCES

1. T. A. Prevost, and T. V. Oommen, IEEE Electr. Insul. Mag. **1**, 28-35 (2006).
2. Y. Du, M. Zahn, B. C. Lesieutre and A.V. Mamishev, IEEE Electr. Insul. Mag. **15**, 11-20 (1999).
3. T. V. Oommen, IEEE Trans. Power App. Sys. **PAS 103**, 3063-3067 (1984).
4. L. J. Zhou, G. N. Wu and J. Liu, IEEE Trans. Dielec. Electr. Insul. **15**, 872-878 (2008).
5. W. Hribernik, W. Kubicek, G. Pascoli, and K. Frohlich, "Verification of a model-based diagnostic system for on-line detection of the mositure content of power transformer insulation using finite element calculation," in IEEE Condition Monitoring and Diagnostics Conference Proceedings (Beijing, CN, 2008), pp. 475-478.
6. J. Li, Z. Zhang, S. Grzybowski, and M. Zahn, IEEE Trans. Dielec. Electr. Insul. **19**, 1615-1622 (2012).
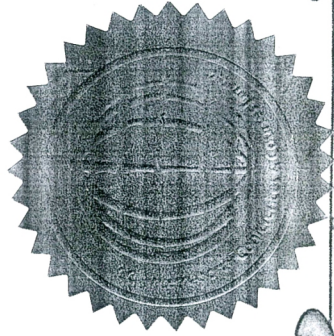
Certificate of Participation DSL337

We certify that **Dr. Manish Vashishtha** successfully attended the 10th International Conference on Diffusion in Solids and Liquids - DSL-2014, in Paris-France, from the 23rd to the 27th of June, 2014.

During the conference, Dr. Manish Vashishtha presented the work entitled:

Diffusion of Moisture from Insulation in an Oil-Paper-Air System Inside a Power Transformer
M. Vashishtha, S. Chakraborty

_____
Prof. Dr.-Ing. Andreas Öchsner, D.Sc.
DSL-CONFERENCE - Chairman

Continuing Education

ICC - International Conferences & Courses Limited

10th International Conference on Diffusion in Solids and Liquids (DSL)
Le Tapis Rouge, 67, rue du Faubourg, Saint-Martin
Paris, France
Paper ID: DSL337

Diffusion of Moisture from Insulation in an Oil–Paper-Air System inside Power Transformer

M. Vashishtha, S. Chakraborty*

*Corresponding author: 2012rch9520@mnit.ac.in

Malaviya National Institute of Technology, Jaipur, RAJASTHAN 302017, INDIA

The experimental and mathematical method of calculating the diffusivity has widely studied and applied in many fields of science and technology where diffusion is concerned. In the present paper the peculiar behaviour of oil immersed transformer insulating solids which are cellulose based components and porous in nature is studied. It is an established fact that presence of external or internal moisture not only hampers the performance but also reduces the life of an oil-filled transformer. The time required by the migrated moisture to diffuse and generate equilibrium conditions can devour information about the dielectric resistance of the insulation system against increasing moisture concentrations and subsequent failures. This equilibrium time constant is inversely proportional to the diffusivity and therefore is a function of varying moisture concentrations.

The paper gives an insight on laboratory scale transformer based diffusion experiments performed on Oil Impregnated Paper (OIP) of high porosity and dielectric stability at 100^0C. The results obtained from these experiments were divided into two sections for understanding i.e. *firstly* the impact of diffusivity on varying moisture concentration (1%, 3%, 5%) and subsequent equilibrium time, and *secondly* improved moisture profiling by discretizing the whole system in to small elements for location oriented measurement of moisture. These results can be used in designing an intelligent black box system for effective assessment for in service on-line transformers.

References
[1] R. Liao, M. Zhun, L. Yang, X. Zhou and C. Gong, J. Physica B: Condensed matter, 406, p1162-1168, (2011)

[2] D. F. Garcia, R. Villarroel, B. Garcia and J. C Burgos, Vol.29(2), p 40-49, IEEE Electrical Insulation Magazine, (2013)